PCCP

PERSPECTIVE

View Article Online
View Journal | View Issue

Cite this: *Phys. Chem. Chem. Phys.*, 2014, **16**, 19790

Photocatalytic generation of solar fuels from the reduction of H_2O and CO_2: a look at the patent literature†

Stefano Protti,* Angelo Albini and Nick Serpone

Received 27th June 2014,
Accepted 28th July 2014

DOI: 10.1039/c4cp02828g

www.rsc.org/pccp

The application of photocatalysis in environment remediation as well as in the generation of useful fuels from the reduction of water (hydrogen) and of carbon dioxide (methanol, carbon monoxide and/or methane) has been investigated largely in the last four decades. A significant part (12–13%) of the literature on the generation of such fuels is found in patents. Accordingly, the present article presents a selection of the patent literature on the theme. Photocatalysts, whether pure or doped, solid solutions or composites, reported in patents are reviewed along with the corresponding preparative methods and the photocatalytic performance. The absorption of light by such materials has been extended toward the red side of the spectrum, so that a better use of solar irradiation has been obtained, but the expected improvement of the catalytic effect has not always been achieved. The causes of these results and the way for improving the performance in the various steps of the process (*e.g.* avoiding charge recombination or catalyst corrosion) have been documented. The correct use of the term *water splitting* and the fundamentals of photochemical hydrogen evolution in the presence of a sacrificial electron donor (*e.g.*, alcohols) are discussed. Quantitative data about the amount of hydrogen evolved or carbon-based fuels produced are indicated whenever available.

1. Introduction

1.1 General considerations

Nearly forty years have passed since Fujishima and Honda[1] reported the photo-assisted electrolysis of water that generated stoichiometric amounts of hydrogen and oxygen upon irradiating a TiO_2 electrode (water oxidation; evolution of O_2) while maintaining the Pt counter-electrode in the dark (water reduction; evolution of hydrogen). The 1973 oil crisis established a favorable climate for funding research on water splitting since the production of a convenient energy carrier, such as hydrogen, seemed to be a reasonable and environmentally friendly approach of exploiting an abundant and inexhaustible energy source, namely solar energy. In a similar manner, the photocatalytic reduction of carbon dioxide was also demonstrated as a sensible approach to obtain useful fuels (CO, methanol, and/or methane).[2] However, to provide a stable and constant energy flux, as modern society expects, energy harvested from sunlight, a variable and low-density light source, has to be transformed into chemical energy by producing a fuel that can be transported, stored and used on demand. At that time, there was a general consensus that producing hydrogen by photocatalytic water splitting would offer an appealing opportunity to achieve this target under eco-friendly conditions. The reasons for this situation have been discussed in many books and reviews and will not be considered here, nor will other forms of producing hydrogen considered such as photovoltaic electrolyzers and the like.[3] Our focus is on the use of (heterogeneous) photocatalysis with light-photoactivated semiconductor inorganic materials to induce the formation of fuels from the reduction of water and carbon dioxide.

Years subsequent to the oil crisis of the early 1970s saw a sustained development of research by a large number of laboratories. A 1978 article by Bolton argued that the photocleavage of water by visible light counted amongst the most attractive options for the photochemical conversion and storage of solar energy, and that there were several possible photochemical systems that could produce hydrogen from water in a homogeneous medium.[4] Unfortunately, the euphoria that existed and the promise of a quick fix to the energy crises (another one occurred in 1979) failed to materialize with the consequence that much of the generous research funding by governments began to shrink and ultimately dried up. Nonetheless, research activity continued at a sustained pace, as demonstrated by the large number of publications.[5–22] Although the field of photocatalysis originated in the early years of the 20th century, the concentrated efforts to achieve

PhotoGreen Lab, Department of Chemistry, University of Pavia, via Taramelli 12, Pavia 27100, Italy. E-mail: stefano.protti@unipv.it

† Electronic supplementary information (ESI) available. See DOI: 10.1039/c4cp02828g

water splitting in homogeneous media were spurred by the short note in the journal *Nature*[1] and subsequently by the studies of Bard's group in heterogeneous media[21] in the late 1970s and early 1980s at the University of Texas. The extensive literature of the last three decades on heterogeneous photocatalysis has been summarized briefly in several reviews,[23–31] which included historical[19–21] and methodological aspects.[22]

The societal perception that non-renewable fossil fuels have to be substituted by some other energy source is now well enshrined in the mindset of society. That an important contribution to the energy needs of modern society might arise by exploiting solar energy through the generation of hydrogen from water splitting[5–16] and/or through the photocatalytic reduction of carbon dioxide[15–18] to fuels (CO, CH_3OH, and CH_4) is now widely recognized. Moreover, combining the reduction of carbon dioxide with the photochemical splitting of water and using a recyclable hydrogen donor might offer the opportunity to develop a non-biomimetic photosynthesis.[32] The actual challenge is not about the general idea, but rather on establishing whether or not these goals can be met in a cost effective way at the terawatt scale,[33,34] as well as to confront human rights and bioethical issues.[35] Accomplishing these goals has led to the founding of important government-supported research centers such as, for example, the Solar Energy Research Center at U.C. Berkeley in 2012, from which fast progress is expected in achieving the generation of eco-friendly useful fuels. Importantly, a detailed techno-economic analysis of photochemical water splitting commissioned by the U.S. Department of Energy[36] demonstrated that it is possible to produce hydrogen at an acceptable price. However, the technology available can at best be classed to be in the early Research & Development stage. To devise a system that is efficient, robust and scalable, many technological barriers have yet to be overcome, which have stimulated further work on specific aspects. In view of this situation, one must wonder how much investors and industry believe as to whether an effort in this direction is worthwhile. The position of industry will no doubt contribute, along with social pressure towards a *green* production and use of energy, to the trend of significant funding in this area. To evaluate this point, *patents*, rather than open scientific publications, are the measure of potential applicative interest. A significant number of patents have been granted in the last four decades that concern the photogeneration of hydrogen from water or of fuels such as carbon monoxide, methanol and/or methane from the photoinduced reduction of carbon dioxide. Although the practical significance of such systems depends on many factors that must interact in a synergistic manner, the very fact that a finding has been patented testifies to the potential feasibility of the application.

Far too many claims have been made in the scientific and patent literature that hydrogen produced photocatalytically is generated through a process referred to as *water splitting*, which in the strictest scientific sense refers to a process whereby water is decomposed to hydrogen and oxygen in a 2 to 1 ratio in the presence of a photocatalyst whether in homogeneous or heterogeneous media. Water splitting by photochemical or photocatalytic means is equivalent to the electrolysis of water, whereby the reduction of water occurs at the cathode (H_2 evolution) while oxidation of water occurs at the anode (O_2 evolution) with the half-cell reactions involving two reducing equivalents for hydrogen formation and four oxidizing equivalents for oxygen formation with the energy being provided by an electrical source (Fig. 1a; reactions (1) and (2)).[37]

$$\text{Cathode (reduction):}\quad 2H_2O(l) + 2e^- \rightarrow H_2(g) + 2OH^-(aq) \quad (1)$$

$$\text{Anode (oxidation):}\quad 4OH^-(aq) \rightarrow O_2(g) + 2H_2O(l) + 4e^- \quad (2)$$

Years of studies have shown that optical excitation of a semiconductor nanoparticle with energy equal to or greater than its corresponding band-gap energy by a light source ultimately causes formation of charge carriers: photo-holes in the valence band and photo-electrons in the conduction band, which in part recombine and in part migrate to the surface, where they interact with

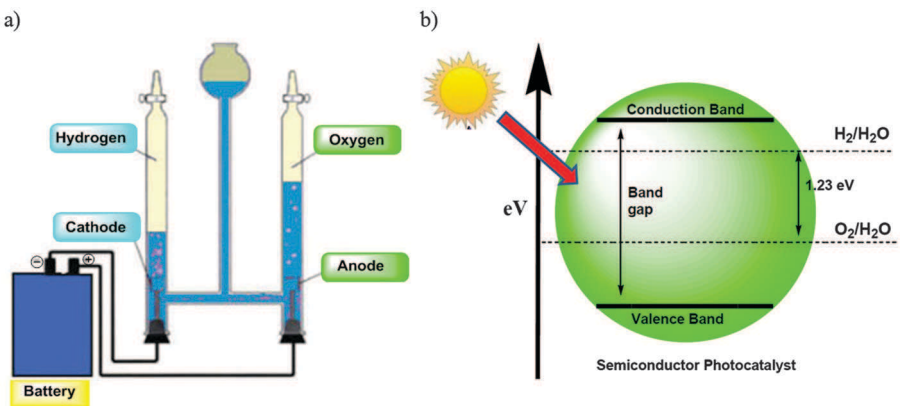

Fig. 1 (a) An electrolysis cell for the decomposition of water into hydrogen and oxygen. Adapted from http://msnucleus.org/membership/html/jh/physical/atomictheory/lesson4/atomic4c.html. (b) Cartoon illustrating the thermodynamic feasibility of carrying out the water splitting process upon illumination of a semiconductor photocatalyst with artificial UV/visible light or solar light; here the anode is the valence band and the cathode is the conduction band when the catalyst particle is photo-activated.

adsorbed molecules and initiate oxidative and reductive chemical reactions, respectively. The standard free energy for splitting a water molecule into H_2 and O_2 is 1.23 eV. When the band-gap of the semiconductor photocatalyst is such that it entrenches both the reductive and oxidative steps, water splitting becomes a thermodynamically feasible process (Fig. 1b). However, whenever hydrogen is generated from water/photocatalyst dispersions in the presence of a sacrificial electron donor (for example, alcohols or similar electron donor systems) then the process is *definitely not water splitting* and cannot be claimed to be so.

A recent critical review on the photocatalyzed reduction of carbon dioxide over metal-oxide materials by Li and co-workers[38a] highlighted several key factors for efficient CO_2 photoreduction and recent development in catalysts and photocatalytic reactor designs. Some of the key factors that limit the efficiency of the photoreductive process regard (i) the mismatch between the absorption of light by the semiconductor (most often TiO_2) and the solar spectrum, (ii) the poor efficiency in charge carrier separation, (iii) the low solubility of CO_2 molecules in water (*ca.* 33 μmol in 1 mL of water at 100 kPa and ambient temperature), (iv) the back reactions during the reduction of CO_2, and (v) the competition between the reduction of CO_2 to carbon-based fuels and water to hydrogen – see Fig. 2.[39] It is fairly well-known now that to reduce CO_2 into CO and other carbon-based fuels (*e.g.*, CH_3OH and CH_4), the photogenerated electrons in the semiconductor photocatalyst must have a more negative redox potential, while for water oxidation, where water would act as a sacrificial electron donor, the photogenerated holes must be at more positive redox potential levels. The following half-cell reactions and the corresponding redox potentials (reaction (1)–(8); E° (V) *versus* NHE) illustrate the thermodynamic feasibility for the generation of carbon-based and hydrogen solar fuels at neutral pH.[28] As highlighted in eqn (3)–(10), the first one-electron reduction of CO_2 (eqn (3)) to the corresponding radical anion $^\bullet CO_2^-$ is the rate limiting step, due to the highly negative electrochemical reduction potential involved.[38b]

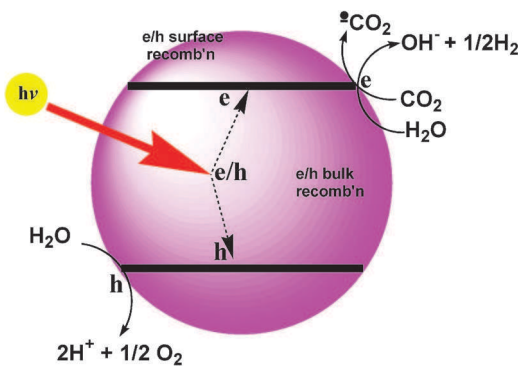

Fig. 2 Schematic diagram of photoexcitation of a semiconductor photocatalyst and electron transfer processes in the ultimate reduction of CO_2 to CO or HCHO or CH_3OH or CH_4 *via* initial capture of photogenerated electron by CO_2 in competition with water reduction present in much greater quantities.

It should also be noted that the pH of the aqueous solution will also play a role, since above pH *ca.* 5 CO_2 is present as a carbonate anion (CO_3^{2-}), a good hole scavenger.

$$CO_2 + e^- \rightarrow {}^\bullet CO_2^- \quad -1.90\ V \qquad (3)$$

$$CO_2 + 2H^+ + 2e^- \rightarrow HCOOH \quad -0.61\ V \qquad (4)$$

$$CO_2 + 2H^+ + 2e^- \rightarrow CO + H_2O \quad -0.53\ V \qquad (5)$$

$$CO_2 + 4H^+ + 4e^- \rightarrow HCHO + H_2O \quad -0.48\ V \qquad (6)$$

$$CO_2 + 6H^+ + 6e^- \rightarrow CH_3OH + H_2O \quad -0.38\ V \qquad (7)$$

$$CO_2 + 8H^+ + 8e^- \rightarrow CH_4 + 2H_2O \quad -0.24\ V \qquad (8)$$

$$2H_2O + 4h^+ \rightarrow O_2 + 4H^+ \quad +0.81\ V \qquad (9)$$

$$2H^+ + 2e^- \rightarrow H_2 \quad -0.42\ V \qquad (10)$$

Clearly, formation of the carbon-based fuels involves multielectron processes, particularly for the generation of methane. The review by Li *et al.* also emphasized that there should be more efforts (a) to improve the efficiency of the photoreduction reaction, (b) to develop novel heterostructured photocatalysts with considerable activity, high reaction selectivity for CO_2 reduction and stability, (c) to further investigate the crucial role of the co-catalysts (*e.g.*, noble metals), and (d) to unravel the little understood mechanisms of the photochemical process.[38a]

Based on the available scientific literature to the mid-2007, Osterloh[40] reviewed inorganic semiconductor materials that served as catalysts in photochemical water splitting, concluding that the only useful visible-light-driven catalysts that required no sacrificial electron donors or acceptors were $NiO/RuO_2/Ni{:}InTaO_4$, the tandem system composed of Pt/WO_3 and $Pt/SrTiO_3/TaON$, the Cr/Rh-GaN:ZnO system and $(Zn_{1.44}Ge)(N_{2.08}O_{0.38})$. Trends in the H_2/O_2 evolution rates were roughly proportional to the magnitude of the semiconductor band-gaps. However, the reported quantum efficiencies[40] were tenuous at best as they were often determined on the basis of the incident radiation emitted by various light sources *impinging* on the reactor for a range of wavelengths, and not on the basis of the radiation actually *absorbed* by the photocatalysts at a given wavelength.[41]

Fresno and co-workers[42] recently examined achievements and near-future trends of different photocatalytic materials in (heterogeneous) photocatalysis with the intent to assess the state-of-the-art of this continual developing technology with specific reference to materials and systems, emerging aspects, and potential new directions of the technology in the near future. These authors concluded, among others, that blind chemical doping or small variations in synthesis conditions affecting the most widely used metal-oxide photocatalyst, TiO_2, will not likely lead to significant advances, although small improvements might be achieved by chemical, morphological and textural modifications of this material, which has the potential to significantly improve the results in specific niches. They further proposed that an integrated and more comprehensive use of published results may be a more sensible approach for successful outcomes, rather than repetitive attempts at improving the characteristics of TiO_2 by time-consuming trial-and-error.[42]

1.2 The patent literature

Despite the large number of patents published on photocatalysis in the last decade (2000–2011; Fig. 3),[43] the patent literature on the photo-induced generation of fuels has received limited attention.[44–49] Accordingly, the topic is examined in the following sections, limitedly to the production of hydrogen from water and carbon-based fuels from the reduction of carbon dioxide (*e.g.* CO, CH_3OH, CH_4), see reactions (11)–(14).

$$2H_2O \rightarrow 2H_2 + O_2 \quad (11)$$

$$2CO_2 \rightarrow 2CO + O_2 \quad (12)$$

$$4H_2O + 2CO_2 \rightarrow 2CH_3OH + 3O_2 \quad (13)$$

$$2H_2O + CO_2 \rightarrow CH_4 + 2O_2 \quad (14)$$

The extensive patent literature on water depollution, air purification, printing and many other applications of photocatalysis has not been considered in the present review.

Patents on photocatalytic water splitting are a significant fraction of those for which proprietary protection is sought. The flow of patents issued in photocatalysis on these topics began a couple of years before publication, rapidly reaching a level of 12–13% of the overall number of publications during the rather dramatic increase in the last decade (Fig. 4a). It is noteworthy that China and Japan hold the largest number of patents in the field (Fig. 4b). Moreover, most Chinese patent applicants (represent more than 50% of the patents cited in this review) are from the academic community. Patents arising from industry have been highlighted in the text and in the references (see also ESI†).

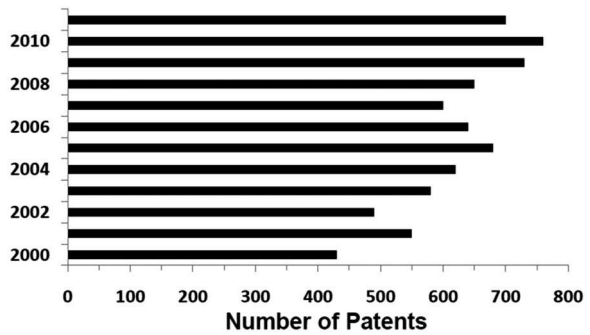

Fig. 3 Number of patents filed in the years between 2000 and 2011 in the field of photocatalysis. Adapted from ref. 43.

All of the main issues investigated in fundamental studies are reflected in patents. For instance, with regard to the photocatalysts used, titanium dioxide (TiO_2) dominates with almost identical percentage among patents and in the overall scientific literature, followed by groups 5 and 6 metal-oxide derivatives (Fig. 5a). However, there appears to be a greater focus towards sulfides in patents relative to oxides (22.1 and 15.1% of the overall number, respectively), probably because of the good performance of the sulfide systems that make it worthwhile to devote a bigger effort to technological development and to overcome corrosion in *applied* science. By contrast, *fundamental* science tends to look for new catalysts, typically new metal oxides.

Somewhat on the same line, composites have received greater attention in the patent literature, whereas other approaches for improving the performance, such as sensitizing, doping or going to nano-sized systems, are considered less often (Fig. 5b). This is a manifestation of the general trend towards exploiting a smaller number of variations to more depth, which is typical of industrial chemistry. Also, the proportion of patents devoted to the production of carbon-based fuels from the reduction of CO_2 relative to those on the production of hydrogen from water is lower (25.4% *versus* 29.5%). The number and quality of work reported in the patents suggest that the photocatalysis technology is being considered seriously for near-future industrial applications.

Nearly all of the patents filed contain an introduction that explains the significance of solar energy conversion for the needs of modern society and the appropriateness of the energy vector considered, hydrogen from water or various fuels from CO_2. The specific invention is presented in some detail, with a number of examples followed by the claims. As one may expect, patents tend to claim as large an area as possible. Such claims refer to the catalyst structure, preparative methodologies and irradiation methods, and to other significant features such as separation of H_2 and O_2 when co-generated, the choice of the medium and the sacrificial electron donor, among others.

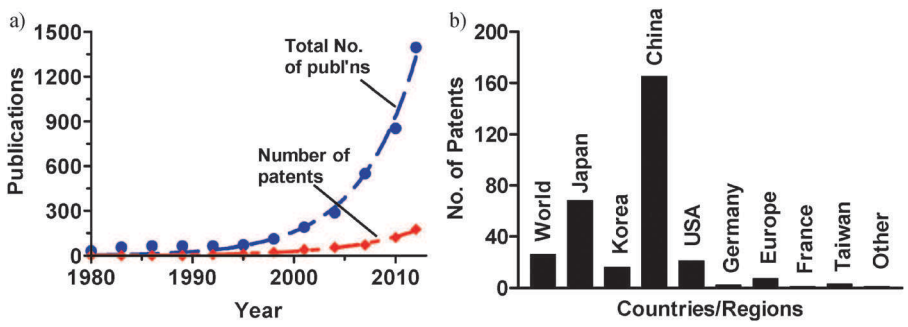

Fig. 4 (a) Total annual number of publications in the literature (open literature + patents) relative to the number of patents granted on the photocatalyzed production of hydrogen from the reduction of water and formation of carbon-based fuels from the reduction of CO_2 since 1980. (b) Countries/regions where patents on the formation of fuels were issued and quoted in this review; note that many of the World and US patents also originate from China and Japan.

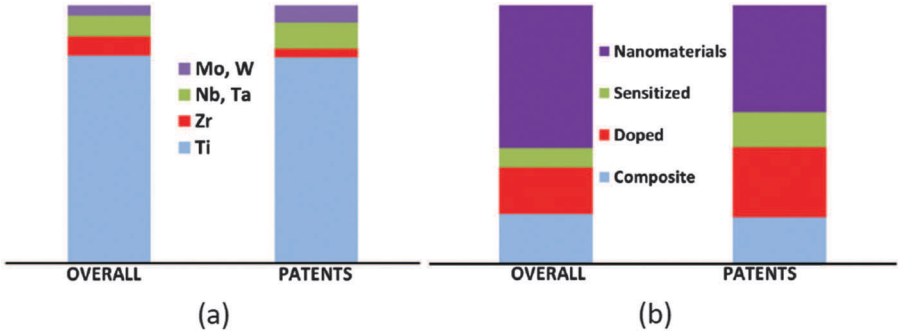

Fig. 5 Contribution of specific topics to the patents relative to the overall number of publications. Photocatalyst used: (a) metal oxides; (b) characteristics of the photocatalytic materials.

The most distinctive element is the structural features of the potential photocatalyst.

As hinted above, the most investigated photoactive semiconductors have been the metal oxides TiO_2, ZnO, WO_3, and the mixed metal oxides $BiVO_4$ and the analogous Nb and Ta oxides in which the metals have either a d^0 or d^{10} electronic configuration. To some extent, the activity appears to depend on the crystalline forms of the metal oxide (*e.g.* in the case of TiO_2: anatase, rutile and brookite), the morphology (nanostructured material, *e.g.* zero dimensional, 0D, such as spherical nanoparticles and quantum dots, 1D such as nanorods, 2D such as nanosheets, *etc.*..), the loading of metallic co-catalysts capable of facilitating electron exchange, and release of molecular hydrogen. Doping with metallic and non-metallic dopants into the bulk of the nanoparticles, or the use of solid solutions of different semiconductors, introduces new levels within the band-gap that may considerably extend the range of active wavelengths into the visible spectral region. Composites have also been used with great advantage. In the following section, key details for the preparation of the photocatalysts are gathered. The performance is reported as the rate of hydrogen and oxygen evolution (μ (or) mmol h^{-1} g^{-1}) per gram photocatalyst (when appropriate, the scale of the experiment, of obvious importance for application, is also mentioned). Quantum efficiency or % light exploitment is mentioned where available.

2. Photocatalysts for hydrogen generation and CO_2 reduction: group 4 metal oxides

2.1 Undoped metal oxides for hydrogen generation

Samples of titanium dioxide for use as photocatalysts are most often prepared from a precursor either by forming a sol gel, followed by aging, drying and calcining, or by a hydrothermal reaction, followed by drying and calcining. The mode of preparation and the temperature of the pretreatment stage can have a large effect on the crystalline structure, dimension and surface characteristics of the particles formed, and thus on the photoactivity, as abundantly documented in the patent literature; a selection of some representative examples is reported in Table 1.[50–66]

Table 1 Photocatalyzed generation of hydrogen in various TiO_2 systems in aqueous media in the presence of a sacrificial electron donor

Ref.	Catalyst system	Solution/electron donors	Light source[a]	R (H_2)/mmol h^{-1} g^{-1} (% efficiency)
50	2.2% W/C on TiO_2	MeOH (50 $vol\%_{aq}$)	500 W, Hg	5.35
51	Pt/TiO_2/Carregeenin[b]	MeOH (50 $vol\%_{aq}$)	740 mW cm^{-2}, Hg	1.95
52	19% Printex-G + 65% TiO_2 + 16% (5 wt% RuO_2/TiO_2)	EtOH–H_2O	50 mW cm^{-2}	0.045
53	Ni/TiO_2-CNT	MeOH–H_2O	300 W, Hg	Up to 1140
54	(5 wt%)Ag/TiO_2 NT	MeOH (5 $vol\%_{aq}$)	Hg or Xe	3.2
55	Pt/TiO_2	Glycerol (20 $vol\%_{aq}$)	300 W, Xe	7.28
56	(3 wt%)Pt/TiO_2 pulp	EtOH–H_2O	400 W, Hg	0.0077
57	C,N-co-doped TiO_2	Na_2S–Na_2SO_3	8 W, Hg (365 nm)	0.38
58	(1 wt%)Pt/TiO_2 nanoboxes	MeOH–H_2O	300 W, Xe	Up to 1
59	C,N-co-doped TiO_2	Water	150 mW cm^{-2}	0.153
60	C,N-co-doped TiO_2	Na_2S–Na_2SO_3	145 mW cm^{-2}, Xe	0.056
61	TiON/TiO_2	Na_2S–Na_2SO_3	500 W, Xe	0.114
62	$TiO_2/BiVO_4$	MeOH–H_2O	300 W, Xe	1.24
63	TiO_2/MIL-101 (Cr)	MeOH–H_2O	Xe	2.68
64	Cu nanowires/TiO_2	MeOH–H_2O	365 nm	(10.5%)
65	TiO_2/Cu_2O	MeOH–H_2O	300 W, Xe > 420 nm	1.52
66	Ag/AgBr/TiO_2	HCOONa	300 W, Xe	0.143
		HCOONa–MeOH		0.393

[a] Power and lamps used (Hg or Xe arc "fluorescent lamps") whose emitted light impinged on the sample; indicated where available. [b] Carregeenins are a family of sulfated linear polysaccharides.

As evidenced in Table 1, titania-based photocatalysts are the most investigated systems for the photodecomposition of water in the presence of an electron donor(s) because of the relatively large band-gap and conveniently situated for this process, albeit TiO_2 is photoactive only under UV radiation. Indeed, a limitation to the use of TiO_2 in its pristine form is that it absorbs only a small fraction of the solar light (*ca.* 4%, the absorption edge for anatase is at *ca.* 3.2 V, corresponding to 387 nm). Unaltered TiO_2 samples, including the largely used commercial Degussa P25 (now Evonik P25) that consists of a mixed phase of anatase (*ca.* 80%) and rutile (~20%), do exhibit some photoactivity under UV/visible irradiation. Despite much work, however, a convincing explanation as to why a mixed-phase material such as the P25 titania outperforms the individual polymorphs has not been reached.

Nonetheless, through a combination of state-of-the-art materials' simulation techniques and X-ray photoemission experiments, Scanlon and co-workers[67] demonstrated that a staggered band alignment of *ca.* 0.4 eV exists between the anatase and rutile phases with anatase possessing the higher electron affinity (or work function; Fig. 6). Their results explain the robust separation of photogenerated charge carriers between the two phases. For practical reasons, the characterization of useful photocatalysts is most often done in a laboratory environment with the use of artificial Hg or Xe lamps; this raises questions as to the validity of the data for assessing the suitability of such systems in practical solar energy conversion schemes.

Many of the patents examined suggest that the morphology of the metal-oxide photocatalyst plays a key role in process efficiency. Hydrothermal processes were the best choice for the preparation of differently structured materials that include brookite titania (patented by Daicel Corporation),[68] mesoporous TiO_2 samples,[69] coating material containing needle-shaped nanocrystals (anatase structure; length, 100 nm; thickness, 20 nm),[70] and flower-like anatase titania monocrystals with a double pyramidal configuration.[71] In a similar manner, photoactive mesomorphous nanobelt titania materials (length: few μm; width: dozens to hundreds of nm; mesopore diameter: 4.6–4.8 nm) have been prepared under solvothermal conditions using commercially available P25 TiO_2 in strong caustic soda (NaOH) and absolute ethyl alcohol (EtOH at 180 °C).[72]

The use of surfactants, such as poly(ethylene/propylene glycol) triblock copolymers (*e.g.* Pluronic P123) and sodium dodecyl sulfonate (SDS), cetyltrimethylammonium bromide, polyethylene glycol (PEG), and triethanolamine, have been exploited to synthesize mesoporous titania catalysts in aqueous media with uniform pore size and specific surface areas in the range 100–180 $m^2\ g^{-1}$.[73] Analogously, pure anatase TiO_2 with a surface area of 350–450 $m^2\ g^{-1}$ and pores with an average diameter of 20–30 nm and a pore volume of 0.2–0.3 $m^3\ g^{-1}$ was obtained in the presence of ethanol–glycerol; the resulting photocatalyst synergistically produced hydrogen, while efficiently degrading high concentrations of dyes in wastewaters.[74]

Photocatalytically active materials can be supported on substrates such as quartz, conductive glass, and indium tin oxide (ITO). Metals have also been used as supports; for instance, an ultrathin film of TiO_2 nanoparticles supported on a stainless steel wire net has been prepared by immersion-drawing from a stable titanium alkoxide solution, followed by a high temperature treatment at 300–600 °C. It was claimed that the resulting small TiO_2 grain material had high photocatalytic activity.[75] The use of a flexible polymer support (*e.g.*, polyethylene terephthalate, PET) was recently introduced to prepare TiO_2-containing flexible films[76] and transparent coatings of TiO_2 on water-soluble polyurethanes and acrylic derivatives.[77]

Doping a semiconductor photocatalyst particle, such as TiO_2, can lead to the formation of an *extrinsic* band-gap without changes to its *intrinsic* band-gap (Fig. 7). However, the extrinsic band-gap can also form by subjecting the metal oxide to a *physical* stress[78,79] without addition of any chemical additive. For instance, vacuum-coating a thin film of titania onto a substrate, preferably with a different Young's modulus, led to bending undulations on the surface of a spatial radius similar to the film thickness. The resulting electrical activity induced in the band-gap shifted the absorption of light from the UV toward the visible spectral region. The undulated coating also served to self-focus and concentrate the incident light required for the process, to increase the photocatalytic surface area, and to prevent delamination of the film from the substrate.[79] Furthermore, this stress-induced *shortened*

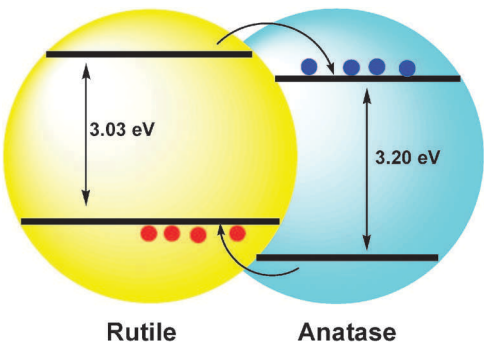

Fig. 6 Suggested valence and conduction band alignment mechanisms for the anatase–rutile interface in a mixed phase TiO_2 material such as the P25 TiO_2: red dots represent photogenerated holes and blue dots denote photogenerated electrons.

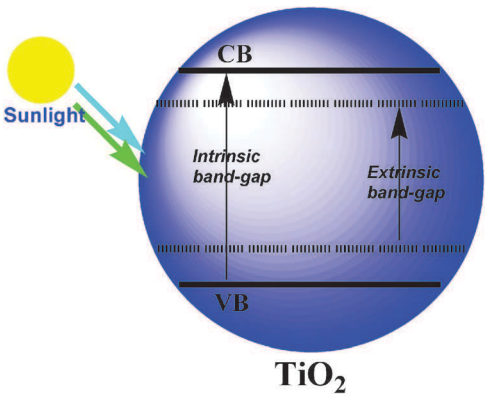

Fig. 7 Illustration of a sunlight-irradiated TiO_2 nanoparticle with an *intrinsic* band-gap and an *extrinsic* band-gap. The latter results from a physical modification of the nanoparticle through formation of oxygen vacancies as a result of doping or through some physical stress.

band-gap of the titania photocatalytic surface could be used in photoelectrolysis for the production of hydrogen gas from water.

Other than through doping, a metal-oxide photocatalyst with band-gap energy in the UV region can also be photoactivated indirectly by visible light through a photosensitization process. This can be achieved either through the use of organic dyes (*e.g.*, rhodamine-B) or transition metal complexes (*e.g.*, metal-loporphyrins or ruthenium-polypyridyls) that act as photo-sensitizers,[80–84] or through electron-transfer sensitization by coupling the metal oxide with a smaller band-gap semi-conductor that possesses an absorption edge well into the visible region (*e.g.*, CdS). The latter process was first reported in 1984 by Serpone and co-workers[85] as the Inter-Particle Electron Transfer (IPET) process for sensitization and was later confirmed by these[86–90] and other authors[91] (Fig. 8).

One of the first patents on the photochemical TiO_2-assisted production of hydrogen and oxygen over extended periods was allocated to Grätzel and co-workers.[92] The catalyst system consisted of ruthenium dioxide (RuO_2, 0.1 wt%) and Nd-doped TiO_2 (grain diameter *ca.* 100–200 nm) that served as the carrier of finely divided platinum (2.5–3.5 nm); the resulting particulates performed the function of both oxidation (RuO_2) and reduction (Pt) catalysts. Exposure of the catalyst suspension that also contained the well-known inorganic ruthenium(II) photosensitizer, $Ru(bipy)_3Cl_2$ (10^{-4} M; bipy = bipyridyl) and methylviologen (MV^{2+}; 5×10^{-3} M) acting as the electron relay to filtered visible light illumination (250 W halogen lamp, IR and UV filters) led to an initial hydrogen evolution rate of 5.35 mmol h^{-1} g^{-1} with concurrent evolution of oxygen at 2.14 mmol h^{-1} g^{-1}. The lower than expected evolution rate for oxygen was attributed[92] to adsorption of the oxygen on the metal oxides. However, the expected stoichiometric ratio of 1 mol of O_2 to 2 mol of H_2 was reached later. Optimal yields of products were obtained at pH ~ 4–5.[92] Importantly, after 18 hours of irradiation, the hydrogen generated was 18 times the amount produced in the first hour of illumination. Another viable combination was based on the excitable proflavine and thionine photosensitizers, with the inert $Fe(bipy)_3^{2+}$ complex acting as the electron donor. Also present were co-catalysts to activate the release of the gases produced.[92]

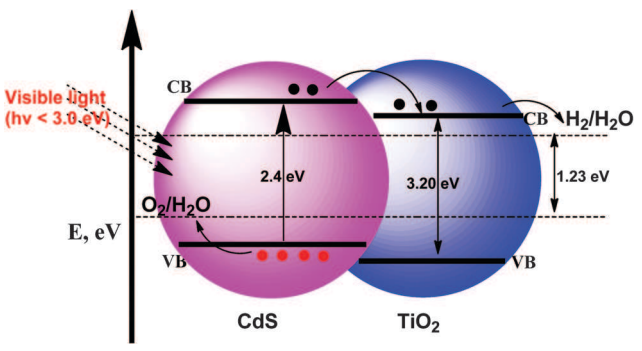

Fig. 8 Illustration of the Inter-Particle Electron Transfer (IPET) process in the photosensitization of a wide band-gap metal-oxide semiconductor photocatalyst (*e.g.* TiO_2) coupled to a smaller band-gap semiconductor (*e.g.* CdS) in the photo-induced cleavage of water.

A patent on the sensitization of a semiconductor-based oxidation/reduction photocatalyst, and the use of the photocatalyst for the photooxidation of aqueous or aqueous-organic liquids or the photodecomposition of aqueous liquids with visible light was allotted to Duonghong, Grätzel and Serpone for the specific purpose of producing hydrogen from water decomposition.[93] In fact, the unusually sensitized photocatalyst made it possible to generate stoichiometric quantities of hydrogen and oxygen from the water splitting process with satisfactory efficiency under visible light illumination, even at wavelengths between 590 nm and 665 nm. These authors discovered that it was possible to obtain such a redox photocatalyst by attaching a ruthenium(II) polypyridyl complex (tris-bipyridyl or tris-phenanthrolyl type) chemically onto the surface of TiO_2 particulates loaded with Pt deposits and RuO_2 through a Ru(II)-bis-polypyridyl fragment. In the presence of a sacrificial electron donor (triethanolamine) and subsequent to irradiation of an aqueous suspension of the photocatalyst (0.01 g; pH = 10) at wavelengths greater than 405 nm (Xe light source) the H_2 evolution rate was 1038 μmol g^{-1} h^{-1}, while for irradiation at wavelengths longer than 590 nm the H_2 evolution rate was 223 μmol g^{-1} h^{-1}.[93] In the absence of any sacrificial electron donor (*i.e.* pure water, pH 2), however, irradiating the aqueous suspension of $TiO_2/Pt/RuO_2/RuL_2^{2+}$ (L = the polypyridyl fragment) at wavelengths longer than 420 nm gave an initial H_2 evolution rate of 134 μmol h^{-1} g^{-1} and the amount of hydrogen evolved after 20 hours of illumination was 400 μL. A chromatographic analysis of the gases evolved after 12 hours of irradiation showed the presence of both H_2 and O_2 in a virtual 2-to-1 stoichiometric ratio.

2.2 Doped metal oxides for hydrogen generation

The presence of foreign atoms in a host lattice and their difference in size, with respect to the native atoms, can introduce a physical strain in the lattice. When the dopant ions have a different valency relative to those ions in the host lattice, the effective charge will affect the electroneutrality condition and thus the defect equilibria. These titania photocatalysts, now commonly referred to as second generation photocatalysts, absorb a more or less extended part of the visible light wavelengths as a result of embedding the dopant impurities into the lattice. Whether doping the metal-oxide semiconductor leads to an intrinsic shift of the absorption edge of titania (this is the so-called band-gap narrowing proposed by some workers[94,95]) or whether the introduction of oxygen vacancies by doping leads to the formation of color centers is a topic of current debate.[96–99] Other than what was noted above, this point will not be discussed here. In general, we have adopted a phenomenological classification with little attention to mechanistic issues.

2.2.1 Self-doped metal oxides. A method to bring about chemical changes in a metal-oxide system is altering the oxidation state of one of its constituting element. For TiO_2 this would be the introduction of Ti^{3+} ions, which has been achieved by heating titania in a hydrogen atmosphere. This led to the formation of a partially reduced (colored) form of titania.[100] A new energy level attributed to Ti^{3+} was thus generated and located at *ca.* 0.8 eV below the conduction band. The resulting surface-hydrogenated

titania microspheres (3–6 nm) consisted of nanowires with a surface area of ~ 75 m^2 g^{-1} and an overall pore volume of 1.02 cm^3 g^{-1}. A markedly increased visible light absorption ability resulted and ensured the generation of a large number of $^{\bullet}OH$ radicals and a H_2 evolution efficiency nearly three times greater than that from the commercially available Evonik P25 titania.[100] By contrast, self-doped TiO_2 nanorods (average length: 50–80 nm; average diameter: 8–15 nm) could also be prepared by direct reduction of the Ti^{4+} ions in a liquid phase containing hydrazine and ethylene glycol as the reductants; no thermal treatment was required in this case.[101]

2.2.2 Anion-doped titania photocatalysts. Although visible light absorbing N-doped TiO_2 was first described in 1986, it received considerable attention only after the study reported by Asahi and co-workers in 2001,[94a] in which they took the view that doping caused a *narrowing* of the band-gap of the doped titania. This was based on density functional theory (DFT) calculations of the band-gap energy, not universally accepted, since with pristine TiO_2 the calculated gap was lower by >1 eV with respect to the experimental value of 3.0–3.2 eV. However, the adoption of improved methods such as (DFT + U calculations) overcame most of the limitations of the DFT method in calculating band-gap energies of semiconductors.[94b–d]

As in the case of non-doped oxides, the hydrothermal methodology has also been employed to synthesize boron-doped titania crystals (precursor: titanium boride, TiB_x, $0 < x < 5$; B content in TiO_2: 0.05 to 5 atom%) that have specific crystal planes and recognizable surface composition.[102] Preparation of the anion/cation-co-doped titania photocatalysts $TiO_{2-x-y}A_xM_y$ (M = metal ion dopants not described; A = B, C, N, F, Si, P, S, Cl, Br, or I) has also been reported; the as-prepared B,N-co-doped titania had a surface area of 94.43 m^2 g^{-1}.[103] Addition of minerals of the tourmaline class (crystalline boron silicate minerals) to P25 TiO_2 increased the quantum efficiency of hydrogen generation more than twofold (Fig. 9a and b) in what the patent (from Nanoptek Corporation) claimed to be a water splitting process, yet no evolution of oxygen was reported.[104] The greater efficiency was attributed to the electric field on the surface of the polar tourmaline mineral deposits.

Mixing and heating a mixture of titania and carbon powder at temperatures ≥ 1000 °C under an inert atmosphere, followed by treatment in an oxidizing atmosphere at 300–1000 °C produced a visible-light activatable photocatalyst that contained *ca.* 3% Ti–C bonds.[105] The visible-light-active titania so-formed could be used for point-of-use dissociation of an aqueous medium into hydrogen gas along with other products that depended on conditions.

Films and powders of nitrogen-doped materials ($TiO_{2-x}N_x$) have revealed an improved activity under visible light (wavelength, 500 nm) with respect to titanium dioxide (TiO_2), larger than that obtained with other non-metal dopants.[94] Such materials are usually prepared from titanium precursors, or TiO_2 and nitrogen sources that include amines, nitro compounds, heterocyclic derivatives,[106] and urea[107] allowing the formation of materials with N-to-Ti ratios up to 10%,[106] with a significant absorption in the visible spectral region (up to 830 nm).[108] Similarly, the hydrothermal method has proven useful in the synthesis of N-doped titania nanotubes of controlled dimension either from TiO_2 sols or nanoparticles as precursors.[109] By contrast, an alternative methodology was reported by Anpo and co-workers,[110] who used RF magnetron sputtering of TiO_2 in a nitrogen-containing atmosphere and achieved the formation of a N-doped TiO_2 (N content $>$ 1.5 atom%) thin film with no rutile structure. Placing a titanium sheet in a 3–10% hydrogen peroxide solution led to the formation of a peroxo-titanium acid nano-flower-like thin film on the metal surface.[111] Subjecting this film to a hydrothermal reaction, carried out in an oven, yielded a titania nano-film, which when placed in a reactor with urea at both ends followed by calcination in a muffle furnace produced a catalyst that was sensitive to visible light.[57]

Preparation and use of X,N-co-doped titania photocatalysts (X = additional dopant) have been described. For example, C,N-co-doped titania materials were obtained by heating TiCN powder at a temperature of 400–600 °C for about 0.5 to 2 hours. Thus, irradiation of a mixed aqueous dispersion of the so prepared C,N-co-doped titania containing the sacrificial electron donors Na_2S and Na_2SO_3 (500 W xenon light source; light intensity, 120 mW cm^{-2}) produced H_2 at a rate of 0.38 μmol h^{-1} g^{-1}.[57] Another procedure to prepare C,N-co-doped titania involved the calcination of black TiN under oxidative conditions (in air at 400–600 °C for 0.5–2.5 hours) followed by treatment with CO, also at 400–600 °C for 0.5–2.5 hours.[59] The as-prepared

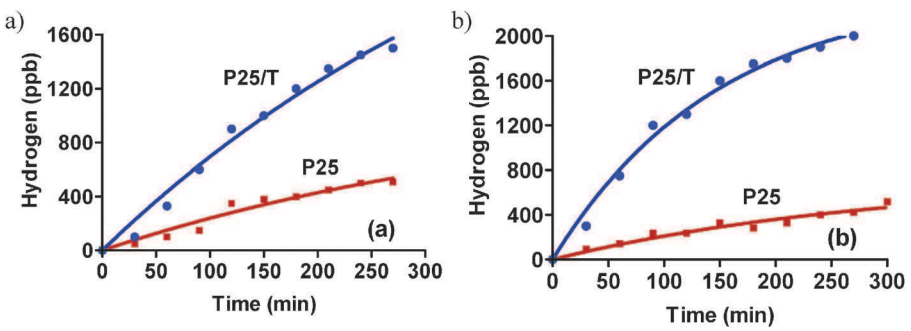

Fig. 9 (a) Graph illustrating the evolution of hydrogen from water as a function of time for P25 TiO_2(P25) and for P25 TiO_2 integrated with tourmaline (P25/T); (b) graph illustrating the evolution of hydrogen from water for P25 TiO_2 (denoted, P25) and a P25 TiO_2 integrated with tourmaline (P25/T) in acidic media at pH 4.8, adapted from the data given in ref. 104.

C,N-co-doped TiO_2 displayed good photocatalytic activity toward methylene blue degradation, as well as a higher hydrogen evolution rate (64.4 μmol h^{-1} g^{-1}) than either N-doped TiO_2, obtained by heating TiN, (48.0 μmol h^{-1} g^{-1}) or P25 titania (41.4 μmol h^{-1} g^{-1}).[60] After 80 min of illumination and under identical experimental conditions in the presence of the two sacrificial electron donors (Na_2S/Na_2SO_3), the hydrogen evolution efficiency of the C,N-co-doped titania was greater (56.0 μmol h^{-1} g^{-1}) than for pristine P25 TiO_2 (37.4 μmol h^{-1} g^{-1}). Moreover, when used as the photoanodes in dye-sensitized solar cells the C,N-co-doped TiO_2 exhibited a higher energy conversion efficiency (3.31%) than did either the N-doped TiO_2 (2.44%) or the P25 titania (1.61%).[60]

The patent by Parida and co-workers[112] reported the intercalation of ruthenium(II) polypyridyl complexes (bipyridyl (bpy) and phenanthroline) in N-doped and N,S-co-doped titania pillared montmorillonite samples that proved useful as multifunctional photocatalysts towards a variety of light driven redox reactions: *e.g.*, organic dye degradations, photocatalytic water splitting and various organic transformation reactions oriented to the synthesis of fine chemicals. Although claimed that the evolution of H_2 originated from the photocatalytic water splitting process, the patent indicates the presence of significant quantities of methanol as the sacrificial electron donor (hole/$^{\bullet}$OH radical scavenger). As such, the process cannot be considered as water splitting as noted earlier in this article.[112] Nonetheless, under the conditions of (i) catalyst loading, 20 mg, (ii) 20 mL of 10 vol% methanol, (iii) illumination time, 3 hours, and (iv) light source, 125 W Hg visible lamp, the observed rates of H_2 evolution in the presence of different photocatalysts were rather high.

- N-doped TiO_2 pillared montmorillonite: 28 246 μmol H_2 h^{-1} g^{-1}
- N,S-co-doped TiO_2 pillared montmorillonite: 33 500 μmol H_2 h^{-1} g^{-1}
- Ru(II)-bpy intercalated N-doped TiO_2 pillared montmorillonite: 63 466 μmol H_2 h^{-1} g^{-1}
- Ru(II)-bpy intercalated N,S-co-doped TiO_2 pillared montmorillonite: 75 166 μmol H_2 h^{-1} g^{-1}

Thus, the ruthenium(II) complex enhanced the hydrogen evolution process by photosensitization; co-doping also improved the rate of hydrogen evolved.

The use of a Ti sheet as the anode in an NH_4NO_3 solution produced amorphous N-doped titania, which when subsequently used as the cathode in a $Gd(NO_3)_3$ solution yielded N,Gd-co-doped titania nanotube arrays.[113] The nitrogen and gadolinium co-dopants generated a synergism and raised the photoelectric performance and photocatalytic activity of titanium dioxide.

Addition of a fluoride ion source during the preparation of mesoporous titania under mild hydrothermal conditions gave a fluorinated material that displayed a greater photocatalytic activity (threefold greater than P25 titania); however, the patent is silent as to what was used to ascertain the photoactivity of the materials prepared. Whatever the method, the greater photoactivity was attributed to a larger surface area, smaller grain sizes, and to its mesoporous structure.[114] Treatment of titania particles with F_2 gas followed by treatment with H_2O_2 afforded colored particles.[115] It was reported that Br-doped TiO_2 nanomaterials with Br inserted into the crystal lattice at interstitial positions (Br content up to 10 atom%) absorbed visible light up to 750 nm.[116]

An arc discharge process, in which titanium or a titanium alloy substrate was used as the anode in the presence of oxygen and other buffering gases (*e.g.*, H_2, Ar, He, N_2, NH_3, CH_4, CH_3CH_3, $CH_2{=}CH_2$, C_2H_2, *n*-$CH_3CH_2CH_3$, or a mixed gas) at controlled pressures led to the formation of nanometer spherical fibrous carbon-doped and nitrogen-doped titania systems (N and C dopant concentrations: 0.001–5 atom%) of different crystalline forms and different crystal grain sizes that absorbed visible light for the use in photocatalytic processes.[117]

2.2.3 Cation-doped titania photocatalysts. Metal-ion-doping of TiO_2 is recognized as an appropriate method to tune both the photochemical and the photophysical behaviors of titania. In particular, transition metal ions such as Fe^{3+}, Ru^{3+}, V^{4+} or Ni^{2+} increased the photocatalytic activity of the semiconductor.[118] Titanium dioxide doped with 2.5% transition metal borides, carbides or nitrides exhibited satisfactory photocatalytic activity for H_2 evolution in 50 vol% aqueous methanol.[119] By comparison, co-doping with Cr and B (2.2 atom%) led to a H_2 generation rate of 1.71 mmol h^{-1} g^{-1} of the catalyst, the best result being obtained amongst the boride-doped materials. However, co-doping TiO_2 with W and C led to an even better overall result with a nearly threefold greater hydrogen evolution rate.

Electrochemical anodic oxidation of titanium plate substrates containing various quantities of metallic impurities (M = Zr, Hf, Nb, Ta, Cr, W, Bi, Al, Zn, In, and Cu; alloying dopant contents: 0.5–20%) for 1 to 15 hours led to the formation of amorphous cation-doped TiO_2 nanotubes, which subsequent to a heat treatment in air at 500–600 °C for 1 to 20 hours yielded crystalline titania nanotube arrays (the anatase phase or the mixed rutile-anatase phase; the rutile phase varying from 5 to 75%) with dimensions of 50–250 nm (diameter), thickness of 1–100 nm and lengths up to 10 μm.[120] Similarly, anodic oxidation of a titanium surface in the presence of metal glycerol-phosphates and acetates (of alkaline metals or lanthanides) has been used to prepare films of doped titania and titanium-containing mixed oxides.[121]

Visible-light-responsive titanium dioxide photocatalysts doped with V, Cu, Fe, Ni, Sr, or Cd were prepared from titanium alkoxide precursors in mixed ethanol–ethylene glycol solvents in the presence of various compounds of the dopants; ethylene glycol was used to control particle size (10–20 nm). The materials so-formed were fairly photoactive in the wavelength range 400–700 nm (*e.g.*, with 2% Cu the sample absorbed light up to 480 nm).[122]

2.2.4 Metal-loaded metal oxides. Loading metal particle co-catalysts onto a metal-oxide photocatalyst often results in increased charge separation and, as a consequence, in a significant improvement of the efficiency of hydrogen generation. Highly-active noble metal-supported photocatalysts have been prepared by photo-electrodeposition upon irradiating TiO_2 samples in an

aqueous solution of noble metal precursors (including Au, Ag, Ir, or Ru). Interestingly, Pt-loaded titania exhibited a high initial hydrogen generation rate and maintained a high efficiency for several hours (>70 hours) upon UV irradiation of a methanolic aqueous suspension, although at longer times H_2 evolution rapidly decreased owing to loss of the sacrificial electron donor (methanol) during the process.[123]

Recently, Feng and co-workers[55] prepared not less than 10 different platinum-loaded TiO_2 photocatalysts (0.05 to 2 wt% Pt by photodeposition) from P25 titania as the precursor. The samples were subjected to various heat treatments at temperatures from 400 to 900 °C for periods of 0.5 to 72 hours, with the best TiO_2 material (containing 70–80 weight% rutile) prepared by calcination of P25 at 700 °C for 3 hours and subsequently submitted to the platinization process. The obtained photocatalysts were then used in reforming biomass (glucose and glycerol were the model sacrificial substrates) that caused significant evolution of hydrogen and very little CO relative to pristine P25 titania: for P25 TiO_2, the hydrogen evolution rate was 1.49 mmol h^{-1} g^{-1} and the quantity of CO formed (undesired in an industrial environment) was 6390 ppm. As for the Pt-loaded TiO_2s, the rate of evolution of H_2 ranged from 4.18 to 7.38 mmol h^{-1} g^{-1}, while the amount of CO evolved ranged from less than 5 ppm to a maximum of 248 ppm.[55] Clearly, the prepared photocatalysts were about 3 to 5 times more efficient in generating hydrogen. Analogously, a United States patent allotted to Chung and co-workers[56] reported the preparation of TiO_2-based photocatalysts by hydrolyzing titanium alkoxide precursors, which yielded colloidal sols into which were then added various metal salts ($AgNO_3$, H_2PtCl_6, or $LaNO_3$) affording a ''pulp'' that was subsequently subjected to thermal treatment at temperatures varying from 130 to 300 °C for 10 to 24 hours and then cooled (particle size: 5 to 150 nm). Exposure of the Pt/TiO_2 photocatalyst (0.5 g) to UV irradiation (400 W Hg light source; 12 hours) in an ethanolic aqueous suspension caused the evolution of hydrogen gas (rate, 7.7 μmol h^{-1} g^{-1}) in the presence of the sacrificial electron donor ethanol. A look at Table 2 shows that under these conditions the prepared platinized titania material was twofold more efficient *vis-à-vis* the platinized P25 titania under the same conditions (note that under the conditions used the pristine P25 TiO_2 evolved no hydrogen).[56]

Photoactive materials have also been prepared by placing a catalyst layer, typically TiO_2, on a support followed by addition of metal nanoparticles prepared by a hydrothermal treatment, yielding semiconductor grains with metal particles loaded on the surface of the metal oxide (*e.g.*, Ag/TiO_2).[124]

Table 2 Photocatalytic activity of various TiO_2 based photocatalysts in hydrogen evolution from the photodecomposition of water in the presence of a sacrificial electron donor (ethanol)[56]

Catalyst	Solution volume and composition	Hydrogen yield (μmol h^{-1} g^{-1})
(3 wt%)Pt/TiO_2	600 mL (H_2O + 0.57 M EtOH)	7.7
(3 wt%)Pt/P25 TiO_2	600 mL (H_2O + 0.57 M EtOH)	3.8
P25 TiO_2	600 mL (H_2O + 0.57 M EtOH)	0

A titania microsphere array (anatase, 100–300 nm diameter particles), prepared by a two-step template method and loaded with platinum by immersion in a chloroplatinic acid solution and then subjected to a reduction process with H_2, absorbed well into the visible wavelength region.[125] The photoactivity was ascertained by the degradation of the rhodamine dye, a practice that is not recommended because the dye absorbs much of the light in the visible spectral region. A photolysis sedimentation method followed by an impregnation–drying–calcination scheme was used by Li *et al.*[126] to obtain a Pt,F-loaded TiO_2 photocatalyst. Irradiation of an aqueous suspension of the resulting material in the presence of tetrachlorophenol (the sacrificial donor) led to the latter's degradation and to significant, though unspecified amounts of hydrogen. A similar behavior has been observed when using a TiO_2 photocatalyst loaded with Pt and PO_4^{3-} anions on the surface.[127]

Sunlight-sensitive TiO_2 particles loaded with iron or tungsten deposits have been prepared by treating pristine titania particulates in a hydrogen plasma in the presence of ferric nitrate or tungstic acid.[128]

Multi-dimensional structures offer another route to improve catalytic performance. For instance, it appears that in the case of Au/Ga_2O_3, Ag/Ga_2O_3, Ni/Ga_2O_3, Ni/TiO_2 and Pt/ZnO, the organized system had a large effect. Structures such as spherical or zero-dimensional nanoparticles have a capability for H_2 production of 250 mmol h^{-1} g^{-1}, whereas for one-dimensional nanowires the evolution rate was up to 500 mmol h^{-1} g^{-1}. With two dimensional nanosheets the rate was 800 mmol h^{-1} g^{-1}, while for three-dimensional gyroids the rate was up to 7000 mmol h^{-1} g^{-1}.[129] A stable and non-toxic system consisting of nanometer-sized Fe particles loaded onto TiO_2 was obtained from a titanium dioxide–ferric oxide gel subsequent to reduction of the latter oxide by hydrogen at 350–500 °C. The presence of nanosized iron deposits on the metal oxide made it possible to recover the catalyst by an iron magnet after each use.[130]

2.2.5 Mixed metal-oxide photocatalysts. Titanate derivatives have been exploited extensively in carrying out photocatalyzed processes. Methods for the preparation of these materials have included, among others, flame spray pyrolysis, which in a patent was used to prepare the highly porous $SrTiO_3$.[131] This photocatalyst, prepared at high temperatures using a solid-phase method (1000–1250 °C; $SrCO_3$ and TiO_2), gave a modest performance in the formation of H_2 by irradiating a methanolic aqueous solution (10 vol% methanol; 300 W xenon light source; $\lambda > 440$ nm) in the presence of 0.5 weight% Pt loaded onto the $SrTiO_3$ photocatalyst (band-gap, 3.2 eV) surface. This was improved, however, by doping it with either Rh (0.1 to 3.0 weight%) or Ir (0.05 to 0.5 weight%). The 1.0 wt% Rh-doped system evolved H_2 at 126 μmol h^{-1} g^{-1}, while the best rate for the Ir-doped system was 37.3 μmol h^{-1} g^{-1} (0.3 weight% Ir).[132] In the presence of a sacrificial electron acceptor, some O_2 could also be evolved under similar conditions (6 μmol h^{-1} g^{-1} for 0.1 wt% Ir-doped $SrTiO_3$). Analogously, efforts to increase the photoactivity in the decomposition of water by the RuO_2/$BaTi_4O_9$ photocatalyst were reported.[133] $BaTiO_3$ was prepared by a solid-phase method by firing titania and barium carbonate

in air. The resulting material was subsequently doped either with Ru (from co-firing with RuO_2) or with Ir (IrO_2), Ta (Ta_2O_5) or La. The photoactivity of (1 weight%)$RuO_2/Ba_{1-x}La_xTi_4O_9$ increased by 24% when $x = 0.1$, when compared to the $RuO_2/BaTi_4O_9$ photocatalyst. With the doped system, 46.4 μmol h^{-1} g^{-1} of H_2 and 23.2 μmol h^{-1} g^{-1} of O_2 were evolved, while for the undoped system 37.4 μmol h^{-1} g^{-1} H_2 and 18.2 μmol h^{-1} g^{-1} O_2 were evolved in what can appropriately be described as a water splitting process (400 W xenon lamp, 20 mL ultrapure water, 250 mg of photocatalyst). Note that the Ti constituent in the titanate could also be substituted in part by Hf and Zr.[133]

Irradiation of a suspension of $SrTiO_3$ in a solution containing Rh, Ru, Ir, Pd, Pt, Os, Re, or Co cations led to loading of the titanate onto the corresponding metals, thereby yielding highly photoactive materials for the water splitting process. The most efficient photocatalyst was the Rh-loaded $SrTiO_3$ that produced 28.0 μmol h^{-1} g^{-1} of H_2 and 14.1 μmol h^{-1} g^{-1} of O_2.[134]

2.3 Composite nanomaterials for hydrogen generation

Significant improvements of photocatalyst properties were obtained with phase separated materials, often using different metal oxides. Various approaches have been used to prepare such composites. For instance, semiconductor metal-oxide catalysts have been prepared by sputtering Fe_2O_3, TiO_2, Ta_2O_5 or WO_3 onto a support and then heating the thus formed film at 550–600 °C. The patent also describes a hydrogen generating apparatus for the photodecomposition of water using the semiconductor oxide films in the presence of an organic redox electrolyte.[135] Similarly, a hydrogen generating device (patented by Sharp Corporation) using photocatalytic films obtained by sputtering iron oxide on a support and then covering it with a layer of titanium oxide was reported.[136,137] Deposition of an organic template on the surface of a TiO_2 thin film followed by a layer of Cu_2O by magnetron sputtering and calcination in air of the material obtained resulted in an effective photocatalyst, the performance of which toward the sunlight-assisted decomposition of pure water and an aqueous solution containing electron donors to produce hydrogen was further improved by addition of Pt nanoparticles.[138] However, although the claim was made, no quantitative data for the production of H_2 were reported with or without the sacrificial electron donor. A nanocomposite powder with UV photocatalytic activity was prepared by vapor phase oxidation from mixed drops of Ti, Fe and V compounds using flame spray pyrolysis.[139]

Composite catalysts formed between graphene oxide and TiO_2, as well as with various other inorganic compounds (ZrO_2, MnO_2, CdS, ZnS, and others) have been prepared by ultrasonic treatment (20 min, 200 Watts) and UV-visible irradiation (400 W light source) for the photocatalytic production of H_2 from water under UV-visible irradiation. The composite formed by heating titania and graphene oxide (0.5 to 3.5 wt%) was active for the evolution of hydrogen from the photodecomposition of H_2S under irradiation by lamps with emissions similar to the solar spectrum. At the end of the process, 90% of the photoactivity of that of the fresh catalyst was regenerated by washing the system with organic solvents (CCl_4 or CS_2).[140] Composites such as graphene–TiO_2 (titania being self-doped with Ti^{3+}) could be prepared ultrasonically by using dispersed graphene oxide in water after vacuum activation at 300 °C. The active material was prepared from 0.05 g of the catalyst dispersed in 60 mL of 25 volume% methanol containing 0.5 mL of H_2PtCl_6 (1 g L^{-1}), followed by irradiation with a 300 W high pressure Hg lamp for 120 min. This led to the deposition of Pt on the catalyst surface. Subsequent irradiation of this system with visible light (Xe lamp, wavelengths >420 nm) produced H_2 from the photolysis of water.[141] Titania microspheres coated with graphene oxide were prepared by Liu *et al.*[142] and the resulting material had good perspectives toward industrial applications owing to convenience of operation, rapid synthesis, high efficiency, and low energy consumption. In a patent assigned to The Hydrogen Solar Production Company Limited, photocatalysts for producing hydrogen from the photodecomposition of water or aqueous solutions of organic compounds using light energy include carbon black (Printex-G or Printex-L) and a semiconducting photocatalytic material.[52] In one claim, the photocatalysts consisted of one or more of the metals or the corresponding metal oxides selected from Pt, Ir, Rh, Pd, Os, Ru, Ag, Ni (or a combination of two or more of them), which were deposited on light harvesting semiconductor materials selected from TiO_2, ZnO, $SrTiO_3$, $BaTiO_3$, WO_3, CdS, CdSe, Fe_2O_3, and ZnS (or a combination of two or more). In other claims, the photocatalysts further included a light harvesting semiconducting material with no deposit on it, selected from TiO_2, ZnO, $SrTiO_3$, $BaTiO_3$, WO_3, CdS, CdSe, Fe_2O_3, ZnS; these were doped with one or more of the elements selected from Nb, Fe, In, Ga, Li, P, Si, B.[52] One experiment involved 50 mg of the catalyst {19% Printex-G, 65% of TiO_2 and 16% of (5% RuO_2/TiO_2)} in 10 mL water and 0.2 mL white wine (*i.e.*, 0.13% ethanol). Irradiation with UV-visible light (sun lamp) led to the evolution of H_2 gas at a rate of 45 mmol h^{-1} g^{-1}.

A simple and environmentally-friendly method of synthesizing nanocomposites consists of impregnating titania nanotubes obtained by anodic oxidation of a titanium sheet in a copper sulfate solution. Photoreduction afforded the Cu_2O–TiO_2 composite catalyst that could be activated by visible light.[143] An invention by Zhang and Xiu described a process for enriching precious metals on abandoned printed circuit boards and synthesizing the highly reactive Cu_2O/TiO_2 nano-photocatalyst simultaneously. In the process, copper was selectively loaded on the surface of nano-TiO_2 in the form of Cu_2O and the resulting material was more active than the commercial P25 TiO_2 toward the degradation of a dye.[144] Low-cost catalysts based on TiO_2 containing Al_2O_3 and Cu_2O as co-catalysts were obtained by firing a mixture of the three oxides at temperatures in the range 200–1800 °C. UV-visible irradiation of aqueous suspensions of one of the catalysts in the presence of alcohols as the electron donors led to the evolution of unreported quantities of hydrogen.[145]

Visible light active composite titania coatings containing up to 20% silica nanoparticles and up to 10% nanoparticles of metals (Ag, Cu, Pt, Fe) or their corresponding oxides or sulfides have also been used as photocatalysts and are notable for their antibacterial effects.[146] By comparison, Ni nanoparticles loaded

onto TiO_2 nanotube composite arrays were prepared by anodic oxidation of a titanium foil followed by a pulsed electrodeposition procedure. The patent further claimed, though no specific data were provided, that these arrays can find application niches in super-capacitors as well as photocatalysts for hydrogen generation and as magnetic materials, among others.[147] A rather intriguing patent reported by Dasheng[148] described a hydrogen generating device and a method to produce a composite system constituted of nanoparticles of MoO_2, TiO_2 and MnO_2 supported on stainless steel meshes forming layers. Under UV irradiation and ultrasounds (28 kHz, 50 W) the device functioned as a high-yield, low-cost photocatalyst toward the production of hydrogen from water. As an example, from a water flow of 5 L h^{-1}, it is claimed that 401.5 mol h^{-1} of H_2 were produced.[148]

A recent Korean patent by Kim and Yoon[149] described the preparation of a hydrogen ion transport membrane formed using a porous thin film having a plurality of regularly aligned holes, a membrane for generating hydrogen, and a method for manufacturing the hydrogen ion transport membrane and the membrane for generating hydrogen. The membrane for the generation of hydrogen included a photocatalyst layer formed from various metal oxides, such as TiO_2, and anions that can absorb UV and/or visible radiation, such as titanates, niobates, and tantalates. Titania involved in a nanostructure that contained non-noble metals in galvanic contact with a noble metal (for example, TiO_2/Fe–Au/Au) performed better than pristine titania in the evolution of hydrogen in the photochemical electrolysis of water.[150] The synthesis of the catalyst composite was carried out by first performing a potentiostatic electrosynthesis of semiconducting TiO_2 and subsequently incorporating Au/Fe–Au multilayer nanowires onto the semiconductor surface. Such a nanostructure was more resistant to potential corrosion (up to 240 days) owing to the action of the non-noble (Fe) metal. The catalytic performance of the catalyst composite materials was assessed by using aqueous solutions of NaOH (0.05 M) and utilizing a photoelectrochemical cell with a quartz window. The Au–Fe/TiO_2 composite sitting on the stainless steel substrate was the working electrode (WE), a platinum mesh was the counterelectrode (CE), and an Ag/AgCI electrode was the reference electrode (RE) – see Fig. 10. Only the WE was UV-irradiated with a 10 W low-pressure Hg lamp.[150]

A silver bromide/titanium dioxide (P25) photocatalyst was reported recently in a Chinese patent by Tian and co-workers.[66] UV irradiation of the Ag/AgBr/TiO_2 composite catalyst resulted in a greatly improved hydrogen evolution from aqueous media, albeit in the presence of sodium formate or of sodium formate–methanol mixtures as the sacrificial electron donors. With a catalyst loading of 0.2 g in 250 mL containing 0.3 M of sodium formate the rate of hydrogen evolution was 143 μmol h^{-1} g^{-1}, some 9–10 times better than without the sacrificial agents, while with further addition of methanol (60 mL) the rate of H_2 evolution was 393 μmol h^{-1} g^{-1}, some 26 times better than in the absence of formate–methanol.[64]

Efficient evolution of hydrogen was also claimed in a patent that used titania nanospheres as photocatalysts prepared by

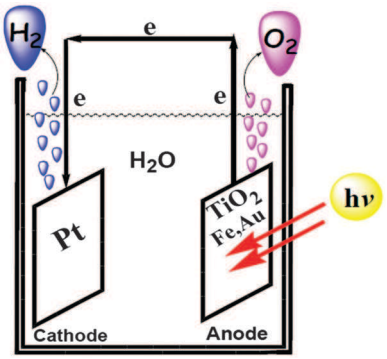

Fig. 10 Diagram of the photocatalytic electrolysis system in which the photocatalyst of the invention (see ref. 150) was utilized at the anode; also depicted is the electrochemical process operating in the system, in which water is split to form hydrogen gas at the Pt cathode and oxygen gas at the TiO_2/Fe–Au anode under UV irradiation.

hydrothermal reaction from various titanium compounds, followed by heating in a muffle furnace at 300–400 °C and subsequently spin-coated on the surface of F-SnO_2. A multi-layered TiO_2 semiconductor material was made by assembling, electrochemical deposition, and sintering at 200–500 °C for 0.5 to 2 hours to serve as a nano-anode electrode (Pt was the cathode) in the photoelectrochemical decomposition of water.[151] The maximal light efficiency to produce hydrogen from decomposition of water was 1.78%.

A simple method characterized by low energy consumption, a short preparation cycle, and facile industrial production has been patented for the preparation of carbon-coated anatase TiO_2 nano-composite powders. These were prepared through various steps that included heating (200–450 °C) TiO_2 in the presence of acetylene–argon or acetylene–argon–hydrogen gas mixtures; no attempts were made to ascertain its photoactivity under UV-visible radiation.[152] Reacting titanium alkoxides in water in the presence of oxidants (hydrogen peroxide) and alkyl amines (or pyridine derivatives) under an atmosphere of CO_2 in alcohol solvents led to a yellow-colored powder containing carbonate anions. This was followed by a heat treatment at 400 °C and produced a visible-light-responsive black titania anatase composite powder. The photoactivity of this material under UV-visible light was tested by methylene blue decomposition.[153] Composite titania nanotube photocatalysts have been prepared from the alkoxide precursors by a sol–gel method in alcohol solvents in the presence of metal salts (*e.g.*, nitrates and acetates of Ag and Cu) followed by drying, sintering and then reacting under pressure in the presence of NaOH.[53] Under visible light irradiation, these nanotube composites decomposed water, methanol, ethanol, aqueous methanol, aqueous ethanol or propanol to produce hydrogen at rates spanning from 0.01 to 0.5 mmol h^{-1} g^{-1}, while under UV irradiation the rates of hydrogen evolution ranged from 0.01 to 15 mmol h^{-1} g^{-1} of the catalyst.

Titania (92% rutile) photocatalysts containing a carbon nanotube and up to 3 wt% Ni were prepared by precipitation and calcination, followed by treatment in a hydrogen atmosphere.

Irradiation of the resulting catalyst with a 300 W high pressure arc in aqueous media containing 2 vol% MeOH (the sacrificial electron donor) produced hydrogen at a rate of 1.96 mol h^{-1} g^{-1}.[53] A carbon nanotube composite with highly crystallized porous monocrystalline TiO_2 (dimension: 40–60 nm) also displayed good photocatalytic activity toward the reduction of Cr(VI) compared with the commercial P25 TiO_2.[154] With the addition of the carbon nanotube, the composite material displayed good electron–hole separation efficiency and better reactive sites, and thus suitable in applied fields such as production of hydrogen from water photolysis, solar cells, bacterial inhibition, and pollutant remediation.

Calcination of a core–shell material consisting of a rutile TiO_2 single crystal core and a polyphenol shell yielded carbon-wrapped single crystal nanowire arrays, which when used as the working electrode in a photoelectrochemical cell for hydrogen production resulted in a light-induced water splitting efficiency of 2.38%, while for the TiO_2 nanowire arrays alone the efficiency was only about 0.15%. With the modified carbon coating the efficiency improved *ca.* 16 times.[155] Photocatalysts involving surface-modified composites based on silica-titania mixed oxides have also been reported that could include additional metal oxides or metals deposited on the surface (*e.g.*, Pd).[156]

A 2013 patent reported the preparation of micron-sized hollow spheres of titania containing other metal oxides (metal = Zn, Cr, *etc.*..) by using a simple, low cost, environmentally friendly process. The visible light activity of the resulting materials was ascertained by the decomposition of methyl orange (*ca.* 90% compared to P25 TiO_2).[157] Test results from a dye-sensitized solar cell assembly also showed that for the ZnO composite with the titania hollow spheres the battery open circuit voltage and short circuit current were significantly improved with conversion efficiencies by up to 3.56% compared to titania hollow spheres alone. A porous nanocomposite in the form of a powder (specific surface area, 75–150 cm^2 g^{-1}) consisting of hydroxyapatite (a basic calcium phosphate) and titania (ratio: 4 to 1) to be used as a photocatalyst was prepared by an ultrasonic method. No photoactivity data were given.[158] A composite comprising a metal organic framework (MIL-101) and TiO_2 was prepared for the specific purpose of carrying out the photocatalyzed water splitting process to generate hydrogen from the decomposition of water. Although the rate of H_2 production was 2.68 mmol h^{-1} g^{-1}, the dispersion also contained a sacrificial electron donor, and thus hydrogen did not evolve from water splitting.[63]

The composite of titania and attapulcite (a magnesium aluminum phyllosilicate occurring in clay soil in the Southern United States) displayed photoactivity when subjected to visible light irradiation. Further treatment with Fe^{3+} and Fe^{2+} ions gave a magnetic material that could easily be recovered after use.[159] The patent also claimed that the composite photocatalyst displayed a good visible light degradation effect, magnetism, and had good application prospects and economic benefits with regard to photocatalyst recycling.[159] The photoactivity was tested by the decomposition of methyl orange (>90% after 3 hours of irradiation). Platinum loaded onto Y-doped strontium zirconate–titania heterojunction compounds, such as Pt–$Sr(Zr_{1-x}Y_x)O_{3-\delta}$–$TiO_2$ ($0 \leq x \leq 1$; Y doping, 3–7 mol%; weight ratio of Sr salt to titania, 2 : 4 to 8 : 6; amount of Pt, 0.80–1.00 wt%), have been reported as photocatalysts. The rate of hydrogen generation from the photodecomposition of water in the presence of the sacrificial oxalic acid electron donor was up to 2.8 mmol h^{-1} g^{-1} (Fig. 11).[166] A non-TiO_2 composite system consisting of a polymer gel, a photocatalyst and a nanoscopic encapsulated hydrogenase enzyme (*e.g.*, from *Clostridium pasteurianum* or a hydrogenated mimic) produced hydrogen from the photodecomposition of water in the presence of electron donors (*e.g.*, metal sulfite, thiosulfate and dithionite). The system was not sensitive to O_2 poisoning, and maintained its photoactivity even when heated at 85 °C.[167]

2.4 Photocatalysts for CO_2 reduction: TiO_2 systems

One-electron reduction of CO_2 is a highly unfavorable process owing to the large kinetic *overvoltage* that results from the geometric change from a linear to a bent structure associated with the electron transfer process. By contrast, the proton-assisted multi-electron CO_2 reduction follows a much more favorable course. The reaction has been studied particularly in water, wherein the main product is often methanol. Important factors that affect the process are the concentration of CO_2 in solution, its adsorption on the photocatalyst and the

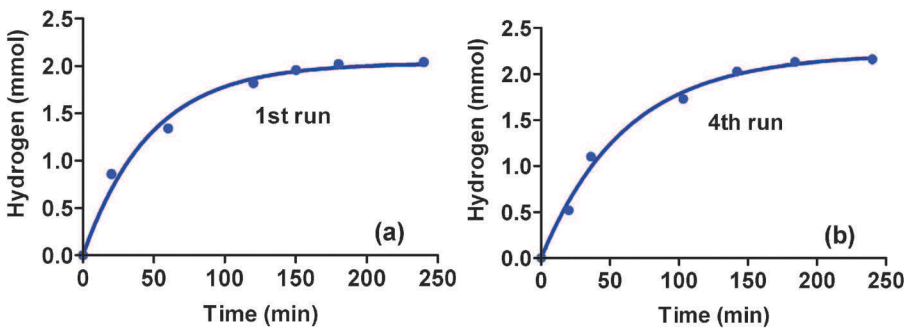

Fig. 11 Plots showing the stability of the photocatalyst over five runs and the formation of hydrogen from the photodecomposition of water in the presence of the Pt-loaded Y-doped strontium zirconate–titania heterojunction photocatalyst; oxalic acid was the sacrificial electron donor. For the 1st run, k = 0.021 ± 0.003 mmol min^{-1}, whereas for 4th run k = 0.016 ± 0.002 mmol min^{-1}. Adapted from the data of ref. 166.

Table 3 Photocatalytic reduction of CO_2 to carbon-based fuels[a]

Ref.	Photocatalyst	Medium/other species	Light source	Products (rates; mmol h^{-1} g^{-1})
162	Cu,Bi-co-doped TiO_2	Water	300 W, Xe >400 nm	CH_4 (0.673) CH_3OH (0.373) CH_3CH_2OH (0.055)
163	Pt/TiO_2;TiO_2/Fe_2O_3	Steam	20 W, Fluo	HCHO (0.0055)
164	$Cu(X\text{-bpy})_2/TiO_2$	Water	300 W, Xe	CH_4 (0.004)
165	$Ru/Cu_xAg_yIn_zZn_kS_j$	$NaHCO_3$, H_2, Na_2S, Na_2SO_3	1000 W, Xe	CH_3OH (0.185)
166	Ag/AgX (X = Cl, Br)	$NaHCO_3$	300 W, Xe	CH_3OH (4.6) CH_3CH_2OH (1.5)
167	Fe_3O_4@SiO_2–Ag/AgI	$NaHCO_3$	300 W, Xe	CH_3OH, EtOH, i-PrOH, (overall, 7 products)
168	Cu_2O/RuO_2	Water	Concentrated sunlight	CH_3OH (1.54) HCHO (0.52)
169	$NaNbO_3$ nanowires	Water, 0.4 mL	400 W, Hg	CH_4 (653 ppm)

[a] Power and lamps used whose emitted light impinged on the sample are indicated where available.

competitive reduction of water. Semiconductor oxides such as titania have received the largest attention with regard to this process (Table 3).[162–169]

A major breakthrough in the area of generating solar fuels, *e.g.* hydrogen, was achieved by coupling biomimetic carbonation with photocatalysis, an approach that could technically advance the efforts in solar fuel production that require a carbon neutral fuel such as hydrogen.[170] In addition to carbonates as end products during the biomimetic carbonation process, the production of hydrogen could make the process commercially viable and thus could be adopted by industries that emit significant quantities of carbon dioxide, as would be the case of cement producing industries. The carbonate rich stream was reduced photocatalytically to HCHO (0.0004 to 0.345 ppm). This method opens up a new route to sequester CO_2 and generates clean energy vectors such as hydrogen, methane and methanol. In fact, the patent by Rayalu and co-workers,[170] whose main goal was to produce hydrogen and syngas ($CO + H_2$), reported maximum hydrogen evolution up to *ca.* 101 μmol mg^{-1} in the presence of free carbonic anhydrase (CA, an enzyme used as a biocatalyst to increase the rate of hydration of CO_2), 156.8 μmol mg^{-1} with immobilized CA, and 6684.5 μmol mg^{-1} with stabilized CA in the presence of TiO_2/Zn/Pt as the photocatalyst. Either zinc metal and/or ethanol were used as the sacrificial electron donor systems.

Conversion of carbon dioxide to methanol or formaldehyde was also achieved with high conversion efficiency and selectivity using titania nanocrystals (>90% anatase) doped either with non-metal or metal-ion dopants (N, F, Fe^{3+}, Mo^{5+}, Ru^{3+}, Os^{3+}, Re^{5+}, V^{4+}, and Rh^{3+}) as the photocatalysts to effect the reduction of carbon dioxide saturated with water vapor.[171] A change of the hydrogen source in the feed stream led to different products. For instance, when H_2 gas was the hydrogen source, the observed primary product was either CH_4 or CO, whereas if H_2O was used, as much as 90% of the reduced product was CH_3OH. By contrast, a mixture of HCHO and formic acid was obtained when methanol was the source of hydrogen.[171] More intriguingly, irradiation of a Au-doped titania photocatalyst (particle diameter < 20 nm) led to the reductive dimerization of CO_2 to oxalic acid.[172]

A co-doped catalyst containing 0.2 to 3 mol% Cu and 0.5 to 5 mol% Bi, prepared by a hydrothermal reaction from TiO_2 nanoparticles of uniform dimensions, resulted in a material active in converting CO_2 to CH_3OH and CH_4 with a high light quantum efficiency as a result of the large surface area, the strong CO_2 adsorption capacity, and the high rate of sunlight utilization (Table 3).[162] In addition, a material that included the combination of a highly oxidizing photocatalyst (*e.g.*, TiO_2–CuO, or TiO_2–Fe_2O_3–CeO_2, or TiO_2–Fe_2O_3–Pt on the electroconductive CeO_2 substrate) coupled to a Pt/TiO_2 system, which acted as the reducing photocatalyst, selectively reduced a stream of CO_2 and water vapor to HCHO under UV irradiation.[173] Likewise, passing water and CO_2 through a microfluidic reactor having a microchannel coated with a Pt-loaded titanium oxide led to the reduction of CO_2 to CH_3OH,[174] whereas the anatase titanium–cobalt oxide catalyst $Ti_{1-x}Co_xO_{2-a}$ ($0.03 < x < 0.07$; $-0.1 < a < 0.1$) produced CO from CO_2 (photocatalyst patented from Nippon Telegraph and Telephone).[175] Heating titanium and cobalt mixed hydroxides at temperatures in the range 650–750 °C yielded the anatase-type metal-oxide catalyst $Ti_{1-x}Co_xO_{2-a}$ ($0.03 \leq x \leq 0.07$; $-0.1 \leq a \leq 0.1$) that could also reduce carbon dioxide.[176] Composite catalysts consist of a Pt loaded semiconductor ($K_2Ti_6O_{13}$) and a copper–zinc oxide-based carbon dioxide reducing catalyst. When exposed to sunlight the composite transformed a mixture of H_2O and CO_2 into the reduced products HCOOH, HCHO and CH_3OH.[177] Zhao and co-workers[178] described a device involving UV-active rare earth-loaded titania systems, Cu-loaded titania, and $InTaO_4$ to reduce CO_2 in flue gas into an oxygen-enriched combustion power plant, whose purpose was to carry out the reduction of CO_2 to methanol and other organics. Rare-earth titanias were preferred because of their visible-light activity.

A composite with graphene was used in a heterojunction with a surface photocatalytic material that consisted of a graphene layer film with a semiconductor photocatalyst film wrapped around the graphene layer; irradiation of the photocatalyst in the presence of a 10 vol% aqueous solution of triethanolamine and methanol led to the formation of hydrogen.[179] A noble metal co-catalyst loaded onto a titanium composite oxide support has also been used in the reduction of CO_2.[180] A three-phase photocatalyst system consisting

of titania and/or silica, a metallo-phthalocyanine and NaOH has been used to reduce CO_2 photocatalytically upon irradiation with visible light in conjunction with ultrasounds (100 W; 50 kHz); after an 8 hour treatment, the reduction led to the formation of formic acid (199.2 μmol h^{-1} g^{-1} of catalyst), formaldehyde (8.46 μmol h^{-1} g^{-1}), and methanol (3.86 μmol h^{-1} g^{-1}).[181] Quartz glass powders carrying TiO_2 adhered on perfluoroethylene propylene resin and gave a composite that produced MeOH from the reduction of carbon dioxide upon UV irradiation.[182] The reduction of a mixture of carbon dioxide and water – as the hydrogen source – to formic acid, formaldehyde and methanol with a light-active material comprising selected transition metal oxides and sulfides and titanates of earth-alkaline metals was reported as long ago as 1984 by Aurian-Blajeni and co-workers.[168] A boron-doped graphene nanosheet was prepared by vacuum reduction of graphene oxide combined with ultrasounds, following which a composite with P25 TiO_2 was ultrasonically dispersed in water and then used in the sunlight-induced (300 W Xe lamp to simulate sunlight) reduction of carbon dioxide in the presence of Na_2SO_3 as the electron donor (hole scavenger) to yield methane. The B-doped graphene–TiO_2 displayed significantly greater activity than either the graphene or the graphene-oxide composite TiO_2 photocatalysts.[183]

The copper(I) 2,2′-dipyridyl complex, $Cu(NN)_2PF_6$ (see Fig. 12), was prepared by reacting $Cu(MeCN)_4PF_6$ with the bipyridine (NN) ligands at a molar ratio of 1 : 2 in dichloromethane and methanol. The complex was subsequently combined with TiO_2 to yield a composite that was used as the photocatalyst in the visible-light photocatalyzed reduction of carbon dioxide to methane.[164] As illustrated in Fig. 12, the quantity of methane formed in the absence of the semiconductor TiO_2 catalyst was negligible by comparison. A photocatalytic process comprising the reaction of carbon dioxide and water by a composite capable of chemisorbing carbon dioxide and UV/visible-light irradiation at wavelengths from 200 nm to 700 nm produced methanol and other oxygenated fuels. The photocatalytic materials consisted of nanoparticles of titania, ceria, titanates and the hydrotalcites, $Mg_6Al_2(CO_3)(OH)_{16}{\cdot}4H_2O$.[184]

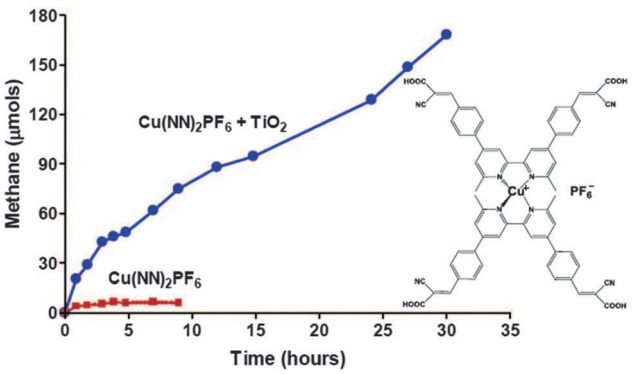

Fig. 12 Formation of methane from the photocatalyzed reduction of carbon dioxide by the visible-light irradiated composite consisting of TiO_2 and the $Cu(NN)_2PF_6$ complex. Adapted from the data given in ref. 164.

3. Photocatalysts for hydrogen generation and CO_2 reduction: group 5 oxides

3.1 Undoped, doped, and mixed oxides for hydrogen generation

The vanadates MVO_4 with M = Y or one of the lanthanides (La, Ce, Pr, Nd, Pm, Sm, Eu, Gd, Tb, Dy, Ho, Er, Tm, Yb, and Lu) possessing a zircon-type structure are, in some cases (see *e.g.*, Table 4[130,160,161,185–207]), active for water splitting under UV and/or visible light irradiation. These materials may include one or more further component, such as a metal or an oxide chosen among Pt, Ni, NiO_{0-1}, IrO_2, and RuO_2 as an auxiliary catalyst.[208] Many of these catalyst materials absorb light in the visible spectral region; for example, YVO_4 absorbed up to *ca.* 600 nm (estimated band-gap, 2.1 eV). Irradiation of the platinized (0.1 wt%)RuO_2/YVO_4 system (loading, 1 g) in 370 mL of water with a 400 W high-pressure Hg lamp yielded both hydrogen and oxygen. The rate for H_2 evolution was 150 μmol h^{-1} g^{-1}, while the rate for O_2 evolution was 75 μmol h^{-1} g^{-1}. In the absence of RuO_2 and Pt only H_2 was detected, while for the NiO_x/YVO_4 system efficient formation of hydrogen (1500 μmol h^{-1} g^{-1}) required the presence of a sacrificial electron donor (methanol).[208]

A series of monocrystalline powders and films of catalyst materials with formula $Bi_2La_xV_{1.6-0.6x}O_7$ or $Bi_2Y_xV_{1.6-0.6x}O_8$ ($0.8 \leq x \leq 1$), or a film of $Bi_2La_xV_{1.6-0.6x}O_7$ or $Bi_2Y_xV_{1.6-0.6x}O_8$ ($0.8 \leq x \leq 1$) doped with N or S has been prepared from the oxides Bi_2O_3, V_2O_5, La_2O_3 or Y_2O_3 by a high-temperature solid phase method. Their applicability in the water splitting process (*no* sacrificial agents) has been studied. The undoped and doped composite films were prepared using either high-vacuum ion-sputtering or magnetron-sputtering the catalyst target in oxygen, ammonia or a SO_2–Ar mixture.[209]

Irradiation of $Bi_2La_xV_{1.6-0.6x}O_7$ ($0.8 \leq x \leq 1$) powder (1 g) in 300 mL pure water (300 W Xe lamp, $\lambda > 420$ nm or 400 W high-pressure Hg lamp, $\lambda > 390$ nm) yielded 18.2 μmol h^{-1} g^{-1} of H_2 and 9.2 μmol h^{-1} g^{-1} of O_2 (Xe lamp); with the Hg lamp the yields were 50.8 μmol h^{-1} g^{-1} and 25.4 μmol h^{-1} g^{-1}, respectively.[209] Under similar conditions, but with the $Bi_2Y_xV_{1.6-0.6x}O_8$ powdered catalyst, the yields of H_2 and O_2 were 12.6 μmol h^{-1} g^{-1} and 8.3 μmol h^{-1} g^{-1}, respectively, under Xe lamp irradiation, whereas under Hg light irradiation the yields were 40.7 μmol h^{-1} g^{-1} and 20.7 μmol h^{-1} g^{-1}. By contrast, in the presence of methanol (50 mL methanol and 300 mL of water), irradiation of the composite catalyst (0.2 wt%)$Pt/Bi_2Y_xV_{1.6-0.6x}O_8$ ($0.8 \leq x \leq 1$) with the 400 W Hg light source yielded, after 14 hours, 403 μmol h^{-1} g^{-1} of H_2, whereas with the composite (1.0 weight%)$NiO/Bi_2Y_xV_{1.6-0.6x}O_8$ ($0.8 \leq x \leq 1$) the yield of H_2 was 298 μmol h^{-1} g^{-1} and with the composite (1.0 weight%)$RuO_2/Bi_2Y_xV_{1.6-0.6x}O_8$ the yield of hydrogen was only 124 μmol h^{-1} g^{-1}.[209]

Tantalum-based hollow nano-photocatalytic materials were prepared in a high pressure reactor followed by a nitriding heat treatment in the presence of ammonia. The hydrothermal approach gave urchin-like shaped particles with visible

Table 4 Various photocatalysts used for the generation of hydrogen with and without the presence of sacrificial electron donors

Ref.	Catalytic systems	Solution	Light sources[a]	Hydrogen production rate (mmol h^{-1} g^{-1})
185	[Bis(tetramethylammonium)Zn dithiolene]	THF–H_2O	125 W, Hg	0.93
186	$CH_3C_5H_4Mn(CO)_3$	H_2O-cellosolve 1–3 $NaHCO_3$	100 W, Hg	70.7
187	(0.1 wt%)$Pt/In_{0.9}Ni_{0.1}TaO_4$	MeOH–H_2O	300 W, Xe	0.30
188	$RuO_2/K_4Ce_2Nb_{10}O_{30}$	Na_2SO_3	300 W,	0.67
		Water	Xe >420 nm	0.071
189	(0.5 wt%)$Ni/LaTaO_4$	Water	450 W, Hg	3.25
190	$InVO_4$	Water	500 W, Halogen	1480
161	Pt-Hsp protein cages composites	MV^{2+}, 0.5 mM; Ru(bipy), 0.2 mM; EDTA, 200 mM; pH = 5	150 W, Xe	1.34
161	*C. pasteurianum hydrogenases*	Water, pH = 8	150 W, Xe	7.58
191	$BaCsFeWO_6$	MeOH–H_2O	400 W, Xe	0.135
192	$Ni/La_2O_2CO_3$	CO_2 saturated water	125 W, Hg	Up to 1.28
193	$BaRbFeMoO_6$	MeOH–H_2O	400 W, Xe	0.0725
194	ZnO	H_2S	500 W, Xe	Up to 2.90
195	(1.5 wt%)RuO_2/(0.5 wt%)$Pt/BiYV_2O_8$	Water	300 W, Xe (>420 nm)	0.079
196	$Ti_2La_xBi_{2-x}O_7$ ($0.7 < x < 1$)	Water	400 W, Hg	1.22
197	$Bi_2Al_xV_{(1.6-0.6x)}O_7$ ($0.8 < x < 1$)	Water	400 W, Hg	1.31
198	(1 wt%)$RuO_2/(KTaO_3)_{0.5}(LaCoO_3)_{0.5}$	MeOH–H_2O	250 W, Hg (>420 nm)	3.99
199	$CuY_{0.08}Fe_{1.92}O_4/CuCo_2O_4$	$H_2C_2O_4$	—	2.77
160	(1.0 wt%)Pt/Y-doped $SrZrO_3/TiO_2$	$H_2C_2O_4$	250 W, Hg	2.8
200	(0.2 wt%)$Pt/Cd_2Ta_2O_7$	MeOH–H_2O	300 W, Hg	8.23
201	Eosin Y/MWNTs/CuO/NiO (CuO : NiO, 1 : 1)	TEOA (15 $vol\%_{aq}$)	1000 W, tungsten	0.852
202	$H_2PtCl_6/K_8Na_8H_4$ $[P_8W_6Ta_{12}(H_2O)_4(OH)_8O_{236}]\cdot 42N_2O$	HCl, MeOH–H_2O	250 W, Hg	1.25
203	(1.5 wt%)$Pt/KNbO_3$	MeOH–H_2O	300 W, Hg	4.21
204	$CuAl_2O_4$/grapheme	$H_2C_2O_4$	150 W, Xe	5.2
205	$SnO_x/LaCO_3OH$	Water	—	0.289
206	(0.2 wt%)Pt/Gd_2ErSbO_7	MeOH–H_2O	400 W, Hg	0.267
207	(0.5 wt%)ZnO/cementitious polymer	Na_2S–Na_2SO_3	300 W, Xe	8.03
129	Au/Ca_2O_3,Ag/Ga_2O_3,Ni/Ga_2O_3, Ni/TiO_2, Pt/ZnO	Water	300 W, Xe	Up to 7

[a] Lamp used as well as the flux impinging on the sample indicated when available.

light response.[210] Irradiation of the resulting material (300 W Xe lamp; 200 mL water; catalyst loading, 0.05 g L^{-1} to 2 g L^{-1}) produced H_2, albeit in the presence of the electron donor Na_2SO_3 (efficiency of water decomposition, 9.5%), whereas in the presence of sacrificial electron acceptors such as $AgNO_3$ or La_2O_3 irradiation of the catalyst suspension yielded O_2 with an efficiency of *ca.* 60%. Mixing indium and tantalum oxide sols, and allowing the formation of a gel then followed by a thermal treatment gave the catalyst $InTaO_3$; UV irradiation of an ethanolic aqueous dispersion of this catalyst yielded 370 μmol h^{-1} of hydrogen.[211] Composite photocatalysts responsive to visible light of the type $In_{1-x}M_xAO_4$ (A = V, Nb or Ta; M = Cr, Mn, Fe, Co, Ni, Cu, and Zn; $0 < x < 1$) have been prepared by a solid state reaction of the oxides and the surface of the particulates has been modified by loading with noble metals (*e.g.*, Pt, Pd) or with transition metal oxides (*e.g.* NiO, IrO_2 or RuO_2).[211]

Table 5 summarizes the rates/yields of the evolution of hydrogen and oxygen from the water splitting process on irradiation of some catalyst systems at wavelengths >420 nm (300 W Xe lamp; catalyst loading, 0.5 g in 250 mL water) in the absence of any sacrificial agent.[187] In the presence of methanol (50 mL; 240 mL water), however, and under the same irradiation conditions, illumination of 0.5 g of the (0.1 weight%)$Pt/In_{0.9}Ni_{0.1}TaO_4$ system yielded 292 μmol h^{-1} g^{-1} of hydrogen (see also Table 5), whereas irradiation (400 W Hg light source) of the platinized (1 wt%) systems $Pt/In_{0.8}Cu_{0.2}TaO_4$ and $Pt/In_{0.8}Fe_{0.2}TaO_4$ produced hydrogen at, respectively, 200 μmol h^{-1} g^{-1} and 160 μmol h^{-1} g^{-1}. The catalysts $A_cM_pO_n$ (A = K, Na, Ca; M = Nb, Zr, V) were loaded with a co-catalyst prepared from Rh, Ir, and Pd, and then examined for the production of hydrogen.[212]

Table 5 Rates of the evolution of hydrogen and oxygen from the water splitting process in the absence of any sacrificial agents for various catalyst systems[187]

Catalyst systems	Co-catalyst	X	Rates (μmol h^{-1} g^{-1})	
			H_2	O_2
$In_{1-x}Ni_xTaO_4$	NiO_x	0.05	8.4	4.2
$In_{1-x}Ni_xTaO_4$	NiO_x	0.1	34.0	16.2
$In_{1-x}Ni_xTaO_4$	NiO_x	0.15	16.6	8.2
$In_{1-x}Ni_xTaO_4$	RuO_2	0.05	17.4	8.6
$In_{1-x}Ni_xTaO_4$	RuO_2	0.1	9.6	4.6
$InTaO_4$	NiO_x	—	6.4	2.2
$InTaO_4$	RuO_2		1.6	0.8
TiO_2	Pt		Trace	0

$InVO_4$ prepared from In_2O_3 and V_2O_5 by a solid state reaction and loaded with NiO (0.3–2.0 weight%) becomes an efficient photocatalyst for water splitting. In every case, the expected ratio of 2 hydrogen to 1 oxygen was observed in terms of mmol per gram of the catalyst after 2 hours of irradiation with a 500 W halogen lamp.[213] For instance, irradiation of the (0.3 weight%) $NiO/InVO_4$ system with a 250 W halogen lamp produced 750 μmol h^{-1} g^{-1} of hydrogen at a temperature from ambient to 58 °C. In comparison, irradiation of $InVO_4$ alone with a 500 W halogen lamp (50 mL water; T = 25–60 °C) produced

633 mmol h^{-1} g^{-1} of H_2 and 317 mmol h^{-1} g^{-1} of O_2; the largest quantities of gases obtained after 2 hours of irradiation were achieved with the (1.0 weight%) $NiO/InVO_4$ catalyst under similar conditions, that is 896 mmol h^{-1} g^{-1} and 448 mmol h^{-1} g^{-1} of the catalyst for hydrogen and oxygen, respectively.[213]

Strontium niobate catalysts, Sr_xNbO_3 ($0.8 < x < 0.9$), absorb in the visible and display low energy band-gaps (down to 1.84 eV).[214] The preparation of cadmium tantalate ($Cd_2Ta_2O_7$) was carried out by a sol–gel method in absolute ethanol in the presence of PEG 6000 as the dispersing agent; energy band structure and state density calculations showed that the valence band of the photocatalyst was mainly formed by oxygen 2p orbitals, while the conduction band was formed by the Ta 5d, O 2p and Cd 5s5p hybrid orbitals. This explained the low band-gap and the enhanced photocatalytic activity of $Cd_2Ta_2O_7$.[200] Thus, nanometer-sized $Cd_2Ta_2O_7$ loaded with Pt (0.2 weight%) and irradiated in methanol–water produced 8.23 mmol h^{-1} g^{-1} of hydrogen with a quantum yield of *ca.* 17% and an energy conversion efficiency of *ca.* 6%; when loaded with 0.2 wt% NiO, the quantity of hydrogen evolved was 0.57 mmol h^{-1} g^{-1}; the quantum yield was *ca*. 1.2% and the energy conversion efficiency was 0.43%.[215]

The catalyst $Sr_2Ta_2O_7$ is apparently photoactive under visible light, with an efficiency of *ca.* 5.8%.[216] Similarly, when composite oxides such as $SrNb_2O_6$ were submitted to alternate sulfuration and oxidation cycles, a SO_2 containing Nb compound that was claimed to be photocatalytically active in the visible was formed (photoactivity, *ca.* 7.5%).[217] The materials $K_4Ce_2M_{10}O_{30}$ (M = Ta or Nb) have a tungsten–bronze-type structure and a band-gap energy in the range 1.8–2.2 eV, which places their light absorption between 580 nm and 690 nm. The conduction band involves hybridization between Ta 5d or Nb 4d and Ce 4f orbitals, whereas the valence band involves O 2p and Ce 4f orbitals.[218] Loading these mixed metal oxides with Pt, RuO_2 or NiO_x increased their photocatalytic activity toward the photolysis of water to produce hydrogen (in the presence of Na_2SO_3 as the electron donor). Irradiation of $K_4Ce_2Ta_{10}O_{30}$ in aqueous media with a 300 W xenon lamp at $\lambda > 420$ nm in the presence of the Pt co-catalyst or the electron donor Na_2SO_3 produced hydrogen at 423.8 μmol h^{-1} g^{-1} and 602.3 μmol h^{-1} g^{-1} of the catalyst, respectively, whereas at $\lambda < 420$ nm the yields of H_2 were 33.7 and 56.3 μmol h^{-1} g^{-1}. With 0.5 wt% Pt or in the presence of Na_2SO_3, visible light illumination (>420 nm) of $K_4Ce_2Nb_{10}O_{30}$ produced hydrogen at 85.7 and 461.1 μmol h^{-1} g^{-1}, respectively, while <420 nm the corresponding yields were 5.0 and 13.9 μmol h^{-1} g^{-1}.[218] By comparison, with 0.1 g RuO_2 as the co-catalyst or in the presence of an electron donor, illumination of $K_4Ce_2Ta_{10}O_{30}$ at wavelengths >420 nm yielded hydrogen at 189.7 and 1040.3 μmol h^{-1} g^{-1}, respectively. Below 420 nm, the yields of H_2 were significantly lower (2.6 and 11.9 μmol h^{-1} g^{-1}). For the niobium analogue, $K_4Ce_2Nb_{10}O_{30}$, the yields of H_2 were 70.6 and 672.3 μmol h^{-1} g^{-1} upon illumination at $\lambda > 420$ nm, and significantly lower upon illumination in the UV region (1.8 and 2.7 μmol h^{-1} g^{-1}). When both RuO_2 and Pt were present, the quantities of hydrogen produced were 497.7 and 93.5 μmol h^{-1} g^{-1}, respectively, for the $K_4Ce_2Ta_{10}O_{30}$ and $K_4Ce_2Nb_{10}O_{30}$ systems upon irradiation at wavelengths greater than 420 nm.[218]

The functional niobate $K_4Nb_2O_{17}$, prepared directly from inexpensive Nb oxide–hydroxide and spin-coated to form a thin film (100 nm), displayed good photocatalytic hydrogen production ability from the photodecomposition of water (0.0483 mL cm^{-2} min^{-1}; amount of saturated hydrogen, 9.7 mL cm^{-2}); no evolution of oxygen was reported.[219] The visible-light responsive mixed oxides $Ti_2La_xBi_{2-x}O_7$ ($0.7 \leq x \leq 1$; band-gap, 2.68 eV) or $Bi_2Sn_xTi_{2-x}O_7$ ($0.7 \leq x \leq 1$; band-gap, 2.43 eV) with *ca.* 2 atom% N or S-doping were likewise effective photocatalysts toward the generation of hydrogen from the water splitting process: evolution of both H_2 and O_2 was observed (300 W xenon lamp; >420 nm or 400 W Hg lamp; >390 nm).[220] Rates of H_2 and O_2 evolution for the $Ti_2La_xBi_{2-x}O_7$ photocatalyst were 439 and 220 μmol, respectively, whereas with the Hg light source the quantities were 18.3 and 9.16 μmol h^{-1} g^{-1}, respectively. For the $Bi_2Sn_xTi_{2-x}O_7$ the rates of H_2 and O_2 observed were 18.4 and 9.91 μmol h^{-1} g^{-1} (Xe lamp), while under Hg light irradiation the quantities were, respectively, 54.5 and 26.3 μmol h^{-1} g^{-1}.[220] The powders were prepared by a multistep procedure including mixing and grinding Bi_2O_3, TiO_2 and La_2O_3 or SnO_2, baking at *ca.* 200 °C, pressing, sintering at 750 °C and then pulverizing. Perovskite-type structures of the type $CsLaSrNb_2MnO_9$ have an optical band-gap that can be continuously tuned by changing the composition.[221] Similarly, the perovskite $H_{1.9}K_{0.3}La_{0.5}Bi_{0.1}Ta_2O_7$ prepared from the $K_{0.5}La_{0.5}Ba_2Ta_2O_9$ precursor was active under visible light. The preparation proposed by Nikon Corporation involved the treatment of Ta, K, La and Bi salts with methanol, citric acid and ethylene glycol at *ca.* 130–135 °C. Roasting of the resulting gel gave the $K_{0.5}La_{0.5}Ba_2Ta_2O_9$ precursor which upon acidification with HCl afforded the desired perovskite.[222]

A photocatalytic system that comprised an early transition metal (d^0 configuration; *e.g.*, Ta^{5+}, Nb^{5+}, Ti^{4+}, or W^+) octahedral-based structure was improved by including a late transition metal (d^6; *e.g.*, Co^{3+}, Fe^{2+}, Ru^{2+}, Os^{2+}, Rh^{3+}, Ir^{3+}, Pd^{4+}, or Pt^{4+}). This yielded a solid solution, so that a larger fraction of the visible light was absorbed by the photocatalyst.[198] For instance, the reaction between lanthanum cobalt trioxide and tantalum oxide and sodium carbonate at 1100 °C gave sodium tantalum oxide/lanthanum cobalt oxide, an effective catalyst for water splitting. Hydrogen was produced at relatively high reaction rates of (>0.5–1.0 mmol h^{-1} g^{-1}) in most cases with a turnover of *ca.* 100 (moles of H_2/moles of compound). The photocatalytic reaction continued unabated for >48 hours in the case of $(KTaO_3)_{1-x}(LaCoO_3)_x$ ($x = 0.5$) loaded with 1 wt% RuO_2. Typically, the photocatalytic production of hydrogen was a factor of ten greater in CH_3OH–H_2O media *versus* pure H_2O, with the highest rate being 10.21 mmol H_2 h^{-1} g^{-1} in the first 2–3 hours for the $(NaTaO_3)_{1-x}(LaCoO_3)_x$ ($x = 0.5$) loaded with 1 wt% RuO_2 – the patent is silent as to the generation of oxygen however.[198] Analogously, solid solutions of $Bi_xM_{2-x}V_2O_8$ (M = Y, La, Ce, Pr, Nd and Sm; $0 < x < 2$) have been prepared with the ratio of the component atoms (Bi + M):V:O = 1:1:4. It was claimed that the material could photocatalyze the decomposition of water

under UV/visible irradiation at wavelengths <600 nm, particularly when the materials were loaded with co-catalysts such as Pt, RuO_2 and NiO_x ($0 < x < 1$).[223] As an example, $BiYV_2O_8$ was obtained from a solution of $Bi(NO_3)_3{\cdot}3.5H_2O$, Y_2O_3 and NH_4VO_3 in ethanol; after drying and grinding, the residue was heated at 800 °C and then at 900 °C. When 0.4 g of $Bi_{0.1}Ce_{1.9}V_2O_8$ was loaded with 0.5 wt% Pt as the co-catalyst, dispersed in 150 mL of water, and then irradiated at $\lambda > 420$ nm (300 W xenon light source) it produced both H_2 and O_2 at rates of 44 μmol h^{-1} g^{-1} and 21.8 μmol h^{-1} g^{-1}, respectively. Irradiation at wavelengths below 420 nm (UV), but otherwise under similar conditions, produced 6.3 μmol h^{-1} g^{-1} of hydrogen and 2.0 μmol h^{-1} g^{-1} of oxygen.[223]

3.2 Composite photocatalysts for hydrogen generation

An efficient ternary multilayer core–shell composite photocatalyst including a wide band-gap semiconductor oxide such as TiO_2, ZnO, $SrTiO_3$ and $CaTiO_3$ as the shell layer and both n-type (CdO, WO_3) and p-type (Cu_2O, CoO, or $CuMO_2$; M = Al, Fe or Cr) narrow band-gap semiconductor oxides as the heterogeneous composite core layer photocatalyzed the decomposition of water to generate hydrogen. Upon irradiation of 0.5 g of the platinized TiO_2/WO_3–$CuAlO_2$ photocatalyst (using 800 mL deionized water; 0.5 g Na_2CO_3; pH = 11; 300 W xenon lamp) the system produced H_2 and O_2 at a rate of 646 μmol h^{-1} g^{-1} and 282 μmol h^{-1} g^{-1} respectively.[224] Treatment of a mixture of TiO_2 and nanoparticles of MoO_2 and MnO_2 through the combined use of UV irradiation and ultrasonic technology gave a nanocomposite photocatalyst that generated 9 m^3 h^{-1} of hydrogen from 5 L of water.[225] A preparative method for tantalum–tungsten mixed polyoxometallate photocatalysts with efficient hydrogen producing activity was reported in a patent by Liu and co-workers[226] by enabling $K_8[Ta_6O_{19}]$ and $Na_{12}[\alpha\text{-}P_2W_{15}O_{56}]$ to react in a stoichiometric ratio at 45 °C in the presence of hydrogen peroxide; the quantity of hydrogen produced was 375 μmol h^{-1} after 36 hours (1250 μmol h^{-1} g^{-1}) in the presence of a co-catalyst such as molybdate chloride, and methanol or ethanol as the sacrificial electron donors.

Incorporation of $BiVO_4$ into the layers of zirconium–titanium phosphate by combination of ion-exchange and a hydrothermal route yielded $BiVO_4$ pillared $ZrTiPO_4$ materials capable of generating hydrogen at a rate of 2.6 mmol h^{-1} g^{-1}.[202] The bismuth-doped sodium titanate particles $NaBi_xTa_{1-x}O_3$ ($0.001 < x < 0.1$) obtained by spray pyrolysis have shown improved activity.[227] A core–shell structure built with the inner part consisting of grains (size, 0.06–2 μm) of γ-Fe_2O_3–$Y_{3-x}Yb_xSbO_7$ (x = 0.5–1), γ-Fe_2O_3–$Y_{3-x}Ga_xSbO_7$ (x = 0.5–1), SiO_2–$Y_{3-x}Yb_xSbO_7$ (x = 0.5–1), SiO_2–$Y_{3-x}Ga_xSbO_7$ (x = 0.5–1), MnO–$Y_{3-x}Yb_xSbO_7$ (x = 0.5–1), or MnO–$Y_{3-x}Ga_xSbO_7$ (x = 0.5–1) was clad by $Y_{3-x}Yb_xSbO_7$ and $Y_{3-x}Ga_xSbO_7$ (0.07–2.1 μm large). The resulting magnetic photocatalyst was used for water splitting.[227,228] For example, irradiation of 0.8 g of Y_2GaSbO_7 dispersed in water (300 W xenon lamp; >420 nm; or 400 W Hg lamp; >390 nm) produced, after 24 hours, 39.7 μmol h^{-1} g^{-1} of H_2 and 19.7 μmol h^{-1} g^{-1} of O_2. Irradiation with a Hg light source gave 2148.8 μmol of hydrogen and 1069.2 μmol of oxygen. Calcining a mixture of lead, bismuth and niobium oxides and a metal M (M = Pt, Pd, Ag, up to 2 weight%) resulted in the materials $M_x/PbBi_2Nb_2O_9$ that were active in the visible spectral region.[229]

The semiconductor Ta_2O_5–$NaTaO_3$ composite nanofiber obtained from Ta_2O_5 nanowire precursors has also been described. UV irradiation of this composite under certain conditions produced hydrogen at 50 μmol h^{-1} g^{-1} of the catalyst. No mention of oxygen being produced was given, however.[230]

Composites of niobium and cobalt oxides, *e.g.* comprising $Co_4Nb_2O_9$, $CoNb_2O_6$, Co_3O_4, Co_2O_3, and CoO, are visible-light-active catalysts. In one case, the quantities of hydrogen and oxygen produced were, respectively, 2.8 μmol h^{-1} g^{-1} and 1.2 μmol h^{-1} g^{-1} (0.5 g catalyst; 300 mL pure water; 500 W xenon light source; >420 nm).[231] A recent Japanese patent reported that effective photocatalysis resulted from the combination of O_2-evolving particles (scheelite-type, such as $BiVO_4$-based particles having maximal primary particle diameter *ca.* 300 nm) and H_2-forming particles (*e.g.*, Pt/perovskite-type $SrTiO_3$, Rh-based and/or Ru/perovskite-type $SrTiO_3$, Rh-based particles; the diameter was less than a half of that of the O-forming particles); the combination of $BiVO_4$ particulates and Ru/$SrTiO_3$:Rh particles (Fig. 13) produced 47 mmol h^{-1} of H_2 and 22 mmol h^{-1} of O_2. Another combination involved the use of Fe^{2+} and Fe^{3+} ions as electron shuttles (Fig. 14).[232]

3.3 Photocatalysts for CO_2 reduction

Loading NiO onto the $InTaO_4$ photocatalyst led to the reduction of carbon dioxide to methanol.[233] Metal phosphates that include $AM_2(PO_4)_3$, MP_2O_7 or $A_3X_7P_4O_{29}$, (A = alkali metal, M = tetravalent metal, X = pentavalent metal) have been prepared as photocatalysts. An example is $Na_3Nb_7P_4O_{29}$, which when loaded with RuO_2 as the co-catalyst and subsequently irradiated produced CH_4 from CO_2 and water.[234] Platinum nanowires loaded onto sodium niobate also reduced carbon dioxide to methane, a process that took place twenty times faster (1 atm CO_2, 0.4 mL water; solar simulator; 16.3 μmol h^{-1} g^{-1} of CH_4) relative to that of methane formed from a previously examined sodium niobate catalyst.[169]

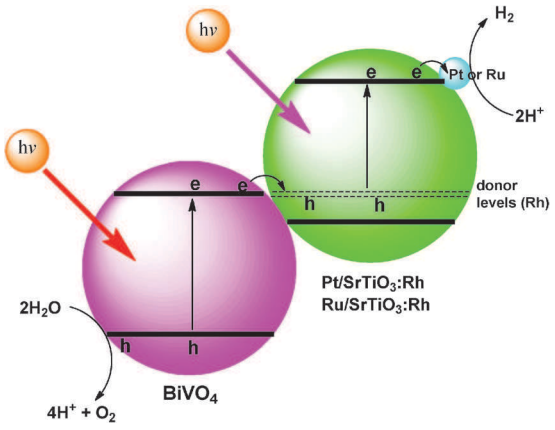

Fig. 13 Potential coupling of the two semiconductor systems, $BiVO_4$ and either Pt/$SrTiO_3$:Rh or Ru/$SrTiO_3$:Rh, in the photoreduction and photooxidation of water to produce hydrogen and oxygen through the water splitting process, see ref. 232.

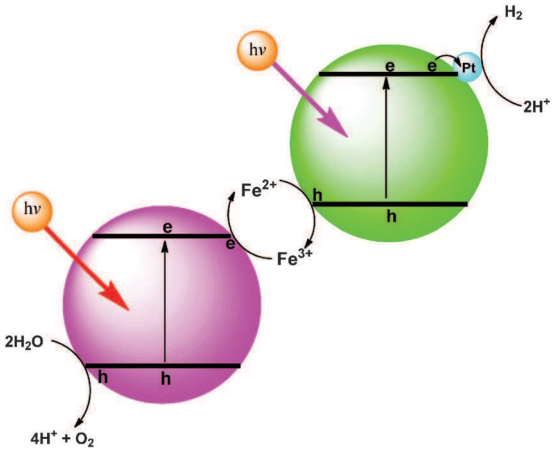

Fig. 14 Potential coupling of two semiconductor systems in the photoreduction and photooxidation of water to produce hydrogen and oxygen through the water splitting process in which the Fe^{2+} and Fe^{3+} species act as electron shuttles between them and promote charge separation.

4. Photocatalysts for hydrogen generation from water: group 6 oxides

As in the case of TiO_2 (Section 2.1), visible-light-activated porous W and Mo oxide catalysts have been prepared by soaking biological templates (butterfly wing, leaf, pericarp, wood brick or rice hull) into an ammonium tungstate or molybdate solution, followed by washing, drying, and baking the samples to remove the templates.[235]

Tungsten trioxide, WO_3, nano composite materials with one-dimensional and two-dimensional nano composite structures were prepared using two-dimensional graphene as an auxiliary material and sodium tungstate as the tungsten source.[236] For the purpose, a WO_3 nanowire (10–30 nm diameter; length, 50–600 nm) was obtained by a hydrothermal synthesis method, subsequent to which mixing the nanowire with graphite oxide dispersed in solution and then photocatalytically reduced yielded the graphene/WO_3 nanowire composite material. The WO_3 nanowire penetrated through or was distributed in the inner layer or on the surface of the layer-shaped graphene main material.[236] Regrettably, the composite material was not tested for the production of hydrogen or for carbon-based solar fuels. A patent by Yokozawa and Ooka[237] described a water splitting system that was made by adding the photocatalyst WO_3 (band-gap, 2.3–2.5 eV), or optionally of N-doped WO_3 as the first layer and TiO_2 (band-gap, 3.0–3.2 eV) as the second layer (and so on). In this way, production of hydrogen and oxygen was achieved photoelectrochemically by means of sunlight irradiation in which a ruthenium(II) dye was the light absorber.[237] Along similar lines, Sato and Ishizuka[193] set out to provide a photocatalyst with significant activity also upon irradiation with sunlight when suspended in water. They prepared laminar composite metal compounds $AMWO_6$ (A = alkali metal and/or H, and M = V, Nb or Ta) and added a semiconductor that could be excited by light and that was included between the layers of the laminar composite metal compound and loaded (0.05–5 wt%) with a metal selected from Pt, Ru, Rh, Ir and Ni, or their oxides as co-catalysts.[193] As an example, calcining a mixture of Nb_2O_5, Li_2CO_3 and WO_3 (24 hours, 800 °C) yielded $LiNbWO_6$, which upon acidification by ion exchange gave $HNbWO_6$ (band-gap energy, 2.96 eV). Upon irradiation of $HNbWO_6/TiO_2$/Pt for 5 hours when suspended in 1.25 L of water (1 g; light source, 450 W Hg lamp; wavelengths > 290 nm) produced 14 cm^3 of gases (mixed H_2 + O_2), whereas in the presence of 10 vol% methanol and under UV irradiation the system produced 70 cm^3 of H_2 (only), while the corresponding $HTaWO_6/TiO_2$/Pt yielded 66 cm^3 of hydrogen.[207] By comparison, Xia *et al.*[238] prepared the visible-light responsive molybdenum-containing semiconductor composite materials $ABFeMoO_6$ (A = Li, Na, K, Rb or Cs; B = Be, Mg, Ca, Sr or Ba) by mixing compounds of A and B with an Fe compound and a Mo compound followed by calcining at 800–1200 °C for up to 160 hours. Although they intended to demonstrate water splitting by sunlight, when the resulting low band-gap material $SrKFeMoO_6$ was irradiated with visible light in a methanolic aqueous medium (20 mL methanol, 480 mL water; 400 W xenon lamp), only hydrogen was produced (48.3 μmol h^{-1} g^{-1}).

5. Photocatalysts for hydrogen generation and CO_2 reduction: metal sulfides

5.1 Undoped, doped and mixed metal sulfides

Cadmium sulfide (CdS) has a band-gap energy (E_{bg}) of 2.4 eV, and thus a relatively significant fraction of the solar spectrum is absorbed by this semiconductor; unfortunately, the compound is not stable in aqueous media under irradiation because it undergoes photocorrosion converting it into either Cd^{2+} ions or CdO and the sulfide into sulfate. Accordingly, most of the work on CdS has been addressed on how to overcome this limitation and produce hydrogen.[239] Representative examples of metal sulfides are collected in Table 6.[240–267]

Noble metal-coated CdS samples have been used as photocatalysts for generating H_2 from aqueous solutions of S-based electron donors. Good results were obtained using (0.8 wt%)Pt/CdS from which hydrogen evolved at 9.36 mmol h^{-1} g^{-1} of the catalyst.[240] Similarly, treatment of CdS with an alkaline solution containing hexachloroplatinate afforded a Pt containing photocatalyst, which upon irradiation developed 58 μmol h^{-1} of hydrogen (see Table 6).[242] A simple and facile method beneficial to large-scale production involves the visible-light-active Pd-loaded CdS material prepared by reduction of a Pd salt with ascorbic acid, which produced cubic palladium nanoparticles possessing a spherical morphology; although Pd/CdS was claimed to be active toward water splitting, only hydrogen was produced: *ca.* 7.6 mmol after nearly 12 hours of irradiation (note that no hydrogen formed until after *ca.* 5 hours).[268] Stable CdS photocatalysts were prepared by loading the nanoparticles with electron acceptors such as Pt, Ru, Ir, Co, Rh, Cu, Pd, Ni, or their oxides (loading, 0.10–2.50 wt%); mixed metal sulfide photocatalysts of the type M/(M + Cd)S, with M selected from

Table 6 Representative examples of the photocatalyzed hydrogen generation by metal sulfides

Ref.	Catalytic system	Solution	Light source[a]	Hydrogen production rate (mmol h^{-1} g^{-1})
240	(0.8 wt%)Pt/CdS	Na_2SO_3	125 W, Hg (>260 nm)	9.36
241	(3 wt%)Pd/ZnS	Na_2SO_3	125 W Hg,	1.43
242	Pt/CdS	Na_2S	500 W, Xe	2.03
243	Cs, Co/ZnS, SiO_2	Water	500 W, Hg	24.3
244	(1 wt%)Ni/Cd[Cr(0.2)]S	Na_2S Na_2SO_3	500 W, Xe (>400 nm)	23.8
245	(1 wt%)Pt/$Sm_2Ti_2O_5S_2$	MeOH–H_2O	500 W, Xe (>440 nm)	0.036
246	(1 wt%)RuO_2/Cd[Cr(0.1)]S	Na_2S, NaH_2PO_2	500 W, Xe (>400 nm)	60.8
247	CdS/TiO_2	Na_2S, Na_2SO_3	350 W, Hg (>420 nm)	17
248	Pt/$HTiTaO_5$/CdS	Na_2S, Na_2SO_3	300 W, Xe (>430 nm)	0.72
249	$H_2Ti_4O_9$/CdS	Na_2S, Na_2SO_3	300 W, Xe (>430 nm)	21.1
250	$ZnS_{(0.9)}CuBr_{(0.1)}$	Na_2S, Na_2SO_3	300 W, Xe (>420 nm)	2.24
251	(0.2 wt%)Pt/(0.1 wt%)Rh/CdS	H_2S	300 W, Xe	64
252	CdS–TiO_2 hollow sphere	Na_2S, Na_2SO_3	Xe (>420 nm)	0.41
253	$(CuIn)_{0.05}Cd_{2(0.95)}S_2$	Na_2S, K_2SO_3	300 W, Xe	0.64
254	Ni-doped $ZnIn_2S_4$/$CdIn_2S_4$ (Zn : Cd = 7 : 3)	Na_2S, Na_2SO_3	250 W, Hg (>400 nm)	3.32
255	(0.6 wt%)Pd/Ni-doped/$Cd_{0.1}Zn_{0.9}S$	Na_2S, Na_2SO_3	350 W, Xe	0.585
256	CdS/Mordenite	Na_2S, Na_2SO_3	250 W, Hg (>420 nm)	16.74
257	WO_xS_y/CdS	Aqueous lactic acid	Xe, (>420 nm)	4.20
258	CdS/*n*-TiO_2	Na_2S, Na_2SO_3	175 W, Hg (>400 nm)	1.21
259	ZnS/CdS	Na_2S, Na_2SO_3	300 W, Xe	Up to 450
260	(0.4 wt%)Pt–Pd/Cr_2O_3/CdS	$(NaH_4)_2S$	1000 W, Xe	50.5% eff.
261	(0.7 wt. %)Mn^{2+}/$CdIn_2S_4$	Na_2S, Na_2SO_3	250 W, Hg (>400 nm)	1.3
262	CdS/TiO_2/conductive polymer fiber membrane	MeOH–H_2O	500 W, Xe	1.8
263	NiS–PdS/CdS	30% lactic acid	300 W, Xe (>420 nm)	31
264	$CdIn_2S_4$/$ZnIn_2S_4$	Na_2S, Na_2SO_3	1000 W, Xe (>400 nm)	Up to 37
265	Wool–Pt(II)/CdS	Na_2S, Na_2SO_3	500 W, Xe (>300 nm)	8.7
266	(1.2 wt%)MoS_2/$ZnInS_2$	Na_2S, Na_2SO_3	n.d.	3.12
267	Pt/CdS	$(NH_4)_2SO_3$	300 W, Xe	6

[a] Lamp used as well as the flux impinging on the sample indicated when available.

V, Cr, Al and P (0.05 to 20.0 mol%), have also been reported.[246] As an example, admixing $CdSO_4 \cdot H_2O$ and $K_2Cr_2O_7$ as promoters and H_2S in aqueous media produced a Cd[Cr]S material, which when loaded with RuO_2 (1.0 weight%) produced (1.0 weight%)RuO_2/Cd[Cr(0.1)]S that upon irradiation at >400 nm (0.5 g of catalyst; 500 mL water) in the presence of Na_2S and NaH_2PO_2 generated hydrogen at a rate of 60.8 mmol h^{-1} g^{-1}.

Another patent also reported that visible-light-responsive CdS photocatalysts could generate hydrogen by the photocatalytic *water splitting* process, although no oxygen was ever produced. The materials consisted principally of CdS loaded with other metal sulfides such as NiS and an optional additional one chosen from PdS, Ru_2S_3, Rh_2S_3 and Ag_2S.[263] In one case, NiS–PdS/CdS (0.15 g) dispersed in 80 mL water containing 30 vol% lactic acid and then irradiated at wavelengths >420 nm (300 W xenon lamp) produced hydrogen (only) at a rate of 31 mmol h^{-1} g^{-1}. The new Pd–Cr_2O_3 nanocomposite co-catalyst prepared at ambient temperature when loaded onto CdS has been claimed to yield hydrogen evolution at a rate faster than mere Pd/CdS. Fig. 15 shows the case of Pd–Cr_2O_3/CdS.[269] A method to prepare M–Pd–Cr_2O_3 nanocomposite co-catalysts (M = Pt, Ru, Rh, Os, Au and Ag) was also patented.[269] The Ni-loaded mixed sulfide $Cd_{0.1}Zn_{0.9}S$ obtained by a hydrothermal method produced H_2 up to 191 μmol h^{-1} g^{-1} of the catalyst with quantum efficiency of 6.8% at 420 nm.[255] Likewise, loading with 0.6 wt% Pt enhanced the activity to 585 μmol h^{-1} g^{-1} (quantum efficiency ~ 16%).[255] The photocatalytic decomposition of water into hydrogen and oxygen has been found to occur from an aqueous solution containing a visible-light-active semiconductor material such as CdS, ZnS, Cd_xZn_xS or Ag_2S/CdS loaded with Pt or Rh or Ir and a transition metal oxide (*e.g.* RuO_2) in the presence of a dioxygen–EDTA–ruthenium(II) complex, $K[\{Ru(EDTA)(OH)_2\}O_2]$.[270] After 60 hours of irradiation by

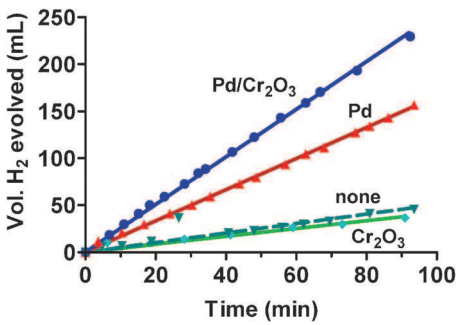

Fig. 15 Graph showing the effect of photocatalyst loading of 1.67 g CdS loaded with Pd and/or Cr_2O_3 per liter of the photolyte and the rate of H_2 evolution from an aqueous 1.0 M NH_4SO_3 solution. Adapted from data in ref. 269. For CdS loaded with Pd(0.4 wt%)/Cr_2O_3(0.1 wt%), the rate of H_2 evolution was 2.35 ± 0.01 mL min^{-1}; for CdS loaded with Pd(0.4 wt%), the rate of H_2 evolution was 1.66 ± 0.01 mL min^{-1}; for CdS alone, the rate was 0.51 ± 0.04 mL min^{-1}, while for CdS loaded with 0.1 wt% Cr_2O_3 the rate was 0.42 ± 0.02 mL min^{-1}.

visible light the quantities of hydrogen and oxygen were, respectively, 3.2 mL and 1.6 mL (CdS/Rh/RuO_2), 2.2 mL and 1.1 mL (CdS/Pt/RuO_2), while the CdS/Ir/RuO_2 system produced only 1.8 mL of hydrogen.[270] CdS that contained Cd as a promoter was effective in separating the photogenerated electron–hole pairs, thereby improving the efficiency of the photocatalytic production of hydrogen by CdS from water; for the (16 wt%)Cd/CdS system. The quantity of hydrogen produced was 12.43 mmol h^{-1} g^{-1} *versus* an average rate of 1.7 mmol h^{-1} g^{-1} for pure CdS.[271]

The semiconductor $Zn_xCd_{1-x}S$ ($x \leq 0.02$) sensitized by CdS quantum dots and activated by visible light did not require noble metal addition to produce hydrogen from water; under UV/visible irradiation the sensitized system produced hydrogen at a rate of 2987 μmol h^{-1}.[272] A method for preparing cadmium sulfide catalysts was also reported whereby a Cd-containing material and an M-containing compound (M = Ni, Pd, Pt, Fe, Ru, Co or their oxides; content of M, 0.001 to 20.0 mol%) were reacted with either H_2S or Na_2S and subsequently loaded with a metal promoter (chosen from V, Cr, Al, P, Sb, and Pb; 0.1–5 wt%) yielding M/Cd[M]S systems.[260] Irradiation of such systems with visible light or sunlight in the presence of 0.05–1.00 mol of Na_2S (as electron donor) and 0.05–1.00 mol of Na_2SO_3 (a reducing agent) led to the generation of hydrogen from the photodecomposition of water. As an example (1 weight%) Ni/Cd[Cr(0.2)]S produced 260 mL h^{-1} of hydrogen (see also Table 6).[260] Loading a semiconductor with a noble metal and a transition metal oxide also gave good results, as in the case of the composite CdS–Rh–RhO_8.[273] Visible-light-sensitive composite photocatalysts consisting of CdS and a lanthanum-manganese based oxide, represented by $La_{1-x}A_xMnO_3$ (A = alkaline earth metal; $0 \leq x \leq 0.6$), when irradiated at wavelengths >420 with a 300 W xenon light source evolved hydrogen in the presence of Na_2S and Na_2SO_3: after 24 hours, 400 μmol of H_2 were obtained for CdS/$LaSrMnO_3$ and 700 μmol for the CdS–$La_{0.4}Sr_{0.6}MnO_3$ composite.[274]

Cadmium and/or indium sulfides also generated hydrogen upon irradiation (300 W xenon lamp; for 24 hours) of a water-containing organic sludge (sewage sludge or digested sludge), previously treated with hot water under pressure in a non-oxidative atmosphere.[275] The amount of H_2 was 150 μmol when the catalyst was In_2S_3, while with CdS no hydrogen was produced except in the presence of Na_2S and Na_2SO_3 (400 μmol of hydrogen).[275] An aqueous suspension of (3 wt%)Pd-coated ZnS yielded hydrogen in the presence of various electron donors such as sulfites, sulfides, hypophosphites, phosphates, and the corresponding free acids; in the presence of Na_2SO_3 the quantity of hydrogen produced was 1.4 mmol h^{-1} g^{-1} of the catalyst.[241] Treating ZnO with either Na_2S or H_2S in aqueous media led the zinc oxide to dissolve forming Zn^{2+} ions that precipitate forming a layer of ZnS fine particles. The resulting material was more efficient in generating hydrogen from the photodecomposition of H_2S when irradiated with THF as the hydrogen donor compared to ZnS, CdS or TiO_2 under similar conditions.[292] Different catalysts of the type (≤0.6 wt%) Cs/X/ZnS have been prepared (X = a promoter selected among Ni, Co, Fe on silica); with the Cs,Co/ZnS-silica catalyst system the quantity of hydrogen evolved from water was 24.3 mmol h^{-1} g^{-1}.[243] Intercalation of benzoic acid in a layered zinc hydroxide followed by reaction with hydrogen sulfide yielded a zinc sulfide–benzoic acid nanocomposite, a convenient photocatalyst in view of its simple preparation and the easily available starting materials; the photoactivity of the composite was ascertained in the photodegradation of methylene blue.[277]

Mixed sulfide photocatalysts of the type (0.1–3.5 wt%)Pt/Zn[M_b]S (b = 0.05–30 mol%; M = Co, Fe, Ni and P) have been prepared by reaction with either H_2S or Na_2S followed by impregnation with a Pt-containing compound (*e.g.*, H_2PtCl_6).[278] Patented was also a method for producing hydrogen, in which ultraviolet or visible light irradiated a suspension of the photocatalyst in water in the presence of Na_2S as the electron donor and NaH_2PO_2 as the reducing agent.[278] Irradiation of an aqueous dispersion (500 mL water) of 0.5 g of (2 wt%)Pt/Zn[Ni(5.0 mol%)]S in the presence of the electron donor and the reducing agent produced 82.0 mmol of H_2 per gram of the catalyst per hour. Likewise, cadmium-zinc sulfide hydrogen generating photocatalysts, represented by $A_a/Cd_xZn_yM_zS$ (A = electron acceptor metal from Ni, Pt, Ru, and their oxides; a = 0.10–5 wt%; M = Mo, V, Al, Cs, Mn, Fe, Pd, Pt, P, Cu, Ag, Ir, Sb, Pb, Ga and Re; x, y = 10.0–90.0 atom%; z = 0.05–20.0 atom%), were prepared by treating the mixed sulfides with a source of M (*e.g.*, $MoCl_5$, VCl_3, among others); depending on conditions, the highest quantities of hydrogen produced by (1 wt%)Ni/$Cd_{49.0}Zn_{49.0}Mo_{2.0}S$ were 41.75 and 45.10 mmol h^{-1}.[279]

Photocatalysts of the type $ZnIn_2S_4$–$CdIn_2S_4$, where the Zn : Cd ratio was 7 : 3, exhibited a low photocatalytic activity toward the decomposition of hydrogen sulfide to evolve H_2 and S.[254] However, when doped with transition metal ions (Cr, Mn, Fe, Co, Cu) the resulting materials were nearly 2 to 6 times more photoactive and produced hydrogen at the rate of 1100 to 3500 μmol h^{-1} g^{-1} – see also Table 6.[254] Other mixed metal sulfides reported had formula ABS (A = Al, Cu, Zn, Ag; B = Pb and Fe).[280] A layered catalyst consisting of 2–5 weight% Pt, 70–80 wt% $HTiTaO_5$, and 15–28 weight% CdS was prepared by calcining a mixture of K_2CO_3, Ta_2O_5 and TiO_2, followed by ion-exchange with nitric acid; CdS was prepared by reaction of cadmium acetate with hydrogen sulfide.[248] The resulting system produced 144 μmol h^{-1} of hydrogen upon irradiation with visible light (>420 nm). The quantum efficiency at 420 nm was 6.3%, while the visible light energy conversion efficiency was 1.67% (see also Table 6). To achieve formation of hydrogen by the water splitting process, the patent by Jiang and co-workers[276,281] reported immobilizing an indium–zinc–silver sulfide solid solution onto thin films consisting of S-doped TiO_2 nanotubes; the photocatalyzed evolution of hydrogen using this architecture after 4 hours of irradiation was more efficient than when using the TiO_2 nanotube (NT) films. For example, irradiation of an aqueous dispersion of the catalyst systems with a 500 W xenon light source in the presence of Na_2S and Na_2SO_3 evolved *ca.* 2150 μL of hydrogen for the ZnS–In_2S_3–Ag_2SOTiO_2 nanotubes films, whereas for the titania nanotubes alone the amount of hydrogen produced for the same time period was *ca.* 1600 μL.

Although water splitting was claimed, no evolution of oxygen occurred. A solid solution consisting of zinc sulfide-copper halide, $(ZnS)_{1-y}(CuX)_y$ ($0.01 < y < 0.2$; preferably $0.05 \leq y \leq 0.2$, and X = a halogen) showed high activity toward the photodecomposition of water under simulated sunlight irradiation (300 W xenon lamp; $\geq$420 nm) in the presence of the electron donor Na_2S and the reducing agent Na_2SO_3 – no co-catalyst was required. The highest quantity of hydrogen produced was 673 μmol h^{-1} for $(ZnS)_{0.9}(CuBr)_{0.1}$ with a band-gap of 2.77 eV – see also Table 6.[250]

The patent by Li and co-workers[253] provided a hydrothermal method to effect the synthesis of a reportedly highly efficient photocatalyst, namely $(MIn)_xCd_{2(1-x)}S_2$ (M = Cu, Ag, Au; x = 0.01–0.3) that was claimed to produce hydrogen by the water splitting process under simulated sunlight with no noble metal being needed; the highest hydrogen yield was 650 μmol h^{-1} g^{-1} of the catalyst, *i.e.* a dozen times more efficient than CdS loaded with a noble metal co-catalyst – the presumed quantum yield was ~10%, although it is not clear how this was reached. Moreover, though water splitting was claimed, no evidence of the simultaneous formation of oxygen was reported.[253] A photocatalyst having visible light activity was prepared from $AgGaS_2$ (band-gap *ca.* 2.56 eV) loaded with Rh, Pt, Ru or Ir promoters. Upon irradiation with visible light metal-loaded $AgGaS_2$ generated hydrogen from aqueous media in the presence of an electron donor (NaS) and a reducing agent (K_2SO_3).[282] The best performing catalyst was (1 weight%) Rh/$AgGaS_2$ which evolved 1340 μmol h^{-1} of hydrogen over a 10 hours period.[282] The order of activity with regard to the co-catalysts was Rh > Pt > Ru ≫ Ir. The patent by Domen *et al.*[283] described a photoelectrochemical setup to achieve water splitting by means of systems such as silver selenide and gallium selenide and their combination involving $AgGaSe_2$ and $AgGa_5Se_8$ that were active in hydrogen generation. The photocatalyst system also contained Rh or Pt as co-catalysts. The electrically biased photoelectrochemical system is illustrated in Fig. 16, wherein the photocatalyst acted as the working photoelectrode that absorbed the UV/visible radiation from an appropriate source, while the potentiostat controlled the potential. The absorption edges of the catalysts extended well into the visible spectral region, to *ca.* 700–710 nm and the amount of H_2 evolved was *ca.* 4 μmol h^{-1}.

A monolithic catalyst system for the photocleavage of water into hydrogen and oxygen involving a first photoactive material is capable of generating O_2 and H^+ from water when irradiated with light at a wavelength of $\geq$420 nm, either alone, or together with one or more auxiliary material and auxiliary catalyst; a second photoactive material selected from GaAs, $CuInS_2$, CuInSe, $CuInGaS_2$, $CuInGaSe_2$,CdS, CdSe, or CdTe having a water resistant coating transparent to visible light is capable of reducing H^+ to H_2 when irradiated with visible light.[284] The first photoactive material and the second photoactive material were supported on at least one substrate and were in direct electrical contact, exclusively *via* one or more electron-conducting materials. Although the patent was declared to disclose a process for cleaving water into H_2 and O_2, no evidence for the evolution of these gases was reported.[284] Semiconductor photocatalyst systems for

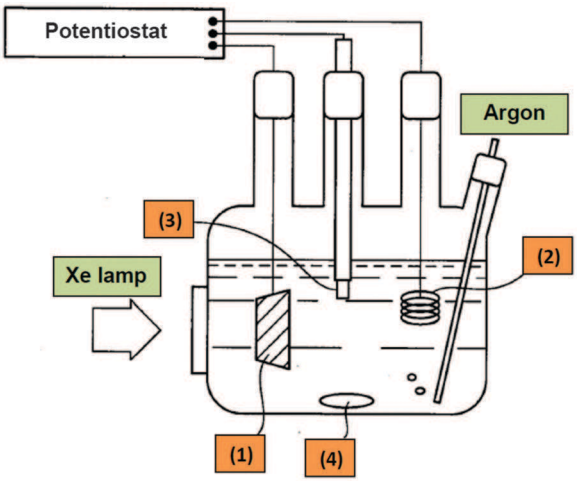

Fig. 16 Schematic view of the apparatus used in photoelectrochemical measurement by Domen and co-workers; (1) is the working electrode, (2) is a Pt wire used as the counter electrode, (3) is the Ag/AgCl reference electrode, and (4) is a magnetic stirrer; the potentiostat controls the applied potential. Adapted from ref. 283.

hydrogen production by the photocatalytic reforming of biomass derivatives (*e.g.*, methanol, ethanol, propanol, butanol, ethylene glycol, glycerol, glucose, sucrose, fructose, maltose, mannose, ascorbic acid, L-proline or L-cysteine) consisting of M ~ N–A_x (M ~ N = II–VI group elements or III–V group elements; A = Co, Ni, Fe, Cu, Cr, Pd, Pt, Ru, Rh, Ir, or Ag; $0.02\% \leq x \leq 1.0\%$) were reported in a patent by Wu and co-workers.[285] The photocatalysts were prepared *in situ* from CdS or CdSe (or CdTe, PbS, PbSe, ZnS, ZnSe) quantum dots by a photoreaction method that did not involve calcination. As an example of the photoactivity of one of the photocatalysts, irradiation of the TiO_2–CdSeS–Ni_x (x = 0.26%) with a high pressure Hg lamp at wavelengths >400 nm produced 71.4 mmol h^{-1} g^{-1} of hydrogen. A film-type photocatalytic system containing a cathode formed by a transparent conducting substrate on which a thin film of a noble metal was coated and the anode was one among either the metal sulfides CdTe, CdSe, CdS, and ZnS or the metal oxides TiO_2 and ZnO has been reported.[286] The oxysulfide $Sm_2Ti_2O_5S_2$ photocatalyst was prepared by calcining samarium sulfide (Sm_2S_3), titanium dioxide (TiO_2) and titanium sulfide (TiS_2) in a 1 : 1 : 1 ratio; platinization and subsequent irradiation of the resulting material at >440 nm (500 W xenon lamp) in a methanolic aqueous solution produced hydrogen at 36 μmol h^{-1} g^{-1} of the catalyst (see also Table 6).[245]

5.2 Composites for hydrogen generation

A patent that claimed to provide a highly efficient water splitting photocatalyst was reported most recently by Jiang and co-workers;[287] it consisted of a composite of CdS and a highly stabilized Metal Organic Framework based on $Zr_6O_4(OH)_4$ octahedra connected by terephthalate or 2-aminoterephthalate bridges (MOFs). The catalyst composite CdS/UiO-66 or CdS/UiO-66(NH_2) was formed by compounding UiO-66 or UiO-66(NH_2) and CdS in the mass ratio of 100 : (1–100). Although two samples of the composite

were more efficient (produced 142 and 284 μmol h^{-1} g^{-1} of H_2) than CdS alone (54 μmol h^{-1} g^{-1}) in producing hydrogen upon irradiation at >420 nm, the process was by no means water splitting, as it required the presence of an electron donor (a sulfide) and a reducing agent (a sulfite).

Photocatalyst composites consisting of CdS and either S,N-doped TiO_2 or N-doped TiO_2 or C-doped TiO_2 were prepared by a hydrothermal method by dispersing TiO_2 in Cd salts followed by addition of a sulfide ion source, together with precursors to dope the TiO_2 (*e.g.* urea or thioacetamide).[274] Irradiation of the composites at wavelengths >400 nm (175 W Hg lamp) in the presence of sulfide–sulfite systems in aqueous alkaline media photodecomposed H_2S yielding hydrogen up to 1209 μmol h^{-1} g^{-1}. Doping increased the photoactivity of the composites by 28 to 52% compared to the CdS–TiO_2 composite.[274] By comparison, the invention disclosed by Zhang *et al.*[252] reported the preparation of hollow-sphere core–shell CdS@TiO_2 composites by first preparing carbon balls followed by a hydrothermal method, a two-step impregnation method and a sol–gel method to obtain the C core wrapped with CdS (first shell) and then wrapped again with TiO_2 (second shell), which upon calcination at 400 °C for 2 hours yielded the core–shell C@CdS@TiO_2 photocatalyst; the composites were photoactive (>420 nm, Xe lamp) in producing hydrogen (up to 68 μmol h^{-1} g^{-1} of catalyst) from water in the presence of Na_2S–Na_2SO_3 systems. The patent also claimed that the technical process is simple and practicable and could realize large scale production.[252] In an additional patent, Zhang *et al.*[304] reported a similar procedure (*i.e.* a hydrothermal method and a four-step impregnation method for compounding p-type and n-type semiconductors) to prepare hollow sphere core–shell systems using the p-NiO semiconductor (the shell) and the n-type semiconductor CdS (the core) to form a p–n junction that produced hydrogen by, supposedly, the photocatalyzed water splitting process. However, the aqueous solution (50 mL) also contained sulfide and sulfite additives as the electron donor and reducing agent, respectively. Irradiation of 0.1 g of the p–n NiO–CdS composite at >420 nm yielded, after 6 hours, 4.05 mmol h^{-1} g^{-1} of hydrogen; the suggested mechanism[288] was absorption of light by the n-CdS semiconductor yielding photogenerated electrons that were rapidly transferred to the p-NiO at the p–n junction thereby enhancing electron transfer efficiency and improving the hydrogen yields.

An alternative method was described in a United States patent[247] for preparing core–shell composite photocatalysts involving a nanoscale particle disposed on a surface of a semiconducting core (CdS, Si, Ge, GaP, GaAs, GaSb, InSb, InP, CdTe, InN, or a metal oxide), wherein the nanoscale particle is an electron carrier having a different composition (TiO_2, NiO, Na_2TiO_3, ZnO, $LaMnO_3$, $CuFeO_2$) than the semiconducting core, with the composite photocatalyst being also loaded with a co-catalyst (Ni, Pt, Rh, Ag, Ru, Pd, IrO_2, NiO, RuO_2) and sensitive to visible light irradiation (350 W Hg arc lamp; ≥400 nm). For the specific case of the CdS@TiO_2 composite (Chart 1), the preparative method consisted of mixing an aqueous solution of Na_2S and an alcoholic (i-PrOH) solution of $Cd(NO_3)_2$ followed by drying, filtering and calcining at *ca.* 800 °C for 1 hour; subsequent

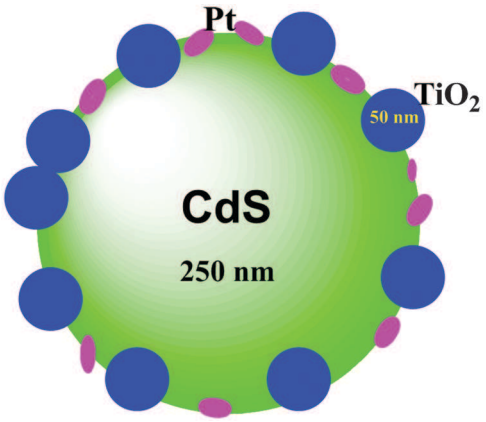

Chart 1 The core–shell CdS@TiO_2 composite.

loading of the composite with 1 wt% Pt by a photodeposition technique and irradiating the resulting material (1 g L^{-1}) in water the presence of the usual Na_2S and Na_2SO_3 additives produced as much as 17 mmol h^{-1} g^{-1} of hydrogen.[247]

The photocatalyst composite consisting of cadmium sulfide nanoparticles supported on mordenite generated hydrogen from the decomposition of H_2S in aqueous media at rates of up to 9.22–16.74 mmol h^{-1} g^{-1} under visible light irradiation.[256] An electrodeposition method allowed the preparation of a multilayered semiconductor photocatalyst in which the band gap between the first semiconductor layer and the second semiconductor layer differed by 1.0–2.5 eV; the semiconductors were ZnS, CdS, or RuS_2.[289] Immersion of the photocatalyst into a H_2S solution followed by irradiation generated hydrogen. To achieve high activity and absorb light across the sunlight visible spectrum, an electrically conductive substrate was used as the cathode that consisted of ZnS as the first semiconductor layer and a second semiconductor (CdS) with a different band gap electrodeposited and fixed on the surface of the substrate while gradually varying the mixing ratio between both semiconductors; the thickness of the multilayer photocatalyst thin films ranged from 100 to 300 nm.[289] Hydrogen was generated photoelectrochemically when this cathode was coupled to a reference electrode (Ag/AgCl) and a counter electrode (Pt) immersed in an visible-light-irradiated alkaline aqueous solution (pH, 8–11), which also contained sulfide–sulfite additives. A composite photocatalyst system was built by alternate layers of ZrO_2 and ZrS_2 deposited on the surface of Zr containing an alkaline earth metal or a composite oxide of Zr and an alkaline earth metal.[290] This displayed good absorption in the visible and appropriate oxidation/reduction properties. When a material prepared from $SrZrO_3$ containing 1.0 wt% Pt was submitted to repeated sulfurization–oxidation cycles the photocatalyst (0.3 g in 20 mL H_2O) generated 67 μmol of H_2 upon irradiation at wavelengths 480–750 nm.[290]

With three objectives in mind, namely (i) to intercalate a ruthenium(II) complex from the bipyridyl/phenanthroline class, as well as N-doped or N,S-co-doped TiO_2 pillared montmorillonite, (ii) to provide a novel approach to prepare photocatalyst systems under mild conditions, and (iii) to provide a material

showing a synergistic effect of nonmetal doping, pillaring and complex intercalation that opened up opportunities for green photocatalytic routes, Parida *et al.*[291] hoped to achieve generation of hydrogen from the water splitting process. Subjecting the resulting photocatalysts to irradiation with a 125 W visible lamp for 150 to 180 min and using different concentrations of the photocatalysts (20 mg to 50 mg), the rate of hydrogen generation ranged from 28.2 to 75.17 mmol h^{-1} g^{-1}. However, this was achieved not by the *water splitting* process, as the aqueous dispersions also contained 10 vol% of the sacrificial electron donor methanol. A photocatalyst composite consisting of 70–80 wt% of $HTiTaO_5$, 15–25 wt% of CdS and 2–5 wt% of Pt was prepared with the intent of greatly improving the efficiency of the water splitting process; $HTiTaO_5$ was first obtained *via* synthesis of $KTiTaO_5$ by mixing the precursors (K_2CO_3 and Ta_2O_5 and TiO_2), followed by grinding and heating at >1000 °C, and then by ion exchange with nitric acid.[292] Irradiation of this composite with a 300 W xenon lamp ($\lambda \geq 430$ nm) in the presence of Na_2S and Na_2SO_3 in aqueous media produced 720 μmol h^{-1} g^{-1} of hydrogen, hardly the result of the water splitting process as no oxygen was evolved under these conditions.

Addition of ZnS by co-precipitation lifted the limitation in the visible absorption of ZnO,[293] and irradiation of the ZnO–ZnS composite in a solution of chloroplatinic acid led to the photodeposition of Pt particles giving a better performing photocatalyst; in both cases no further information was provided.[294] The patent by Yao and co-workers[260] disclosed the fabrication of composite photocatalysts that they hoped would be useful in water splitting. To do so, they loaded a Pt–Pd alloy onto CdS and further added a thin layer of Cr_2O_3. Irradiation of aqueous dispersions of the resulting Pt–Pd–Cr_2O_3–CdS system by simulated sunlight (1000 W xenon lamp) at wavelengths >420 nm in the presence of sulfide and sulfite additives produced at most *ca.* 400 μmol of hydrogen after *ca.* 90 min of irradiation. Existing ternary indium-based sulfide catalysts tend to display low hydrogen yields, but a recent patent by Chen *et al.*[264] reported novel indium-based sulfide catalysts prepared by a one-step hydrothermal method which yielded the cubic and hexagonal phase $CdIn_2S_4$ and $ZnIn_2S_4$ composites; upon irradiation with visible light (300 W xenon lamp; >400 nm) in the presence of Na_2S and Na_2SO_3 in a photocatalytic water splitting apparatus that included a quartz reactor, H_2 evolved at a rate of 32–37 mmol h^{-1} g^{-1}.

A porous p-CuS/n-CdS composite semiconductor with a p–n junction was prepared in the presence of an organic template for the purpose of carrying out the generation of hydrogen by the water splitting process under solar light irradiation.[295] Although the claim was made that the nanocatalyst could be used for the decomposition of water to hydrogen and in the manufacturing of solar cells, no tests were carried out to support these claims.[295] The visible light-responsive composite catalyst Pt/CdS, reported several times in the scientific literature back in the early 1980, was patented and claimed to possess high activity for producing hydrogen by the water splitting process through photocatalysis; the ratio of the co-catalyst to cadmium sulfide was 1 : 200.[267] In the presence of sulfite, irradiation of 0.05 g of Pt/CdS at wavelengths 420 nm < λ < 800 nm (300 W xenon lamp) produced *ca.* 6 mmol h^{-1} g^{-1} of H_2 *versus ca.* 1 mmol h^{-1} g^{-1} when using a different batch of Pt/CdS – the difference was apparently due to the different morphologies of the materials. Clearly, here also water splitting had nothing to do with the formation of hydrogen. The Mn ion-doped $K_4Nb_6O_{17}$ system was prepared by a high-temperature solid phase method, following which CdS was intercalated to obtain the CdS/$K_4Nb_{6-x}Mn_xO_{17}$ composite photocatalyst; illumination with visible light (1000 W xenon lamp) in the presence of Na_2S and Na_2SO_3 resulted in 4.28 mmol h^{-1} g^{-1} of H_2, significantly above the yields from the undoped CdS/$K_4Nb_6O_{17}$ system alone.[296]

Reactions of precious metal ions (Pd, Au, Rh, Pt, Ag) with natural protein fibers (*e.g.* wool, silk wadding, cotton, cow hair, silk and the like) formed precious metal complexes, which upon addition to the traditional photocatalysts (*e.g.*, CdS, ZnS, CuS and the like) produced effective catalysts.[313] In the presence of the usual sacrificial agents, Na_2S and Na_2SO_3, irradiation of the wool–Pd(II) catalyst with visible light (500 W xenon lamp) produced 13.1 mmol h^{-1} g^{-1} of hydrogen; after four cycles the quantity of hydrogen produced dropped to 11.24 mmol h^{-1} g^{-1}, which Wang and co-workers[297] took to mean that the catalyst was fairly stable. A composite material comprising CdSe quantum dots and polycarbonyl di-iron disulfide [$Fe_2S_2(CO)_5L$] clusters (Fig. 17) displayed good performance for hydrogen generation, high stability and the advantage of being prepared from inexpensive and easily available materials; the quantity of hydrogen produced when sampling 10 mL of the total volume was 129 μmol; the highest turnover number was 1286 based on the amount of photocatalyst (Fig. 17).[298]

A composite heterojunction structure comprised of a metal (*e.g.*, Cd) as the core with inlaid zinc oxide particles (10 nm) and with cadmium sulfide as the shell (thickness, 20 nm) contained 50–90 mol% of Cd, 5 mol% of ZnO and 5–45 mol% of CdS. The composite structure exhibited a hydrogen generation rate up to 23 mol h^{-1} g^{-1} from the decomposition of water in the presence of Na_2S.[278] The composite material $ZnIn_2S_4$–$CdIn_2S_4$ (Zn/Cd atom ratio = 7 : 3) was doped with a transition-metal ion (Cr, Mn, Fe, Co, Ni, and/or Cu) and subsequently used to catalyze the generation of hydrogen (1.2 to 3.5 mmol h^{-1} g^{-1}) from an aqueous sulfide solution.[280] Semiconductor heterojunction composites such as ZnS–CdS/TiO_2, SnS/TiO_2, PbS/TiO_2, Bi_2O_3/TiO_2, SnS_2/TiO_2, CdS/TiO_2, or SnS–CdS/TiO_2 (sizes ~ 20–5000 nm) supported on the surface of a conducting polymer {*e.g.*, polyvinylidene fluoride, biphenol-A-type polysulfone, poly(*p*-phenylene)vinylene}, fiber membranes (fiber diameter, 400 nm to 2 μm), and a conducting material such as nano graphite, C black, C nanotubes or polyaniline (1–10 wt% of the polymer) gave an effective photocatalyst that could produce hydrogen synergistically while simultaneously degrading an organic pollutant.[299] As an example, irradiation of 0.2 g of the ZnS–CdS/TiO_2 composite with a 500 W xenon lamp for 20 hours produced 0.5 L of hydrogen (resulting in an overall rate of 5.57 mmol h^{-1} g^{-1}) with 85% of the sacrificial electron donor formic acid being degraded.[299]

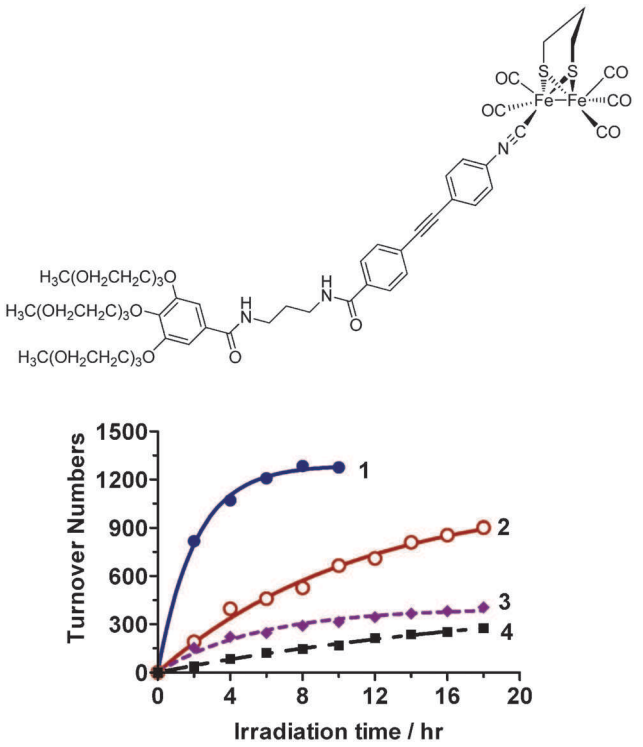

Fig. 17 Turnover numbers (based on the photocatalyst showed below) as a function of irradiation time for the production of hydrogen using the photocatalyst at different concentration and at different pH, the most favourable conditions (line 1) being observed by irradiating a solution of ascorbic acid (0.1 M, pH = 4) in the presence of CdSe quantum dots (0.04 g L^{-1}) and the catalyst (10^{-5} M). Adapted from ref. 298.

5.3 Photocatalysts for CO_2 reduction: metal sulfides

The mixed metal sulfide $Cu_{0.37}Ag_{0.37}In_{0.25}$–$ZnS_2$ selectively reduced CO_2 to methanol (185 μmol h^{-1} g^{-1}) in the presence of hydrogen and with ruthenium (0.01 wt%) as the co-catalyst; the extent of reduction to methanol without the hydrogen was only 21.1 μmol h^{-1} g^{-1}.[165] Similarly, the composite $ZnIn_2S_4$–graphene (band-gap of the $ZnIn_2S_4$, 2.3 eV), synthesized by a hydrothermal method, was able, according to the patent, to reduce CO_2 to alcohols or to hydrocarbons in the presence of H-donating alcohols and in the presence of sulfide and sulfite as sacrificial agents.[300]

6. Other photocatalysts

6.1 Other metal oxides

A controllable preparative method of a rare earth doped lanthanum manganese oxide nanotube consisted of mixing a $La(NO_3)_3$ solution and a $MnSO_4$ solution, followed by dropwise addition on a nanoporous anodic alumina membrane so as to penetrate the channels (the reactors); subsequent calcination, yielded the rare earth doped lanthanum manganese oxide (LaMnOx) nanotubes (external diameter, ≤25 nm; thickness, ≤20 nm; length, ≤10 nm).[301] It was claimed that the materials had large application as hydrogen storage electrode materials, as thermoelectric conversion functional materials, and as light absorption and light conversion catalytic materials.[301] Mixing lanthanum and nickel nitrate solutions in the presence of citric acid gave a gel that upon calcination and activation by CO_2/H_2 at 500–600 °C yielded Ni/LaO_2CO_3 (lanthanum dioxycarbonate); the composite was claimed to be a sunlight active catalyst that could be applied to both water splitting and the reduction of CO_2.[193] The composite photocatalyst $SnO_x/LaCO_3OH$, prepared by a hydrothermal method starting from Sn and La precursors in the presence of either Na_2CO_3 or urea, upon irradiation produced hydrogen at a rate of 0.289 mmol h^{-1} g^{-1} in the presence of methanol (5 mL to 165 mL of water).[205] Zinc–titanium hydrotalcite nanosheets (layered double oxides; particle size, *ca.* 40 nm) were prepared by an anti-phase microemulsion method; subsequent to platinization of the nanosheets, irradiation of aqueous suspensions containing lactic acid (sacrificial electron donor) with visible light produced hydrogen at 1032 μmol h^{-1} g^{-1}, nearly 60-times greater than the more conventional $K_2Ti_4O_9$ catalyst.[302] In a subsequent patent, Wei *et al.*[303] used a co-precipitation technique to prepare the layered hydrotalcite systems $[M_{(1-x-y)}^{2+}M_x^{4+}M_y^{3+}(OH)_2]^{(2x+y)+}\cdot(A^{n-})_{(2x+y)/n}\cdot mH_2O$, wherein M^{2+} was Ni^{2+}, Zn^{2+}or Mg^{2+}, M^{3+} was Al^{3+}, and M^{4+} was Ti^{4+} ($0.14 \leq x \leq 0.33$; $y = 0$ or $0.14 \leq y \leq 0.33$; A = anion with $n = 2$ or 1; $m = 0.5$–9). Subsequent to addition of the Pt co-catalyst, 0.05–0.2 g of the material in 150 mL of water in the presence of lactic acid produced, upon irradiation with the full UV/visible light spectrum, 15.3 μmol h^{-1} g^{-1} of hydrogen, nearly 10 times more than the traditional $K_2Ti_4O_9$ catalyst that produced only 1.7 μmol h^{-1} of hydrogen per gram of the catalyst under similar conditions.

The hydrated salts $[Cu_2(OH)_3]^+Y^-\cdot nH_2O$ possessing a laminar oxide structure have been used as photocatalysts,[304] as $CuFeO_2$ was prepared from the solid phase oxides by heating at 1050 °C in a hydrogen atmosphere. By contrast, the Chinese patent by Yan and co-workers[199] reported that the composites $CuY_xFe_{2-x}O_4$–$CuCo_2O_4$ ($0 \leq x \leq 0.2$) are notable for their simple preparation, low cost and long service time, as well as being photoactive under visible light. For instance, irradiation of the $CuFe_2O_4$–$CuCo_2O_4$ system at the wavelengths 400–700 nm (250 W xenon lamp) in aqueous media in the presence of oxalic acid yielded hydrogen at a rate of 2.46 mmol h^{-1} g^{-1} of the catalyst. By comparison, the $CuY_{0.2}Fe_{1.8}O_4$–$CuCo_2O_4$ composite produced hydrogen at 2.55 mmol h^{-1} g^{-1} of the catalyst under similar conditions.[199] An interesting method to prepare composite photocatalysts, which does not require Pt as the co-catalyst has been reported by Mu and co-workers.[305] Replacement by a copper-based mixed metal oxide in the photocatalytic reduction of water to hydrogen, was reported recently in a patent; it involved multi-walled carbon nanotubes (MWCNTs) as the carrier and photoinduced electron channel and a copper metal-oxide complex.[201] Placing the MWCNTs and the copper-based mixed metal oxide systems (CuO–NiO, CuO–Co_2O_3, CuO–Cr_2O_3, CuO–CeO_2, CuO–MnO_2, CuO–FeO, CuO–Fe_2O_3, CuO–Fe_3O_4, CuO–ZnO, CuO–PbO, CuO–Bi_2O_3) into a nitrogen-purged aqueous solution that contained eosin-Y as a photosensitizer followed by irradiation at >420 nm (1000 W halogen light source) produced hydrogen from the photodecomposition of water.

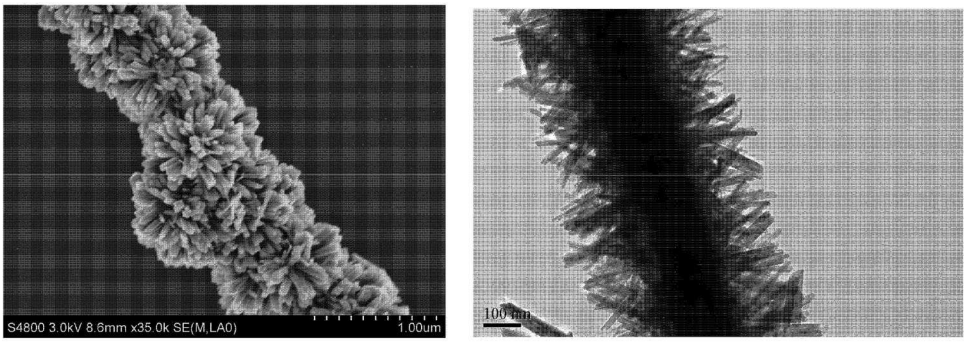

Fig. 18 (a) Emission scanning electron micrograph of the rutile TiO_2 nanorods along the same crystallographic growth and tightly wrapped around the copper nanowires. (b) TEM photograph illustrating the inner layer of the one-dimensional structure of copper nanowires with the rutile nanorod-like structure tightly wrapped externally. Reproduced from ref. 306.

The largest amount of H_2 was obtained for the eosin-Y/MWCNT/CuO–NiO system: 810 μmol h^{-1} g^{-1} of the catalyst. Following nearly identical lines, in an earlier patent the same group[201] reported the formation of a eosin-Y/MWCNT/CuO system by loading the CuO on the carbon nanotubes using a mechanical grinding process. Depending on the preparative method (temperature), the highest rate of hydrogen production in this case was 369 μmol h^{-1} g^{-1}.

Somewhat different from previous patents, a microwave-assisted synthesis (microwave power, 800–1400 W; heating rate 13–30 °C min^{-1}; initial pressure, 0–35 bar; reaction temperature, 140–200 °C; reaction time, 10–30 min) was used to prepare rutile TiO_2 nanorods loaded onto superlong copper nanowires (Fig. 18), which in the absence of a noble metal co-catalyst but in the presence of sacrificial electron donors (methanol, or oxalate or EDTA) and under monochromatic UV irradiation at 365 nm (0.5 g catalyst; 60 mL water; 20 mL methanol) produced 0.5 mL of hydrogen with an efficiency of 10.5%, significantly greater than with P25 TiO_2.[306] A $CuAl_2O_4$–graphene composite prepared by a hydrothermal method in the presence of polyethylene glycol (PEG-4000) was active under visible light generating H_2 at a rate of 5.2 mmol h^{-1} g^{-1} of the catalyst in the presence of methyl orange as the sacrificial agent that degraded almost quantitatively.[204] The composite material comprising ZnO and steel slag cementitious material (mass%: 39.1% CaO, 17.28% SiO_2, 18.74 Fe_2O_3, 4.4% Al_2O_3, 4.92% MgO, 3.58% MnO, 1.52% TiO_2, 0.93% V_2O_5, 0.31% SO_3, 0.2% BaO, 0.11% K_2O, 0.13% Na_2O, and 8.78% others) decomposed water under solar photocatalytic conditions producing hydrogen with high production efficiency; for instance, in the presence of both Na_2S and Na_2SO_3 the ZnO–polymer catalyst (50 mL water; irradiated with a 300 W xenon lamp; 6 hours) produced hydrogen in the amount of 4.58 to 6.34 mmol h^{-1} g^{-1} of the catalyst, depending on conditions.[207]

6.2 Additional catalysts involving transition metals

The large availability and tunable properties of transition metal complexes make them a favorite choice as sensitizers, with the added possibility of using polymeric ligands for more organized systems. In this regard, a colloidal Pt catalyst operated in the presence of the ruthenium-bipyridine functionalized polymeric sensitizer and a methylviologen polymer as the electron acceptor has been reported.[307] A photocatalyst complex system was reported that comprised a photocatalyst and co-catalyst particles (Pt, Au, Ag, Pd, RuO_x or a mixture) surrounded by ion conducting polymers on which a photosensitizer was immobilized (a bipyridine or a porphyrin complex).[308] Linear polymers based on the bipyridine or the 1,10 phenanthroline system complexed to Ru(II) as the sensitizers, colloidal Pt and an electron acceptor have been patented to serve as photocatalysts.[309] Mori and Kataoka[310] reported a material that involved an organic ruthenium compound selected, among others, from ruthenium terephthalate, ruthenium terephthalate chloride and ruthenium terephthalate tetrafluoroborate; the product evolved *ca.* 47 μmol of hydrogen over a 4 hour irradiation period – the turnover number was 93. Ruthenium bipyridine or phenanthroline-based heterooligonuclear complexes that comprised the chromophore, the catalytic unit, and the collector ligand have proven to be highly active photocatalysts. Methane was produced from the reforming of an organic compound.[311] A novel organic ligand, a chelate complex, and a multi-electron storage type photomolecular device for photoinduced charge separation for use in artificial photosynthesis consisted of a Ru(II) chelate, which, together with the PF_6^- anion, functioned as a photomolecular device that could reproduce the behavior similar to the cooperative behavior of both photosystem I and $NADP^+$ reductase. When combined with a platinum complex catalyst it could produce hydrogen gas from the photodecomposition of water by a one-step two-electron mechanism in the presence of EDTA as the sacrificial agent (see Fig. 19).[312]

A photocatalytic hydrogen production system containing a Fe-hydrogenase model compound, a photosensitizer, a sacrificial electron donor, a proton source and a solvent was patented by Wu *et al.*;[313] the photosensitizers were either CdSe quantum dots, CdTe quantum dots, Ru(II) tris-terpyridine or zinc porphyrin. Hydrogen was generated upon irradiating the photocatalytic systems at wavelengths >400 nm; with the most active catalyst producing, in the presence of ascorbic acid (the sacrificial agent), 1.41 mL of hydrogen after 8 hours of irradiation.

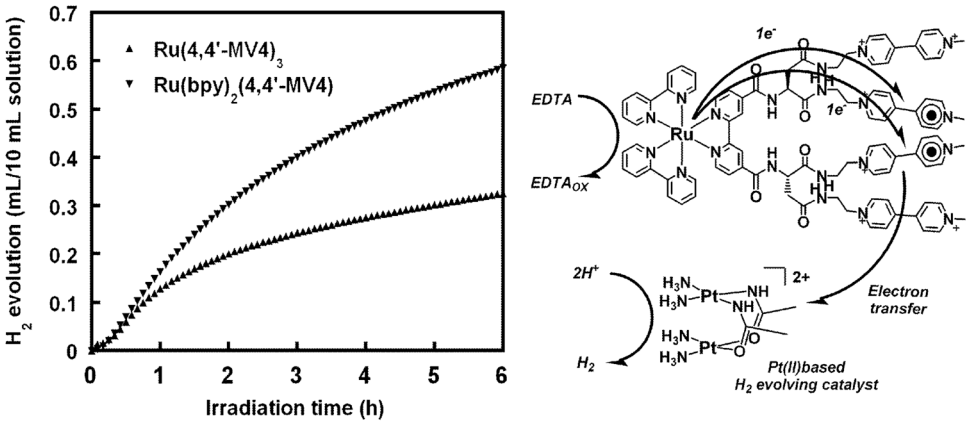

Fig. 19 Scheme showing the one-step, 2-electron mechanism for the hydrogen generation from Ru(II) complexes and a platinum(II)-based hydrogen evolving catalyst. Reproduced from ref. 312.

A catalytic process was described by Kisch[185] in the early 1980s for splitting water by irradiating an aqueous solution of the catalyst with light. The solution contained a metal dithiolene or dithiooxamide complex as the catalyst, with the metal chosen from Ti, V, Cr, Mo, W, Mn, Re, Fe, Os, Co, Ni, Pd, Pt, Cu, Au, Zn, Cd, or Mg, with the ligands linked to the metal atom *via* two sulfur atoms or *via* one sulfur atom and one nitrogen atom. The iron and nickel system showed a larger catalytic activity than either the cobalt or palladium compounds. The patent claimed that maximum conversion rates amounted to several thousand mol of H_2 per mol of the catalyst.[185] Tungsten tris-dithiolene compounds have also been used as photocatalysts.[314] Atomic quantum clusters with up to some hundred atoms may not have metal, but rather semiconductor or insulating character because of their quantum confinement and the consequent separation of the energy levels. Nanoparticles to which at least a semiconductor consisting of an atomic quantum cluster of between 2 and 55 zerovalent atoms were linked have been patented; under these conditions, the interfacial charge transfer rate was increased and recombination much decreased, so that a better performance with respect to traditional oxide semiconductors was obtained.[315]

6.3 Photocatalysts different from oxides and sulfides

A worm-like mesoporous structured C_3N_4 photocatalyst was obtained by mixing an aqueous solution of melamine and low melting point salts followed by calcination in a furnace for 1 to 5 hours (400–680 °C); when irradiated (0.1 g) in 90 mL water in the presence of triethanolamine and 0.5 wt% Pt with a 300 W xenon lamp (>420 nm) the photocatalyst gave *ca.* 1350 μmol h^{-1} of hydrogen, approximately four times more than bulk C_3N_4.[316]

Nanosheets of copolymerization modified graphite-phase carbon nitride having a suitable dimensional nanolayer microstructure and an appropriate band gap improved the surface area and enhanced sunlight utilization compared to the bulk phase; the photocatalyst appears to have broad application prospects.[317] For instance, both the carbon nitride nanosheets and bulk carbon nitride (0.05 g) photocatalytically decomposed water in the presence of triethanolamine and 3 wt% Pt when irradiated with visible light (300 W xenon lamp, $\lambda > 420$ nm) producing 14.8 mmol h^{-1} g^{-1} of hydrogen compared to bulk carbon nitride which produced only 200 μmol h^{-1} g^{-1} of hydrogen, a 74-fold improvement. Silicon carbide (SiC) nanocrystals/graphene heterojunction photocatalysts have been obtained by annealing SiC nanocrystals at 1000–1600 °C *in vacuo* or in an argon atmosphere; they are characterized by an outer surface of a SiC nanocrystalline particle coated with at least one graphene layer – though a claim was made that the photocatalysts may find a niche in the photocatalytic production of hydrogen, none was reported.[318]

Irradiation of the niobium oxynitride NbON system (0.10 g) in 200 mL aqueous solution containing 10 vol% methanol at wavelengths 420 nm to 800 nm (300 W xenon lamp) yielded 8 μmol h^{-1} g^{-1} of hydrogen. However, if a $AgNO_3$ solution was used in the place of methanol, irradiation under the same conditions yielded 0.6 μmol h^{-1} g^{-1} of oxygen.[319] In the same vein, wrapping Ta_3N_5 particles (forming the shell) around Ta, Ta_2O_5 or TaON (the core) produced a heterojunction photocatalyst that was claimed to have a high light quantum conversion efficiency and could be used in hydrogen making from water photolysis; the inventors reported that in the presence of $AgNO_3$ as a sacrificial electron acceptor and irradiation of a 200 mL aqueous solution with a 0.2 g catalyst at 420 ± 15 nm yielded oxygen.[320]

A photocatalyst layer based on a visible-light-absorbing nitride or oxynitride of Ga, Zn, Ti, La, Ta, or Ba and a co-catalyst loaded onto this visible light-responsive optical semiconductor, as well as a hydrophilic inorganic material selected from SiO_2, Al_2O_3 or TiO_2 could, in principle, produce hydrogen and/or oxygen from the photodecomposition of water; for example, Ni,Ta-co-doped TiO_2 would be one such optical semiconductor.[321] A visible light absorbing photocatalyst aggregated on the external surface of a gallium nitride (GaN) crystal was claimed (bot not substantiated) to yield oxygen and hydrogen from water decomposition.[322]

6.4 Other photocatalysts for CO_2 reduction

Ultrathin $In_2Ge_2O_7$–ethylenediamine hybrid nanowires (diameter, 2–3 nm), prepared from indium acetate, germanium oxide and ethylenediamine through a simple and energy saving process,

(no need for high-temperature sintering), photocatalytically reduced CO_2 to CO when loaded with 1 wt% Pt.[323] The photocatalysts Ni/ZnS, Cu/ZnS, tantalum nitride, tantalum oxynitride, tantalum oxide, zinc sulfide, gallium phosphide, indium phosphide, silicon carbide, iron oxide, and an oxide of copper when coupled with a Re or a Ru complex, *e.g.*, $Re(dcbpy)(CO)_3MeCN$, $[Ru(dcbpy)(bpy)(CO)_2]^{2+}$ (dcbpy = 4,4′-dicarboxy-2,2′-bipyridine), and $[Ru(bpy)_2(CO)_2]^{2+}$ (bpy = 2,2′-bipyridine), also reduced CO_2 to CO and to HCOOH.[324] Graphite-phase carbonitride powdered samples (particle sizes, 200 nm to 10 μm) were obtained by heating nitrogen containing compounds, such as melamine and urea at 450–600 °C; visible light irradiation (>400 nm) of a platinized carbonitride sample (band gap, 2.7 eV) in aqueous media produced about 85 μL of hydrogen after *ca.* 50 hours and, although water splitting was claimed, no oxygen was sampled.[325] A system that included nanostructured arrays for converting CO_2 to organic compounds, such as methanol, was built as an array of nanotubes, *e.g.* an ordered array of TiO_2 nanoparticles and Pd nanoparticles; upon irradiation with 300 W simulated solar light the nanotubes (band gap for modified nanotube, 2.2 eV) produced methanol and dimethyl ether from the reduction of CO_2.[326] A US patent claimed that p-type semiconductors such as SiC, GaP, InT and GaAs in the presence of a mediator reduced CO_2 to gaseous hydrocarbons, predominantly methane.[327]

A nano plasma-type photocatalyst was prepared by decorating the surface of AgCl or AgBr particulates with Ag nanoparticles (4–15 wt%); the catalyst had uniform size, regular morphology and a useful activity under visible light for the reduction of CO_2.[328] Monodispersed Fe_3O_4 particles (the carriers) were coated with a SiO_2 shell layer, following which they were decorated with AgI forming a composite that subsequent to being photoreduced with visible light gave the magnetic photocatalyst Fe_3O_4/SiO_2/AgI:Ag, which adopted a magnetic nanocapsule-type structure.[167] Irradiation of this composite led to the photoreduction of CO_2 yielding methanol, ethanol and *n*-propanol; the total yield was 35.84 mmol g^{-1} after 3 cycles.[167] Carbon dioxide could also be reduced to CO with high selectivity on irradiation of Ga_2O_3 decorated with Ag particles at room temperature with no need for additional compounds.[329] In another process, the rhenium complex $Re(CO)_3LX$ (L is a 1,10-phenanthroline derivative; X an anionic or a neutral monodentate ligand) catalyzed the reduction of CO_2 to CO with yields less than 1 μmol after 2 hours of irradiation.[330] A graphene–porphyrin photocatalyst was instrumental in reducing CO_2 to HCOOH on irradiation in a CO_2-equilibrated solution containing (pentamethylcyclopentadienyl-2,2′-bipyridine-chloro)rhodium(III), NAD, and triethanolamine (efficiency, 30.7%).[331]

A system based on two components (Cu or Hg) in contact with each other, one of which catalyzed the reduction of gaseous CO_2 and was supported on an electrically conductive carrier such as carbon black, and the other component (Ag/TiO_2 or Pt/TiO_2) catalyzed the oxidation of water, was patented and claimed to exhibit good performance because the active sites were separated from each other and thus recombination of electric charges was prevented.[332] Another economically manufactured visible-light-responsive photocatalyst was described in a patent assignment to Toyota Corporation; the photocatalyst is based on p-type semiconductor materials comprised of hematite-type iron oxide crystals with nitrogen and metals as the dopants, and optionally with either a metal or a metal complex as the co-catalyst.[333]

A bifunctional catalyst responsive to visible light and consisting of Ag particles decorating AgX (Ag, 4–15 wt%; X = Cl, Br) catalyzed the reduction of CO_2 to methanol and ethanol (more of the former) by dispersing the Ag/AgX in a 50 mL aqueous Na_2CO_3 solution and subsequently irradiating with visible light (300 W xenon lamp); yields of the alcohols were less than 1 mmol h^{-1} g^{-1}.[178] By contrast, a micro-/nano-hierarchical structure bearing octahedral Zn_2SnO_4 with 1 wt% of either RuO_2 or Pt as a co-catalyst reduced CO_2 to CH_4, with the largest yield being *ca.* 17 ppm of methane.[334] A supposedly new and improved method for a light driven photocatalytic reduction of carbon dioxide (or the bicarbonate ion) to useful organic compounds was reported by Lichtin in a 1984 US patent in which silicon dust from solar-cell manufacturing was the catalyst in two different steps to reduce CO_2.[335] In the first step, CO_2 was reduced to methanol and formaldehyde at rates of 0.126 μmol h^{-1} g^{-1} and 0.32 μmol h^{-1} g^{-1}, respectively; in the second one, methanol, formaldehyde and formic acid were produced. The rate for methanol was 0.126 μmol h^{-1} g^{-1} and for formaldehyde 0.46 μmol h^{-1} g^{-1}. A strontium borate-like nano-photocatalyst with good dispersity and highly stable was obtained by a simple preparation method; it displayed photocatalytic efficiency greater than P25 TiO_2 for the reduction of CO_2 to CH_4 The latter photocatalyst produced 0.11 μmol h^{-1} g^{-1}, whereas the strontium borate photocatalyst produced 0.25 μmol h^{-1} g^{-1} of methane.[336]

6.5 Organic materials as photosensitizers/photocatalysts

Organic dyes are typically used as photosensitizers to allow extending the active wavelength range of wide band-gap semiconductor photocatalysts, though they could also act as photocatalysts. Dihydroxy substituted anthraquinone dyes were added in amounts up to 35 μmol g^{-1} to noble metal-loaded inorganic semiconductors in the presence of an organic sacrificial agent.[337] The patent claimed that the resulting visible-light-responsive photocatalyst generated hydrogen by the water splitting process – maximal quantity of H_2 produced was *ca.* 400 μmol over an irradiation period of 12 hours at >420 nm (300 W xenon lamp), with the turnover number being >6300; however, no oxygen was produced to support water splitting.[337] When irradiated with semiconductor materials consisting of metal oxides or sulfides (metal = Ti, Zr, Sr, Zn, In, Yr, La, V, Mo, W, Sn, Nb, Mg, Al, Y, Sc, or Ga), near infrared asymmetric cyanine or squarylium dyes–β-cyclodextrin composite solutions acting as photosensitizers could be used for the photocatalytic production of hydrogen; the patent gave no further details.[338] Xanthylium dyes (Scheme 1) have also been used to sensitize heterogeneous catalysts selected from colloidal Pt, colloidal Pd, Pt/TiO_2 or Pt/ZrO_2; when these were irradiated with visible light in aqueous media containing triethanolamine (the sacrificial electron donor) hydrogen evolved at a maximal rate of 1.30 μmol h^{-1}.[339]

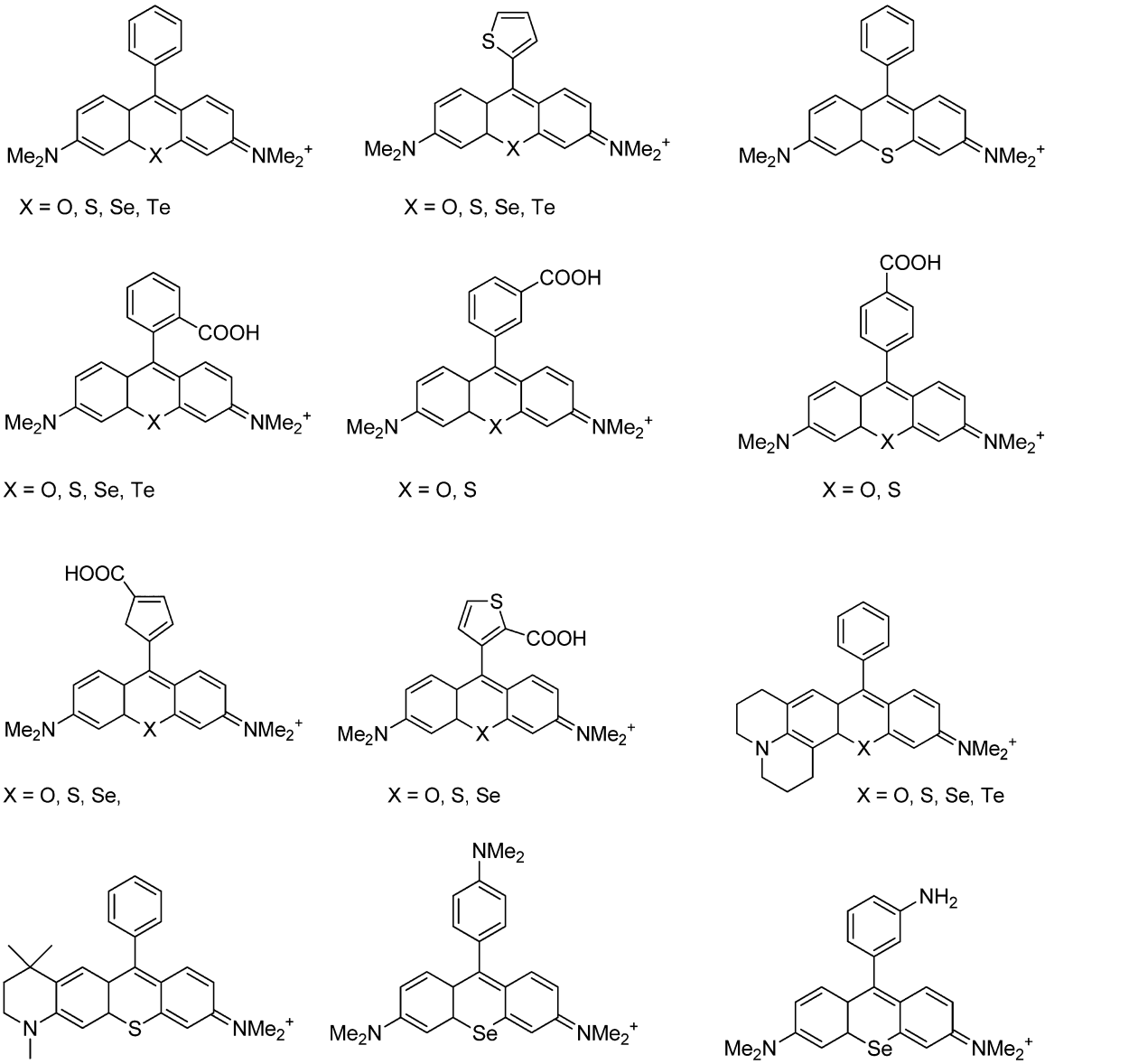

Scheme 1 Examples of compounds useful in the photosensitization of TiO_2. Adapted from ref. 339.

A patent published in 1986 reported a photocatalyst that consisted of an optionally heat-treated electrically conductive polymer such as polyparaphenylene, polythiophene or polymethaphenylene, and an organic substrate consisting of one or more sacrificial electron donors (*e.g.*, diethylamine or methanol); when irradiated at wavelengths 290–366 nm hydrogen was evolved from the aqueous media.[340] A visible-light-responsive photocatalyst was also reported that consisted of three layers, *viz.* (i) a perylene diimide derivative layer; (ii) a layer of a mixture of a perylene diimide derivative and [6,6]-phenyl-C_{61} methyl butyrate; and (iii) a [6,6]-phenyl-C_{61} methyl butyrate layer (Scheme 2); the photocatalyst was supported on an ITO conductive glass and when excited with visible light decomposed water photoelectrochemically into hydrogen and oxygen with the assistance of an electric field.[341] Irradiation with visible light (110 mW cm^{-2}) led to water splitting producing both hydrogen (2.3 μmol) and oxygen (1.1 μmol) in the expected ratio within 100 min. The ITO substrate alone caused no water decomposition.

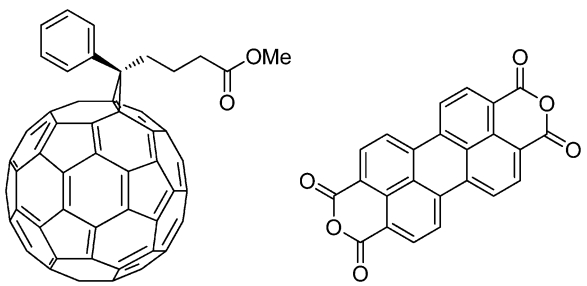

Scheme 2 Structures of [6,6]-phenyl-C_{61}-butyric acid methyl ester and perylene tetracarboxylic dianhydride.

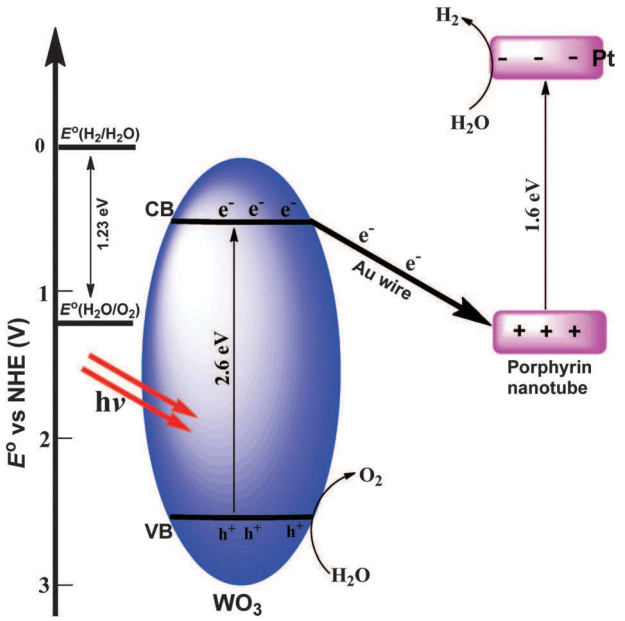

Fig. 20 Cartoon illustrating the electron excitation and transfer steps for a device where reduction of water is occurring at the nanotube composite and oxidation of water is occurring at an oxidation catalyst, WO_3. Adapted from ref. 342.

Porphyrin nanotubes can be formed *via* self-organization by mixing aqueous solutions of two or more porphyrin species, of which some are positively charged and some negatively charged; such nanotubes were used as photocatalysts to generate hydrogen by the photocatalytic decomposition of water – in some cases both hydrogen and oxygen were generated whenever the oxidation catalyst was selected from WO_3, $BiVO_4$, Fe_2O_3, TiO_2, RuO_2, IrO_2, and $Na_2B_4O_7$, and the reduction catalyst was a metal selected from Pt, Pd, Co, Ni.[342] The porphyrin nanotube comprised an inner surface and an external surface. The reduction catalysts could be linked to either surface. Fig. 20 illustrates both the reduction of water to form hydrogen and the oxidation of water to form oxygen. The process occurred by absorption of a photon of at least 1.6 eV by the porphyrin, which excites an electron out of the valence band of the porphyrin. Where the metallo-porphyrin is the tin-porphyrin system, the reduced Sn porphyrin has a redox potential 1.6 eV higher, at approximately −0.6 V, sufficient to reduce water to H_2. The reduction of water is allowed by the reduction catalyst which, in this case, is represented by Pt nanoparticles on the nanotube. Fig. 20 also shows that absorption of a blue photon (2.6 eV) results in the promotion of an electron from the valence band of WO_3 to the conduction band of this oxidation catalyst. The hole left in the valence band of WO_3 is then available to oxidize water to O_2, while the electron in the conduction band travels through the gold wire within the porphyrin nanotube and reduces the photoexcited tin porphyrin components. The solid-state molecule-based solar photocatalytic conversion approach reported in the patent by Shellnutt and co-workers[342] offers certain advantages as no wide band-gap semiconductors with associated sensitizers are required for the production of hydrogen from water reduction. In essence, as indicated in the patent, the porphyrin nanotubes function as organic semiconductors, which offer an inexpensive alternative to the more conventional semiconductors used in photocatalytic devices.

7. Concluding remarks

Quantitative comparison of results

An all important issue in any application is comparing the performance of different photocatalytic systems and some patents are devoted to this issue. The key points are measuring the actual amount of light absorbed (taking into account the reflected fraction) and the determination of the active wavelength range. In this regard, an integrating sphere-type light-catalyzed reaction measuring system was designed (i) to evaluate parameters such as apparent quantum yield in photocatalyzed processes and (ii) to assess the actual efficiency of photocatalyzed processes; of importance, the system involves the synchronous measurement of reactive light absorbing properties and the performance in producing hydrogen photocatalytically.[343] Along similar lines, a low-energy-consumption and highly stable liquid phase light-emitting diode (LED) photocatalysis reaction apparatus has been patented that consists of an integrated system of two parts: (1) a photocatalysis reaction chamber and an LED light source (wavelengths from 254 to 700 nm) and (2) a control system to assess quantitatively the performance of photocatalyzed processes.[344] For an accurate comparison, multichannel reaction devices are now available according to two Chinese patents – one of the apparatuses comprises 4 to 8 sealed reaction systems suited for measuring the hydrogen generated and assesses the photocatalyst performance. Apparently, the system is simple, easy to assemble, easy to operate, and the components are inexpensive. The use leaves a small C-footprint, requires only a small working area and yields credible performance.[345] Yet another multipurpose photocatalytic performance assessment device has been patented for testing the degradation reaction performance of photocatalytic depollution of organic matter and the reaction performance in converting carbon dioxide to carbon-based fuels; the patent also claimed that the multipurpose assessment device is simple, convenient to operate, easy to assemble, can be used for multiple purposes, and affords high treatment efficiency and low consumption costs.[346]

An appropriate glossary is required

An examination of the patent literature shows the variety of materials and methods that have been thought to be worth protecting. Thus it may be concluded that the practical application of methods producing fuels from water and carbon dioxide is, in principle, thought to be credible. Unfortunately, many misunderstandings occur on what the experiments mean, starting from the appropriate wording. First of all, the process is often referred to as *water splitting*. More appropriately the splitting of the water molecule is an appropriately designed process leading from water to hydrogen and oxygen in a ratio of 2 hydrogen

molecules for every molecule of oxygen evolved. Far too often, however, both the patent literature and the open literature claim to produce only hydrogen, but no oxygen (or at least not tested for it), from the photodecomposition of an aqueous solution in the presence of some metal-oxide photocatalyst. Furthermore, this happens in the presence of some sacrificial electron donor, such as alcohols, triethanolamine, EDTA and the like, so that no *water splitting* can be claimed under these conditions. Another issue is how casually the terms *photocatalysis* and *photocatalyst* are being used. We know of only one or two cases where a metal oxide, for example ZrO_2, was experimentally demonstrated to act as a photocatalyst by the determination of the turnover numbers,[347] using no less than three different experimental procedures.[348] In other cases, zirconia was clearly not a photocatalyst.[349,350] The criteria and the conditions by which a metal oxide semiconductor can be referred to as a photocatalyst have been amply described by Emeline and co-workers[347,349,351–353] and need not be repeated here. In particular, patent claimants (similarly in the open literature) often used dyes, such as methylene blue and rhodamine, to determine the photo(catalytic) activity of a metal-oxide substrate. This is a quick and simple experiment, but has to be strongly discouraged since dyes absorb light in exactly the same spectral region as the metal oxide. Thus, when a dye/metal oxide combination is used, the dye can act as a photosensitizer and be decomposed by its own photochemical reaction,[354–361] not necessarily by the activated metal oxide. In fact, the photoactivity of a metal-oxide substrate should be determined by assessing the true photochemically defined quantum yield (not quantum efficiency) of the process, albeit this implies some experimental difficulty.[362,363]

The catalyst issue

Transition from first-generation photocatalysts (*i.e.* pristine metal oxides) to second-generation photocatalysts (*i.e.* anion- or cation-doped materials) resulted from the notion that a greater absorption of the incident light in the visible spectral region would lead to a greater photoactivity of the materials synthesized. In fact, the sole principal goal in transitioning from first to second generation photoactive materials was the extension of the spectral response to longer wavelengths and the assumption that such extension would automatically lead to increased photoactivity. Although the strategy looked promising, in practice, however, it did not lead to the expected results because of numerous side effects typically caused by doping, such as formation of intrinsic defects, for example. In many cases this led to loss of photoactivity and chemical reactivity. An important contribution to this negative result is the likelihood that such induced defects might be good electron/hole recombination centers.[19] With regard to first-generation photocatalysts, studies that spanned the decade between 1965 to 1976 by Basov and co-workers[363–365] on some 35 different pristine metal oxides from NiO (band gap energy, <2 eV) to BeO (band gap energy, >10 eV) demonstrated that their photoactivity toward the photoreduction of oxygen and photooxidation of hydrogen and methane increased with an increase in band gap energy.

The only way for assessing quantitatively the modification of metal oxides by introducing chemical dopants to obtain the second-generation materials is varying the dopant concentration. However, this has the disadvantage that the photocatalytic activity needs to be ascertained at every concentration. In fact, different techniques for doping, or for that matter for any modification of photocatalysts, even a physical one, may result in similar spectral responses, but in different photocatalytic activities.[95–97] From this point of view, as highlighted by Selli *et al.* in their review,[49] the development of preparation techniques (including Magnetron Sputtering[110] and Flame Spray Pyrolysis[139]) capable of tuning the physico-chemical properties of photoactive materials is of crucial importance in the development of efficient photocatalysts.

What has been learned from the multitude of studies of first- and second-generation photocatalysts constitutes a good basis for the preparation of third generation materials; for instance, synthesizing photoactive materials that can be excited through multi(two)-photon events with low-energy photons (visible light) in order to achieve the same excited state as with high energy photons (UV radiation), and utilize heterojunctions to drive the electronic processes in the desired direction.[19]

The contribution of photocatalysis to the hydrogen economy

Returning to more practical matters, though much has been published in the scientific literature and, as demonstrated herein, also in the patent literature, the yields of hydrogen – claimed to be significant in nearly all of the patents – are at present disappointingly low and far from convincing investors and industries that the so-called *hydrogen economy* is upon us.[367]

Currently, steam reforming of fossil fuels remains the ultimate and most convenient choice to produce hydrogen (that is mostly used for the synthesis of chemicals such as ammonia), despite the simultaneous production of carbon dioxide in amounts ranging from 2.5 to 5 times that of hydrogen obtained.[367,368] The use of large-scale capture processes of CO_2 would give access to the conversion (including photocatalytic conversion)[37] of this side product into synthetic fuels but the development of carbon-free hydrogen production protocols is certainly preferable.[368] From this point of view, water is the elective non-carbogenic source and its dissociation *via* electrical, thermal, photochemical, biological or combined processes may prove to be the ultimate way to produce renewable hydrogen.[368] Germane to this, in 2011 Abbasi reviewed the available facilities for the generation of hydrogen from water, highlighting that none of the developed technologies available are yet economic;[368] even the photovoltaic-electrolysis system[366] seems to be attractive for electricity production rather than for the generation of hydrogen, for which the cost lacks of competitiveness. Photocatalysis represents another promising area of research, though still far from a commercial route. In a recent review devoted to TiO_2 photocatalysis for air treatment,[369] Paz highlighted the disparity between the huge number of published scientific papers and the limited number of commercial products that exploited photocatalysts, with practically no positive effect on the day by day life of the average citizen.

Unfortunately, manuscripts analysing the commercial situation of patents on specific arguments are scarcely reported in the literature. With regard to photocatalysis, one of the few reports attributed to Mills and Lee in 2002 listed only patents associated with products for air and water purification.[370]

There is no doubt that great advances have been carried out in the decades following the experiment of Fujishima and Honda,[1] and, as shown by the impressive number of patents published. The interest for these materials is not merely scientific but also applicative. In this regard, we note that the majority of patents examined in this review article originate from academic environments, and are supposedly aimed to act as *trait d'union* between academic and industrial communities.[371]

Perspectives

Much remains to be done in the search for the *holy grail photocatalyst*, a material that when added to pure water evolves both hydrogen and oxygen simultaneously, without the need for either sacrificial electron donors and/or electron acceptors. Perhaps we need to have two different photocatalysts that work in tandem, one that acts as the photocathode (hydrogen evolution) and the other as the photoanode (oxygen evolution) located within the same water bath and with the energy coming only from the incident sunlight radiation to activate both the cathode and the anode.[29,372] In such case, there would be no need to close the circuit as currently done in the photoelectrochemically-assisted water splitting. Fig. 10 points in that direction, although in that case there was a need to close the circuit. A great advancement in this field is represented by the work of Nocera.[3c] Science needs to be more innovative, first in developing novel materials,[373] and subsequently in developing those processes that can achieve the *sustained* availability of energy from hydrogen as the energy source; after all sunlight and water are two inexhaustible resources. It would be useful that future research, whether in patents or in an open forum, will attempt to communicate all the needed key characteristics of the material considered, that is the lifetime of the photogenerated electron–hole pair, the surface area of the catalyst (that also influenced the former factor), the reproducibility and the photo-hydro stability of the employed materials, as suggested by Bowker in a recent review,[374] disregarding oversimplified rationalizations that, as commented above, often have little physical basis. On the other hand, although TiO_2-based photocatalysts generally exhibit low efficiencies, they are nonetheless still considered as the most promising materials in the field of photocatalysis.

Acknowledgements

Financial support from the Fondazione Cariplo (Grant No. 2009–2579) is gratefully acknowledged. S. P. acknowledges MIUR, Rome (FIRB-Futuro in Ricerca 2008 project RBFR08J78Q) for financial support. We are also most grateful to Dr Sara Montanaro for her tireless contribution to the patent literature search.

References

1 A. Fujishima and K. Honda, *Nature*, 1972, **238**, 37–38.
2 T. Inoue, A. Fujishima, S. Konishi and K. Honda, *Nature*, 1979, **277**, 637–638.
3 See for example: (*a*) S. Y. Reece, J. A. Hamel, K. Sung, T. D. Jarvi, A. J. Esswein, J. J. H. Pijpers and D. G. Nocera, *Science*, 2011, **334**, 645–648; (*b*) J. J. H. Pijpers, M. T. Winkler, Y. Surendranath, T. Buonassisi and D. G. Nocera, *Proc. Natl. Acad. Sci. U. S. A.*, 2011, **108**, 10056–10061; (*c*) D. G. Nocera, *Acc. Chem. Res.*, 2012, **45**, 767–776.
4 J. R. Bolton, *Science*, 1978, **202**, 705–711.
5 K. Maeda, *ACS Catal.*, 2013, **3**, 1486–1503.
6 K. Nakata, T. Ochiai, T. Murakami and A. Fujishima, *Electrochim. Acta*, 2012, **84**, 103–111.
7 K. Maeda, *J. Photochem. Photobiol., C*, 2011, **12**, 237–268.
8 M. D. Hernandez-Alonso, F. Fresno, S. Suarez and J. M. Coronado, *Energy Environ. Sci.*, 2009, **2**, 1231–1257.
9 C. H. Liao, C. W. Huang, C. Wie and J. C. S. Wu, *Catalysts*, 2012, **2**, 490–516.
10 Y. H. Hu, *Angew. Chem., Int. Ed.*, 2012, **51**, 12410–12412.
11 Y. Li, H. Liu and C. Wang, *Curr. Inorg. Chem.*, 2012, **2**, 168–183.
12 K. Takanabe and K. Domen, *ChemCatChem*, 2012, **4**, 1485–1497.
13 T. Hisatomi, T. Minegishi and K. Domen, *Bull. Chem. Soc. Jpn.*, 2012, **85**, 647–655.
14 V. H. Nguyen and B. H. Nguyen, *Adv. Nat. Sci.: Nanosci. Nanotechnol.*, 2012, **3**, 023001.
15 G. P. Smestad and A. Steinfeld, *Ind. Eng. Chem. Res.*, 2012, **51**, 11828–11840.
16 P. D. Tran, L. H. Wong, J. Barber and J. S. C. Loo, *Energy Environ. Sci.*, 2012, **5**, 5902–5918.
17 A. Dhakshinamoorthy, S. Navalon, A. Corma and H. Garcia, *Energy Environ. Sci.*, 2012, **5**, 9217–9233.
18 E. V. Kondratenko, G. Mul, J. Baltrusaitis, G. O. Larrazábal and J. Pérez-Ramírez, *Energy Environ. Sci.*, 2013, **6**, 3112–3135.
19 A. V. Emeline, V. N. Kuznetsov, V. K. Ryabchuk and N. Serpone, *Environ. Sci. Pollut. Res.*, 2012, **19**, 3666–3675.
20 J. M. Herrmann, *Environ. Sci. Pollut. Res.*, 2012, **19**, 3655–3665.
21 N. Serpone, A. V. Emeline, S. Horikoshi, V. N. Kuznetsov and V. K. Ryabchuk, *Photochem. Photobiol. Sci.*, 2012, **11**, 1121–1150.
22 B. Ohtani, *Adv. Inorg. Chem.*, 2011, **63**, 395–430.
23 M. A. Fox and M. T. Dulay, *Chem. Rev.*, 1993, **93**, 341–357.
24 A. L. Linsebigler, G. Lu and J. T. Yates, *Chem. Rev.*, 1995, **95**, 735–758.
25 M. R. Hoffman, S. T. Martin, W. Choi and D. W. Bahnemann, *Chem. Rev.*, 1995, **95**, 69–96.
26 X. Chen and S. S. Mao, *Chem. Rev.*, 2007, **107**, 2891–2959.
27 X. Chen, S. Shen, L. Guo and S. S. Mao, *Chem. Rev.*, 2010, **110**, 6503–6570.
28 A. Kubacka, M. Fernandez-Garcia and G. Colon, *Chem. Rev.*, 2012, **112**, 1555–1614.
29 M. G. Walter, E. L. Warren, J. R. McKone, S. W. Boettcher, Q. Mi, E. A. Santori and N. S. Lewis, *Chem. Rev.*, 2010, **110**, 6446–6473.

30 A. J. Nozik and J. Miller, *Chem. Rev.*, 2010, **110**, 6443–6445.
31 T. R. Cook, D. K. Dogutan, S. Y. Reece, Y. Surendranath, T. S. Teets and D. G. Nocera, *Chem. Rev.*, 2010, **110**, 6474–6502.
32 J. Michl, *Nat. Chem.*, 2011, **3**, 268–269.
33 J. R. McKone, N. S. Lewis and H. B. Gray, *Chem. Mater.*, 2013, **26**, 407–414.
34 B. A. Pinaud, J. D. Benck, L. C. Seitz, A. J. Forman, Z. Chen, T. G. Deutsch, B. D. James, K. N. Baum, G. N. Baum, S. Ardo, H. Wang, E. Miller and T. F. Jaramillo, *Energy Environ. Sci.*, 2013, **6**, 1983–2002.
35 T. A. Faunce, Future Perspectives of Solar Fuels, in *Molecular Solar Fuels*, ed. T. J. Wydrzynski and W. Hillier, Royal Society of Chemistry, Cambridge, UK, 2012, pp. 506–524; T. Faunce, *Aust. J. Chem.*, 2012, **65**, 557–563.
36 N. S. Lewis, G. Crabtree, A. J. Nozik, M. R. Wasielewski and P. Alivisatos, *Basic Research Needs for Solar Energy Utilization*, Report of the Basic Energy Sciences Workshop on Solar Energy Utilization, April 18-21, 2005, Office of Basic Energy Sciences, Department of Energy, Washington, D.C., report available at http://www.sc-doe.gov/bes/reports/files/SEU_rpt.pdf, accessed February 2014.
37 A genuine water-splitting process involving rutile TiO_2 powder has been recently reported by Maeda, see K. Maeda, *Catal. Sci. Technol.*, 2014, **4**, 1949–1953; K. Maeda, *Chem. Commun.*, 2013, **49**, 8404–8406.
38 (*a*) K. Li, X. An, K. H. Park, M. Khraisheh and J. Tang, *Catal. Today*, 2014, **224**, 3–12; (*b*) S. N. Habisreutinger, L. Schmidt-Mende and J. K. Stolarczyk, *Angew. Chem., Int. Ed.*, 2013, **52**, 7372–7408.
39 Y. Izumi, *Coord. Chem. Rev.*, 2013, **257**, 171–186.
40 F. E. Osterloh, *Chem. Mater.*, 2008, **20**, 35–54.
41 For the meaning of quantum efficiency *versus* quantum yield see: S. E. Braslavsky, A. M. Braun, A. E. Cassano, A. V. Emeline, M. I. Litter, L. Palmisano, V. N. Parmon and N. Serpone, *Pure Appl. Chem.*, 2011, **83**, 931–1014.
42 F. Fresno, R. Portela, S. Suarez and J. M. Coronado, *J. Mater. Chem. A*, 2014, **2**, 2863–2884.
43 R. Portela and M. D. Hernandez-Alonso, Environmental Applications of Photocatalysis, in *Design of Advanced Photocatalytic Materials for Energy and Environmental Applications*, ed. J. M. Coronado, F. Fresno, M. D. Hernandez-Alonso and R. Portela, Springer, London, UK, 2013, ch. 3, ISBN 2013978-1-4471-5060-2.
44 A. Zaleska, *Recent Pat. Eng.*, 2008, **2**, 157–164.
45 S. M. Lam and A. R. Mohamed, *Recent Pat. Chem. Eng.*, 2008, **1**, 209–219.
46 B. Ohtani, *Recent Pat. Eng.*, 2010, **4**, 149–154.
47 G. Panayiotou, P. Gregoris, S. A. Kalogirou and S. A. Tassou, *Recent Pat. Mech. Eng.*, 2010, **3**, 226–235.
48 G. Panayiotou, S. Kalogirou and S. Tassou, *Recent Pat. Mech. Eng.*, 2010, **3**, 154–159.
49 G. L. Chiarello and E. Selli, *Recent Pat. Eng.*, 2010, **4**, 155–169.
50 H. Nakanishi and T. Nakayama, Toshiba corporation, *Jpn Pat.*, 60044053A, 1985.
51 H. Yamakita, T. H. Masato and T. Kiyoshi, *Jpn. Pat.*, 63035402A, 1988.
52 T. Ravindranathan, The Hydrogen Solar Production Company Limited, *World Pat.*, 2002022497A1, 2002.
53 D. Liao, Y. Ou, J. Lin and S. Fang, *Chin. Pat.*, 100396373C, 2008.
54 G. Chen, Z. Shang and Z. Li, *Chin. Pat.*, 101229514B, 2010.
55 Z. Feng, J. Zhang, Q. Xu, C. Li, X. L. Wang and Y. Ma, *Chin. Pat.*, 101884914A, 2010.
56 J.-C. Chung, Y.-Z. Zeng, Y.-C. Liu and Y.-F. Lu, *US Pat.*, 20100105549A1, 2010.
57 X. Cui and X. Zhang, *Chin. Pat.*, 101513610A, 2009.
58 Z. Wang, B. Huang, X. Zhang and X. Qin, *Chin. Pat.*, 102633303A, 2009.
59 Y. Zhang and L. Zhao, *Chin. Pat.*, 101767023A, 2010.
60 X. Cui and M. Sun, *Chin. Pat.*, 102553626A, 2012.
61 X. Zhang and X. Cui, *Chin. Pat.*, 102357365B, 2013.
62 L. Jing, M. Xie, H. Fu and X. Fu, *Chin. Pat.*, 103157498A, 2013.
63 G. Jiang, Q. Zhang, X. Cui, Z. Zhao, C. Xu, A. Duan, J. Liu and Y. Wei, *Chin. Pat.*, 103240130A, 2013.
64 D. Zhang, S. Xiao, P. Liu, S. Zhang and H. Li, *Chin. Pat.*, 103191739A, 2013.
65 W. Huang, Y. Liu and W. Wang, *Chin. Pat.*, 103263920A, 2013.
66 B. Tian, F. Yang, Y. Li, J. Zhang, T. Wang, T. Xiong, X. Chen, R. Dong and T. Li, *Chin. Pat.*, 102874751A, 2013.
67 D. O. Scanlon, C. W. Dunnill, J. Buckeridge, S. A. Shevlin, A. J. Logsdail, S. M. Woodley, C. R. A. Catlow, M. J. Powell, R. G. Palgrave, I. P. Parkin, G. W. Watson, T. W. Keal, P. Sherwood, A. Walsh and A. A. Sokol, *Nat. Mater.*, 2013, **12**, 798–801.
68 Daicel Corporation, *Jpn. Pat.*, 2013014443A, 2013.
69 N. Lakshminarasimhan, *Kor. Pat.*, KR2009072745A, 2009.
70 M. G. Xu, *Chin. Pat.*, 1724144A, 2006.
71 B. Tian, T. Li, S. Bao, J. Zhang, R. Dong and Z. Lian, *Chin. Pat.*, 102500349A, 2012.
72 X. Wang and C. Liu, *Chin. Pat.*, 102381727A, 2012.
73 H. Fu, T. Li, W. Zhou, L. Wang, Z. Xing, K. Pan, G. Tian, F. Sun and C. Tian, *Chin. Pat.*, CN102744050A, 2012.
74 X. Li, W. Zhong, D. Zhang, G. Li and H. Li, *Chin. Pat.*, 103170319A, 2013.
75 R. Zhou, M. Chen, F. Wu and Y. Zhao, *Chin. Pat.*, 1654118A, 2005.
76 J. Zhi, Y. Li and L. Wu, *Chin. Pat.*, 102863638A, 2013.
77 S. Yokoo and D. Tokunaga, *Jpn. Pat.*, 2001089704A, 2001.
78 J. M. Guerra, *US Pat.*, 20030228727A1, 2003.
79 J. M. Guerra, *US Pat.*, 20090116095A1, 2009.
80 D. Duonghong, N. Serpone and M. Grätzel, *Helv. Chim. Acta*, 1984, **67**, 1012–1018.
81 D. Duonghong, N. Serpone and M. Grätzel, *Sci. Pap. Inst. Phys. Chem. Res.*, 1984, **78**, 232–236.
82 N. Serpone, E. Pelizzetti and M. Grätzel, *Coord. Chem. Rev.*, 1985, **64**, 225–246.
83 M. Wielopolski, K. E. Linton, M. Marszatek, M. Gulcur, M. R. Bryce and J. E. Moser, *Phys. Chem. Chem. Phys.*, 2014, **16**, 2090–2099.

84 Z. Wang, Y. Liu, B. Huang, Y. Dai, Z. Lou, G. Wang, X. Zhang and X. Qin, *Phys. Chem. Chem. Phys.*, 2014, **16**, 2758–2774.
85 N. Serpone, E. Borgarello and M. Grätzel, *J. Chem. Soc., Chem. Commun.*, 1984, 342–344.
86 N. Serpone, E. Borgarello, E. Pelizzetti and M. Barbeni, *Chim. Ind.*, 1985, **67**, 318–324.
87 E. Borgarello, N. Serpone, M. Grätzel and E. Pelizzetti, *Inorg. Chim. Acta*, 1986, **112**, 197–201.
88 P. Pichat, E. Borgarello, J. Disdier, J.-M. Hermann, E. Pelizzetti and N. Serpone, *J. Chem. Soc., Faraday Trans. 1*, 1988, **84**, 261–274.
89 N. Serpone, E. Borgarello and E. Pelizzetti, *J. Electrochem. Soc.*, 1988, **135**, 2760–2766.
90 N. Serpone, P. Maruthamuthu, P. Pichat, E. Pelizzetti and H. Hidaka, *J. Photochem. Photobiol., A*, 1995, **85**, 247–255.
91 R. Peng, C. Lin, J. Baltrusaitis, C.-M. Wu, N. M. Dimitrijevic, T. Rajh, S. May and R. T. Koodali, *Phys. Chem. Chem. Phys.*, 2014, **16**, 2048–2061.
92 M. Grätzel, J. Kiwi, K. Kalyanasundaram and J. Philp, *Ger. Pat.*, 3033693A1, 1981.
93 D. Duonhong, M. Grätzel and N. Serpone, *US Pat.*, 4684537A, 1987; the *Swiss Pat.*, CH1985/000066 on this work was registered on April 30, 1985. Work was also patented elsewhere under the following numbers: DE3571456D1, EP0179823A1, EP0179823B1 and WO1985005119A1.
94 (*a*) R. Asahi, T. Morikawa, T. Ohwaki, K. Aoki and Y. Taga, *Science*, 2001, **293**, 269–273; see for instance: (*b*) R. Long and N. J. English, *J. Phys. Chem. C*, 2010, **114**, 11984–11990; (*c*) R. Long and N. J. English, *Chem. Phys. Lett.*, 2009, **478**, 175–179; (*d*) F. Spadavecchia, G. Cappelletti, S. Ardizzone, M. Ceotto and L. Falciola, *J. Phys. Chem. C*, 2011, **115**, 6381–6391.
95 A. V. Emeline, V. N. Kuznetsov, V. K. Ryabchuk and N. Serpone, *Int. J. Photoenergy*, 2008, 258394.
96 N. Serpone, *J. Phys. Chem. B*, 2006, **110**, 24287–24293.
97 V. N. Kuznetsov and N. Serpone, *J. Phys. Chem. B*, 2006, **110**, 25203–25209.
98 V. N. Kuznetsov and N. Serpone, *J. Phys. Chem. C*, 2007, **111**, 15277–15288.
99 V. N. Kuznetsov and N. Serpone, *J. Phys. Chem. C*, 2009, **113**, 15110–15123.
100 X. Qin, Z. Zheng, X. Zhang and B. Huang, *Chin. Pat.*, 102631909A, 2012.
101 X. Zhou, B. Jin and X. Xu, *Chin. Pat.*, CN103240068A, 2013.
102 G. Liu and H. Cheng, *Chin. Pat.*, 102343260A, 2012.
103 Y. Cao, J. Yuan, E. Wang and H. Long, *Chin. Pat.*, 101444724A, 2009.
104 H. Xu, R. R. Yeredla and K.-S. Hong, *US Pat.*, 20080223713A1, 2008.
105 L. M. Thulin, *World Pat.*, 2012159099A2, 2012.
106 J. S. Gao, *Chin. Pat.*, 1962459A, 2007.
107 W. Shangguan, J. Yuan and M. Chen, *Chin. Pat.*, 1583250A, 2005.
108 Y. Ikuma, A. Srinivasan and K. Niwa, *Jpn. Pat.*, 2009269766A, 2009.
109 S. J. Moon, G. J. Kim, W. U. So, J. U. Baek, J. U. Shin, D. S. Park and H. M. Lee, *Kor. Pat.*, 2009087731A, 2009.
110 S. Anpo, M. Matsuoka, M. Takeuchi and M. Kitano, *Jpn. Pat.*, 2007253148A, 2007.
111 W. Cai, M. Long and Y. Wu, *Chin. Pat.*, 101844077A, 2010.
112 K. Parida, G. B. B. Varadwaj, P. Chandra and S. Sahu, *Eur. Pat.*, 2436439A1, 2012.
113 Y. Zhou, Z. Zhu and M. Dang, *Chin. Pat.*, 102485969A, 2012.
114 J. Yu, W. Wang and B. Cheng, *Chin. Pat.*, 101524642A, 2009.
115 S. Yonezawa, M. Takashima, J.-H. Kim and T. Kubo, *Jpn. Pat.*, 2011207628A, 2011.
116 W. Cai, J. Xu and Z. Wang, *Chin. Pat.*, 1556151A, 2004.
117 (*a*) H. Cheng, *Chin. Pat.*, 1810355A, 2006; (*b*) H. Cheng, Z. Chen, F. Li, H. D. Lu, H. T. Cong and G. Liu, *Chin. Pat.*, 100348313C, 2007.
118 J. Choi, H. Park and M. R. Hoffmann, Effects of Single Metal-Ion Doping on the Visible-Light Photoreactivity of TiO_2, *J. Phys. Chem. C*, 2010, **114**, 783–792 and references therein.
119 Y. Oosawa, *Jpn. Pat.*, 59203701A, 1984.
120 H. Cheng, G. Liu, F. Li, M. Liu and G. Lu, *Chin. Pat.*, 101204649A, 2008.
121 N. Hoshino, M. Fukuda, H. Kita and H. Ito, *Jpn. Pat.*, 09271664A, 1997.
122 Y. Zhou, H. Guo and B. Yang, *Chin. Pat.*, 1327878A, 2001. Also published as *Chin. Pat.*, 1116927C, 2003.
123 Y. Ikuma, K. Niwa and T. Yoshioka, *Jpn. Pat.*, 2009078226A, 2009.
124 C. Shu and T. Kawashima, *Jpn. Pat.*, 2012139613A, 2012.
125 L. Xu, L. Wang, J. Chen, Z. Hu and Y. Huang, *Chin. Pat.*, 103223338A, 2013.
126 Y. Li, Y. Wang, W. Zhang, D. Wang, H. Chen and Q. Wang, *Chin. Pat.*, 103055905A, 2013.
127 Y. Li, Y. Wang, W. Zhang, D. Wang, H. Chen and Q. Wang, *Chin. Pat.*, 103041836A, 2013.
128 Z. Luo, Q. Yan and X. Cheng, *Chin. Pat.*, 1657159A, 2005. Also published as *Chin. Pat.*, CN1290611C, 2006.
129 *World Pat.*, 201301293A1, 2013.
130 M. Gu, M. Zheng and Y. Jin, *Chin. Pat.*, 1288779A, 2001.
131 S. B. Park, H. U. Kang, S. N. Lim and D. S. Song, *Kor. Pat.*, 2013091856A, 2013.
132 A. Kudo, *Jpn. Pat.*, 2004008963A, 2004. Also published as *Jpn. Pat.*, 4076793B2, 2008.
133 Y. Inoue and S. Ashiritsu, *Jpn. Pat.*, 07088370A, 1995. See also http://www.j-tokkyo.com/1995/B01J/JP07088370. shtml.
134 J.-M. Lehn, J.-P. Sauvage and R. Ziessel, *Fr. Pat.*, 2493181A1, 1982. Also published as *Fr. Pat.*, 2493181B1, 1984.
135 Y. Yokozawa, *Jpn. Pat.*, 2010228981A, 2010.
136 Y. Yokozawa and K. Uda, *Jpn. Pat.*, 2008104899A, 2008.
137 Y. Yokozawa and K. Uda, *Jpn. Pat.*, 2008214122A, 2008.
138 J. Zhang, L. Zhu, J. Yang, Z. Chen and T. Wang, *Chin. Pat.*, 102513129A, 2012.
139 H. D. Jang, *Kor. Pat.*, 2005064623A, 2005.
140 F. Fuwen, G. Zhang and X. Lu, *Chin. Pat.*, 102266789A, 2011.
141 J. Zhang, M. Xing, X. Yang, Y. Pan, D. Qi, W. Fang, Z. Xi and Y. Zhou, *Chin. Pat.*, 103007913A, 2013.

142 H. Liu, X. Dong, C. Duan, X. Su, J. Li and Z. Zhu, *Chin. Pat.*, 103285845A, 2013.
143 X. Li, Y. Hou, Q. Zhao, Q. Xie and G. Chen, *Chin. Pat.*, 101537354A, 2009.
144 F. Zhang and F. Xiu, *Chin. Pat.*, 101608263A, 2009.
145 S. Kaneko, C. V. Suresh and K. Sugihara, *Jpn. Pat.*, 2010119920A, 2010.
146 Y. Liu, *Chin. Pat.*, 1786087A, 2006.
147 Y. Zhang, Y. Yang, P. Xiao, M. Zhan and X. Zhang, *Chin. Pat.*, 101613080B, 2011.
148 J. Dasheng, *Chin. Pat.*, 1587026A, 2005.
149 H. S. Kim and K. B. Yoon, *Kor. Pat.*, 20120117074A, 2012.
150 S. Lucatero and E. J. Podlaha-Murphy, *World Pat.*, 2012037478A1, 2012.
151 G. Wang, H. Zhang, J. Li, D. Chen and W. Lu, *Chin. Pat.*, 101143712B, 2011.
152 N. Zhao, J. Sha, E. Liu, C. Shi, C. He and J. Li, *Chin. Pat.*, 102658107A, 2012.
153 H. Matsui, H. Nagai, C. Kiyono and T. Sato, *Jpn. Pat.*, 2008114178A, 2008.
154 D. Zhang, X. Shi, Q. Li, M. Wen, S. Zhang and H. Li, *Chin. Pat.*, 103223335A, 2013.
155 C. Zhao, H. Luo, P. Zhang, Y. Zhang, C. Liao and X. Liu, *Chin. Pat.*, 102107850A, 2011.
156 I. M. Kobasa, W. J. Strus and M. A. Kovbasa, *US Pat.*, 7662476B2, 2010.
157 F. Huang and X. Lu, *Chin. Pat.*, 102234133B, 2013.
158 J. Liu and J. Wang, *Chin. Pat.*, 102274738A, 2011.
159 L. Zhang, J. Zhang, W. Zhang, H. Zhong, S. Zhou and Y. Zhao, *Chin. Pat.*, 103301858A, 2013.
160 J. Yan, L. Zhang, J. Yi, K. Tang, Z. Hou, S. Zheng, Y. Pan and Q. Liu, *Chin. Pat.*, 101623635A, 2010.
161 T. Douglas, T. E. Elgren, J. W. Peters and M. J. Young, *World Pat.*, 2007086918A2, 2007.
162 D. Jun and J. Yang, *Chin. Pat.*, 102500388A, 2012.
163 I. Moriya, *Jpn. Pat.*, 2009275033, 2009.
164 Z. Yu, Y. Yuan and Z. Zou, *Chin. Pat.*, 102532170A, 2012.
165 Y.-C. Ling and J.-Y. Liu, *US Pat.*, 20130252798A1, 2013.
166 C. An, J. Wang, R. Zhang, W. Jiang, S. Wang and Q. Zhang, *Chin. Pat.*, 102658177B, 2013.
167 C. An, X. Ming, J. Wang, R. Zhang, S. Wang and Q. Zhang, *Chin. Pat.*, 102658178A, 2012.
168 B. Aurian-Blajeni, M. M. Halmann and M. Ulman, *US Pat.*, 4478699, 1984.
169 H. Shi and L. Yang, *Chin. Pat.*, 102658139A, 2012.
170 S. S. Rayalu, T. Chakrabarti, M. V. Joshi, P. A. Mangrulkar, N. K. Labhsetwar, R. M. S. Yadav, C. Prabhu and S. R. Wate, *World Pat.*, 2013046228A1, 2013.
171 G. Corti, T. C. Cantrell, M. F. Beaux, T. Prakash, D. N. Mcilroy and G. M. Norton, *World Pat.*, 2011050345A1, 2011.
172 T. Ihara, *Jpn. Pat.*, 2009190981A, 2009.
173 I. Moriya, *Jpn. Pat.*, 2009292821A, 2009.
174 T. Ichimura, Y. Matsushita, T. Suzuki, T. Murata, K. Tanihata, Y. Mizuno, M. Saito and T. Yamazaki, *Jpn. Pat.*, 2009029811A, 2009.
175 Nippon Telegraph & Telephone, *Jpn. Pat.*, 2013035698A, 2013.
176 Nippon Telegraph & Telephone, *Jpn. Pat.*, 2013034915A, 2013.
177 A. Yoshida, K. Kan, T. Kida, T. Harada and M. Isayama, *Jpn. Pat.*, 2004059507A, 2004.
178 Y. Zhao, X. Zhuo, J. Zhang, C. Tian and C. Zheng, *Chin. Pat.*, 102580526A, 2012.
179 J. Liu and W. Chen, *Chin. Pat.*, 101947441B, 2013.
180 A. Yoshida, K. Kan and T. Kida, *Jpn. Pat.*, 2003275599A, 2003.
181 Z. Zhao, J. Wang, J. Fan, Y. Zhao, M. Xie and Z. Wang, *Chin. Pat.*, 101138700A, 2008.
182 H. Ozora, *Jpn. Pat.*, 05146671, 2005.
183 J. Zhang, M. Xing, X. Yang, Y. Pan, D. Qi, W. Fang, Z. Xi and Y. Zhou, *Chin. Pat.*, 102974333A, 2013.
184 P. O'Connor, G. H. Garcia and C. A. Corma, *World Pat.*, 2012168355A1, 2012.
185 H. Kisch, *US Pat.*, 4325793A, 1982.
186 A. D. King Jr, R. B. King and D. E. Linn Jr, *US Pat.*, 4507185A1, 1983.
187 Z. Z. Chen, *Chin. Pat.*, 1321742C, 2007.
188 M. S. Tian, *Chin. Pat.*, 1762583A, 2006.
189 S. Kohei, A. Hiroyuki and S. Yoshiaki, *World Pat.*, 2011068095A1, 2011.
190 Y.-F. Chen, H.-Y. Lin and Y.-W. Chen, *US Pat.*, 7682594B2, 2010.
191 R. Jiang, W. Xia, L. Dai, J. Huang and B. Wang, *Chin. Pat.*, 101301614B, 2010.
192 L. Jia, P. Zhang, Q. Li, J. Gao, W. Fang and J. Li, *Chin. Pat.*, 1014528223A, 2009.
193 T. Sato and M. Ishizuka, *Jpn. Pat.*, 2000189806A, 2000.
194 D.-C. Park and J.-O. Baeg, *US Pat.*, 6300274B1, 2001.
195 J. Shi, J. Yuan, W. Shangguan and H. Liu, *Chin. Pat.*, 100464846C, 2009.
196 J. Zhang, J. Luan, W. Zhao and Z. Zheng, *Chin. Pat.*, 101204651B, 2010.
197 J. Zhang, J. Luan, W. Zhao and Z. Zheng, *Chin. Pat.*, 101199926B, 2010.
198 P. A. Maggard, *World Pat.*, 2007022462A2, 2007.
199 J. Yan, K. Tang, J. Yi, L. Zhang, Y. Pan and H. Yang, *Chin. Pat.*, 101623638A, 2010.
200 X. Liu, H. Yang, L. Guo and C. Zhou, *Chin. Pat.*, 101254462B, 2011.
201 L. Zhang, S. Kang, J. Mu, X. Li and D. Yin, *Chin. Pat.*, 102600901A, 2012.
202 D. P. Das, S. Martha, D. Parida and A. Kulamani, *Ind. Pat.*, 2011DE00268A, 2012.
203 X. Li, S. Mu, M. Shen and X. Yang, *Chin. Pat.*, 101811044B, 2012.
204 L. Zhang, J. Yan and M. Zhou, *Chin. Pat.*, 102553591A, 2012.
205 W. Su, X. Fu, X. Wang, P. Liu, X. Chen, L. Wu, R. Yuan and Q. Xie, *Chin. Pat.*, 102671684B, 2013.
206 J. Luan, D. Pei and B. Chen, *Chin. Pat.*, 103071480A, 2013.
207 Y. Zhang, L. Liu, B. Wang, L. Ni, Y. Wang, Q. Chai, D. Jing, X. Gu and P. Liu, *Chin. Pat.*, 102688764B, 2013.

208 K. Yo, A. Matsuchita, K. In and M. Oshikiri, *Jpn. Pat.*, 2003251197A, 2003.
209 J. Luan, W. Zhao, J. Zhang and Z. Zheng, *Chin. Pat.*, 101176842A, 2008.
210 H. Zhu, Z. Wang, J. Hou, S. Jiao and K. Huang, *Chin. Pat.*, 103084196A, 2013.
211 S. Riyuu, K. Fuchigami and H. Eguchi, *Jpn. Pat.*, 2007175633, 2007.
212 D. C. Park, B.-k. Ahn and H.-j. Lee, *Kor. Pat.*, 9709559B1, 1997.
213 Y.-F. Chen, H.-Y. Lin and Y.-W. Chen, *US Pat.*, 20070297973A1, 2007.
214 J. T. Irvine, X. Xu and C. Randorn, *World Pat.*, 20130610069, 2013.
215 X. Wang, G. Lu, F. Li, G. Liu and H. Cheng, *Chin. Pat.*, 101474558B, 2011.
216 H. Ueda, M Yonemura and T. Sekine, *Jpn. Pat.*, 63107746A, 1988.
217 H. Ueda, M. Yonemura and T. Sekine, *Jpn. Pat.*, 63107815A, 1988.
218 S. W. Tian, *Chin. Pat.*, 1762582A, 2006.
219 M. Z. Zhu, *Chin. Pat.*, 1793036A, 2006.
220 J. Zhang, J. Luan, W. Zhao and Z. Zheng, *Chin. Pat.*, 101204651B, 2010.
221 K. Sasabara and H. Tanaka, *Jpn. Pat.*, 10015394A, 1998.
222 W. Chen, J. Su, W. Shangguan and Y. Sun, *Chin. Pat.*, 102600830A, 2012.
223 H. Y. S. Liu, *Chin. Pat.*, 1899688A, 2007.
224 G. Wang, Y. Wang, G. Zhang and X. Zhao, *Chin. Pat.*, 102188980B, 2013.
225 D. Jin, *Chin. Pat.*, 1587026A, 2005.
226 S. Liu, S. Li and Y. Liu, *Chin. Pat.*, 102773119A, 2012.
227 S. B. Park, H. U. Kang, S. N. Lim and D. S. Song, *Kor. Pat.*, 2013088334A, 2013.
228 Z. Hu, J. Luan, K. Ma and L. Zhang, *Chin. Pat.*, 101850255B, 2013.
229 S. W. Bae, D. W. Hwang, J. S. Jang, S. M. Ji, H. G. Kim and J. S. Lee, *Kor. Pat.*, KR2004110363A, 2004.
230 W. Shi, X. Sun, L. Deng and J. Guan, *Chin. Pat.*, 103265077A, 2013.
231 S. Kiyoakira, A. Tanaka and K. Domen, *Jpn. Pat.*, 11216366A, 1999.
232 R. Shimazaki, A. Sato, S. Shiraki, A. Kudo, Q. Jia, K. Noritake and T. Sasaya, *Jpn. Pat.*, 2013180245A, 2013.
233 *Tw. Pat.*, 317301B, 2009.
234 Y. Inoue, H. Nishiyama, K. Sato, T. Takada, K. Uchida and A. Harada, *Jpn. Pat.*, 2013163153A, 2013.
235 S. Zhu, F. Yao, C. Yin, Q. Yang and D. Zhang, *Chin. Pat.*, 102513164, 2013.
236 J. Yan, M. Zhou, L. Zhang and N. Zhang, *Chin. Pat.*, 102531063A, 2012.
237 Y. Yokozawa and K. Ooka, *Jpn. Pat.*, 2007252974A, 2007.
238 W. Xia, L. Dai, K. Huang, J. Huang and L. Feng, *Chin. Pat.*, 101559371B, 2012.
239 X. Chen and W. Shangguan, *Front. Energy*, 2013, **7**, 111–118.
240 N. Buehler, J. F. Reber, K. Meier and M. Rusek, *Eur. Pat.*, 58136A1, 1982.
241 J. F. Reber, N. Buehler, K. Meier and M. Rusek, *Eur. Pat.*, 100299A1, 1984.
242 Y. Osawa, M. Yonemura and T. Sekine, *Jpn. Pat.*, 62277151A, 1987.
243 D. C. Park and S. Y. Lim, *US Pat.*, 6017425A, 2000.
244 J. W. Baek and D. C. Park, *World Pat.*, 2000078450A1, 2000.
245 K. Domen, M. Hara, A. Ishikawa and T. Takata, *World Pat.*, 2002062467, 2002.
246 D.-C. Park and J.-O. Baeg, *Eur. Pat.*, 1127614B1, 2004.
247 W. Li, S. Oh, J. Lee and J. Jang, *US Pat.*, 20060283701A1, 2006.
248 H. Zhou and L. Guo, *Chin. Pat.*, 100415366C, 2008.
249 Y. C. Li, *Chin. Pat.*, 1978054A, 2007.
250 A. Kudo, K. Tsuji and H. Kato, *Jpn. Pat.*, 2007144304A, 2007.
251 C. Li, G. Ma, H. Yan, X. Zong, G. Wu, G. Luan and Z. Lei, *Chin. Pat.*, 101293632A, 2008.
252 Y. Zhang, C. Min, X. Li, Y. Wang and S. Li, *Chin. Pat.*, 101623644B, 2011.
253 J. Li, Y. Ying and D. Yurong, *Chin. Pat.*, 101337188B, 2010.
254 X. Bai, W. Dan and N. Liu, *Chin. Pat.*, 101927173A, 2010.
255 X. Zhang, D. Jing and L. Guo, *Chin. Pat.*, 101157044A, 2010.
256 X. Bai and Y. Cao, *Chin. Pat.*, 101623646A, 2010.
257 W. Yao, Q. Xu, X. Zhou and Q. Wu, *Chin. Pat.*, 102302941A, 2012.
258 X. Bai, H. Fan and H. Liu, *Chin. Pat.*, 101618329B, 2011.
259 G. Chen, Y. Zhou, Y. Yu, L. Hao, X. Tan and Z. Yang, *Chin. Pat.*, 102285682B, 2012.
260 W. Yao, Q. Xu, X. Zhou and Q. Wu, *Chin. Pat.*, 102302941A, 2012.
261 X. Bai and J. Li, *Chin. Pat.*, 102101055B, 2012.
262 H. Cheng, X. Wang, L. Wang, G. Liu, F. Li and G. Lu, *Chin. Pat.*, 102641741B, 2014.
263 P. Lin, Q. Li, Y. Yang, J. Su, W. Shangguan and Y. Sun, *Chin. Pat.*, 102861597A, 2013.
264 G. Chen, Y. Yu, G. Wang and Y. Zhou, *Chin. Pat.*, 102389824B, 2013.
265 Q. Wang, J. Li, Y. Ding, F. Wang, J. Li, H. Ma, G. Yun, Y. Bai, Z. Zhang and Z. Lei, *Chin. Pat.*, 103111334A, 2013.
266 Z. Li, L. Wei, X. Chen, P. Liu, X. Wang and X. Fu, *Chin. Pat.*, 103071513A, 2013.
267 W. Yao, J. Zhang, B. Zhang, F. Niu, M. Luo and Q. Wu, *Chin. Pat.*, 103055900A, 2013.
268 W. Yao, J. Zhang, M. Luo, P. Wang and Y. Hong, *Chin. Pat.*, 103331174A, 2013.
269 C. Huang, W. Yao, N. Muradov and A. Raissi, *US Pat.*, 8207081B1, 2012.
270 R. C. Bhardwaj and M. M. T. Khan, *US Pat.*, 4889604A, 1989.
271 Q. Wang, J. Li, J. Lian, Y. Liu, J. Hui, Y. Bai, Z. Zhang, H. She, X. Liu and Z. Su, *Chin. Pat.*, 103316693A, 2013.
272 J. Yu, J. Zhang and B. Cheng, *Chin. Pat.*, 101940933B, 2011.
273 M. M. Khan, B. Taqui, C. Ramesh and C. Bhardwaj, *Eur. Pat.*, 281696A1, 1988.
274 T. Kida, A. Yoshida and K. Kan, *Jpn. Pat.*, 2003334446A, 2003.

275 T. Kida, N. Yamada, A. Yoshida, K. Kan and K. Kimura, *Jpn. Pat.*, 2005067973A, 2005.
276 K. Taji, T. Yanagisawa, T. Arai, S. Sakuma and A. Kasuya, *Jpn. Pat.*, 2001190964A, 2001.
277 L. Wang, S. Yue, S. Yang, X. Guo and J. He, *Chin. Pat.*, 103191783A, 2013.
278 S. Y. Lim and D. C. Park, *World Pat.*, 9815352A1, 1998.
279 D. Paku and S. Haku, *Jpn. Pat.*, 2001232204, 2001.
280 J. U. Baek, D. C. Park and Y. J. Park, *Kor. Pat.*, 2004021074A, 2004.
281 Z. Jiang, H. Wan, Z. Yao, F. Jia and Y. Liu, *Chin. Pat.*, 102218332B, 2013.
282 A. Kudo, S. Nagane and H. Kobayashi, *Jpn. Pat.*, 2004255355A, 2004.
283 K. Domen, J. Kubota, T. Minegishi, C. Miwada and H. Nakanishi, *World Pat.*, 2012121034A1, 2012.
284 S. Obenland and C. Fischer, *World Pat.*, 2010127817A1, 2010.
285 L. Wu, Z. Li, C. Li, X. Li and J. Li, *World Pat.*, 2012174844A1, 2012.
286 J. H. Kim, P. E. Hong and J. H. Kim, *Kor. Pat.*, 201322758A, 2013.
287 G. Jiang, X. Mao, Z. Zhao, Z. Jiang, X. Cui, C. Xu, A. Duan, J. Liu and Y. Wei, *Chin. Pat.*, 103316714A, 2013.
288 Y. Zhang, X. Li, C. Min, Y. Wang and S. Li, *Chin. Pat.*, 101623645B, 2011.
289 A. Kasuya and K. Taji, *Jpn. Pat.*, 2003154272A, 2003.
290 H. Ueda, T. Sekine and M. Yonemura, *Jpn. Pat.*, 61068326A, 1986.
291 K. Parida, G. B. B. Varadwaj, P. C. Sahoo and S. Sahu, *Eur. Pat.*, 2436439B1, 2013.
292 G. L. Zhou, *Chin. Pat.*, 1803278A, 2006.
293 C. Kim, S. J. Do, S. J. Lee, S. G. Lee and H. Y. Kim, *Kor. Pat.*, 744636B1, 2007.
294 C. Kim, S. J. Do, H. Y. Kim, S. J. Lee and S. G. Lee, *Kor. Pat.*, 781080B1, 2007.
295 F. Liu, N. Lu, L. Liu, T. Fang, T. Zhu, L. Li, W. Wang and H. Huang, *Chin. Pat.*, 102489318B, 2013.
296 Y. Liang, W. Cui and L. Liu, *Chin. Pat.*, 103285885A, 2013.
297 Q. Wang, J. Li, Y. Ding, F. Wang, J. Li, H. Ma, G. Yun, Y. Bai, Z. Zhang and Z. Lei, *Chin. Pat.*, 103111334A, 2013.
298 L. Wu, F. Wang and C. Li, *Chin. Pat.*, 102744104A, 2012.
299 Z. Zhou, W. Hu, H. Zhang, M. He, F. Ren, W. Xu and A. Ma, *Chin. Pat.*, 102600905A, 2012.
300 M. Zhou, L. Zhang, J. Yan and N. Zhang, *Chin. Pat.*, 102407147A, 2012.
301 Y. Xu, X. Yuan, X. Wang, C. Li and R. Xia, *Chin. Pat.*, 103253712A, 2013.
302 M. Wei, Y. Zhao, W. Gao, B. Li and X. Duan, *Chin. Pat.*, 102872918A, 2013.
303 M. Wei, Y. Zhao, P. Chen, J. Li and X. Duan, *Chin. Pat.*, 102489323B, 2013.
304 A. Tanaka, K. Shinohara and D. Kazunari, *Jpn. Pat.*, 07232079A, 1995.
305 J. Mu, L. Chen and S. Kang, *Chin. Pat.*, 102218322B, 2013.
306 D. Zhang, S. Xiao, P. Liu, S. Zhang and H. Li, *Chin. Pat.*, 103191739A, 2013.
307 K. Murao, Y. Takeda, M. Sato and Y. Morishita, *Jpn Pat.*, 57081836A, 1982.
308 W. Y. Choi and H. W. Park, *Kor. Pat.*, 682033B1, 2007.
309 K. Murao, Y. Takeda, A. Kobi, M. Sato and Y. Morishita, *Jpn. Pat.*, 57030727A, 1982.
310 K. Mori and Y. Kataoka, *Jpn. Pat.*, 2010158627A, 2010.
311 R. Sven and A. Matthias, *Ger. Pat.*, 102008009433A1, 2009.
312 K. Kitamoto, M. Ogawa and K. Sakai, *World Pat.*, 2012002548A1, 2012.
313 L. Wu, C. Li, F. Wang and J. Wang, *Chin. Pat.*, 102924532A, 2013.
314 K. M. M. Bin, I. M. R. Bin and A. Khuzaimah, *Malaysian Pat.*, 145222A, 2012.
315 Q. M. A. Lopez and R. J. Rivas, *World Pat.*, 2013079669A1, 2013.
316 S. Yan, H. Gao and Z. Zou, *Chin. Pat.*, 102992282A, 2013.
317 X. Wang, M. Zhang, H. Ren and J. Zhang, *Chin. Pat.*, 103272639A, 2013.
318 X. Chen, L. Guo, J. Lin, K. Zhu and Y. Jia, *Chin. Pat.*, 102886270A, 2013.
319 T. Suzuki, T. Nomura, S. Tamura, K. Hato, N. Taniguchi, K. Tokuhiro and N. Miyata, *World Pat.*, 2012090390A1, 2012.
320 H. Zhu, Z. Wang, J. Hou, S. Jiao and K. Huang, *Chin. Pat.*, 102423716A, 2013.
321 Mitsubishi Chemical Holdings Corporation and University of Tokyo, *Jpn. Pat.*, 2012187520A, 2012.
322 O. Kimura, K. Okawa, S. Sarayama and S. Takeuchi, *Jpn. Pat.*, 2009195809A, 2009.
323 Y. Zhou, Q. Liu, Y. Ma and Z. Zou, *Chin. Pat.*, 102225782A, 2011.
324 S. Sato, T. Morikawa, T. Mori, S. Saeki, T. Kajino and H. Tanaka, *World Pat.*, 2010018871A1, 2010.
325 W. Chen, J. Liu, T. Zhang and Z. Wang, *Chin. Pat.*, 102218339A, 2011.
326 S. Mohapatra and M. Misra, *US Pat.*, 20130032470A1, 2013.
327 *US Pat.*, 50222970, 1991.
328 *Chin. Pat.*, 102658177A1, 2012.
329 Assigned to Toyota Motor Corp. and Toyota Central Research & Development, *Jpn. Pat.*, 2012192302A, 2012.
330 Assigned to Nippon Telegraph & Telephone, *Jpn. Pat.*, 2013180943A, 2013.
331 *Kor. Pat.*, 2012026656A, 2012.
332 T. Mori, R. Doi, T. Ogawa, H. Hida and O. Kuroda, *Jpn. Pat.*, 04045853A, 1992.
333 *Jpn. Pat.*, 2012250860A, 2012.
334 Z. Yong, T.-D. Lee and Z. Zhigang, *Chin. Pat.*, 102303901B, 2013.
335 N. N. Lichtin, *US Pat.*, 4427508A, 1984.
336 Y. Cao and X. Yang, *Chin. Pat.*, 101879443B, 2013.
337 J. Zhao, Q Li, H. Ji, C. Chen and W. Ma, *Chin. Pat.*, 103041865A, 2013.
338 X. Liu, L. Wang, X. Wang and X. Zhang, *Chin. Pat.*, 101794672B, 2011.

339 M. R. Detty, B. D. Calitree, A. Orchard, R. Eisenberg and T. McCormick, *World Pat.*, 2011090981A2, 2011.
340 S. Yanagida, K. Yoshino, S. Boku, K. Mizumoto and A. Kabumoto, *Jpn. Pat.*, 61191501A, 1986.
341 J. Zhao, G. Liu, C. Chen, H. Ji and W. Ma, *Chin. Pat.*, 102091654B, 2012.
342 J. A. Shelnutt, J. E. Miller, Z. Wang and C. J. Medforth, *US Pat.*, 7338590B1, 2008.
343 L. Guo and H. Liu, *Chin. Pat.*, 101666680B, 2011.
344 B. Cheng, S. Liu and J. Yu, *Chin. Pat.*, 101776588A, 2010.
345 (*a*) B. Ma, C. Li and P. Ying, *Chin. Pat.*, 101315357B, 2013; (*b*) Z. Jiang, F. Jia, Z. Yao and C. Li, *Chin. Pat.*, 101900710B, 2013.
346 H. Shi, Y. Xie, Y. Wang and B. Lan, *Chin. Pat.*, 203216914U, 2013.
347 N. Serpone, A. Salinaro, A. V. Emeline and V. Ryabchuk, *J. Photochem. Photobiol., A*, 2000, **130**, 83–94.
348 A. V. Emeline, A. V. Panasuk, N. Sheremetyeva and N. Serpone, *J. Phys. Chem. B*, 2005, **109**, 2785–2792.
349 A. V. Emeline, V. K. Ryabchuk and N. Serpone, *Catal. Today*, 2007, **122**, 91–100.
350 A. V. Emeline, G. V. Kataeva, A. V. Panasuk, V. K. Ryabchuk, N. V. Sheremetyeva and N. Serpone, *J. Phys. Chem. B*, 2005, **109**, 5175–5185.
351 A. V. Emeline, V. K. Ryabchuk and N. Serpone, *J. Phys. Chem. B*, 2005, **109**, 18515–18521.
352 N. Serpone and A. V. Emeline, *Res. Chem. Intermed.*, 2005, **31**, 391–432.
353 A. V. Emeline, V. K. Ryabchuk and N. Serpone, *J. Photochem. Photobiol., A*, 2000, **133**, 89–97.
354 W. Zhao, C. Chen, W. Ma, J. Zhao, D. Wang, H. Hidaka and N. Serpone, *Chem. – Eur. J.*, 2003, **9**, 3292–3299.
355 C. Chen, W. Zhao, J. Li, J. Zhao, H. Hidaka and N. Serpone, *Environ. Sci. Technol.*, 2002, **36**, 3604–3611.
356 W. Zhao, C. Chen, X. Li, J. Zhao, H. Hidaka and N. Serpone, *J. Phys. Chem. B*, 2002, **106**, 5022–5028.
357 C. Chen, X. Li, W. Ma, J. Zhao, H. Hidaka and N. Serpone, *J. Phys. Chem. B*, 2002, **106**, 318–324.
358 T. Zhang, T. Oyama, S. Horikoshi, H. Hidaka, J. Zhao and N. Serpone, *Sol. Energy Mater. Sol. Cells*, 2002, **73**, 287–303.
359 T. Zhang, T. Oyama, A. Aoshima, H. Hidaka, J. Zhao and N. Serpone, *J. Photochem. Photobiol., A*, 2001, **140**, 163–172.
360 T. Wu, G. Liu, J. Zhao, H. Hidaka and N. Serpone, *New J. Chem.*, 2000, **24**, 93–98.
361 G. Liu, X. Z. Li, J. Zhao, H. Hidaka and N. Serpone, *Environ. Sci. Technol.*, 2000, **34**, 3982–3990.
362 A. V. Emeline, G. N. Kuzmin and N. Serpone, *Chem. Phys. Lett.*, 2008, **454**, 279–283.
363 A. V. Emeline, G. N. Kuzmin, L. L. Basov and N. Serpone, *J. Photochem. Photobiol., A*, 2005, **174**, 214–221.
364 L. L. Basov, Y. U. P. Solonitsyn and A. N. Terenin, *Dokl. Akad. Nauk SSSR*, 1965, **164**, 122–124.
365 L. L. Basov, G. N. Kuzmin, I. M. Prudnikov and Y. U. P. Solonitsyn, in *Photoadsorption processes on metal oxides*, ed. T. H. I. Vilesov, Uspehi fotoniki (advances in photonics), LGU, Leningrad, 1976, 6, pp. 82–120.
366 Apart from the nature of photocatalyst, several factors contribute to the development of a photoelectrolysis device, see for instance ref. 32 and N. S. Lewis, *ECS Interface*, 2013, **22**, 43–49. A review focused on the different devices for the solar production of hydrogen, including photoelectrochemical cells (PEC) and PV-Electrolysis has been recently published, see T. J. Jacobsson, V. Fjällström, M. Edoff and T. Edvinsson, *Energy Environ. Sci.*, 2014, **7**, 2056–2070.
367 (*a*) J. A. Turner, *Science*, 2004, **305**, 972–974; (*b*) A. Sartbaeva, V. L. Kuznetsov, S. A. Wells and P. P. Edwards, *Energy Environ. Sci.*, 2008, **1**, 79–85; (*c*) G. Marbán and T. Valdés-Solís, *Int. J. Hydrogen Energy*, 2007, **32**, 1625–1637; (*d*) N. Armaroli and V. Balzani, *ChemSusChem*, 2011, **4**, 21–36.
368 (*a*) T. Abbasi and S. A. Abbasi, *Renewable Sustainable Energy Rev.*, 2011, **15**, 3034–3040; (*b*) L. Barreto, A. Makihira and K. Riahi, *Int. J. Hydrogen Energy*, 2003, **28**, 267–284.
369 A list of companies in hydrogen production sector is available at http://en.openei.org/wiki/List_of_Companies_in_Hydrogen_Sector, accessed July 14, 2014.
370 Y. Paz, *Appl. Catal., B*, 2010, **99**, 448–460.
371 A. Mills and S. K. Lee, *J. Photochem. Photobiol., A*, 2002, **152**, 233–247.
372 T. Hisatomi, J. Kubota and K. Domen, *Chem. Soc. Rev.*, 2014, DOI: 10.1039/c3cs60378d.
373 R. M. N. Yerga, M. C. A. Galvàn, F. del Valle, J. A. Villoria de la Mano and J. L. G. Fierro, *ChemSusChem*, 2009, **2**, 471–485; D. Y. C. Leung, X. Fu, C. Wang, M. Ni, M. K. H. Leung, X. Wang and X. Fu, *ChemSusChem*, 2010, **3**, 681–694.
374 M. Bowker, *Green Chem.*, 2011, **13**, 2235–2246; see also: B. Ohtani, *Chem. Lett.*, 2008, **37**, 217–229.